

**BOND BEHAVIOUR OF COMMERCIALY PRODUCED STRUCTURAL  
CONCRETE FROM RECYCLED COARSE AND FINE AGGREGATES**

by

Charles Rockson

A THESIS SUBMITTED IN PARTIAL FULFILLMENT  
OF THE REQUIREMENTS FOR THE DEGREE OF

DOCTOR OF PHILOSOPHY

in

The College of Graduate Studies  
(Civil Engineering)

THE UNIVERSITY OF BRITISH COLUMBIA  
(Okanagan)

May 2020

© Charles Rockson, 2020

The undersigned certify that they have read, and recommend to the College of Graduate Studies for acceptance, a thesis entitled:

**BOND BEHAVIOUR OF COMMERCIALY PRODUCED STRUCTURAL CONCRETE  
MADE OF RECYCLED COARSE AND FINE AGGREGATES**

---

Submitted by: Charles Rockson in partial fulfillment of the requirements of  
the degree of Doctor of Philosophy in Civil Engineering

Dr. M. Shahria Alam, School of Engineering

Supervisor, Professor

Dr. Ahmad Rteil, School of Engineering

Co-Supervisor and Committee Member

Dr. Lukas Bichler, School of Engineering

Supervisory Committee Member, Professor

Dr. Sumi Siddiqua, School of Engineering

Supervisory Committee Member, Professor

Dr. Jian Liu, School of Engineering

University Examiner, Professor

Dr. Assem Hassan, Faculty of Engineering and Applied Science, Memorial University,

External Examiner, Professor (please print name and university in the line above)

\_\_\_\_\_  
(Date Submitted to Grad Studies)

## **ABSTRACT**

Recycled concrete aggregates (RCAs) offer a sustainable solution to the multifarious exigent crises involving the ever-increasing demand of virgin aggregates and the disposal of construction and demolition waste arising from demolishing non-serviceable infrastructure. However, the use of RCA in concrete is mostly limited to non-structural purposes at a limited replacement proportion of the virgin aggregates in the standards and codes. Also, using an appropriate test method to quantitatively determine the bond behaviour of steel rebar in recycled structural concrete in addition to other several variables affecting the bond remains unexplored. This study presents the results of an experimental program on the bond behaviour between commercially produced quality recycled concrete and deformed steel rebars.

Seventy beam-end specimens were tested using the ASTM A944-15, where five critical variables affecting bond behaviour, such as cover, bond length, bar size, bar position, and transverse reinforcement were investigated. For the five variables investigated, the normalized bond strengths of recycled concrete mixes were generally comparable to the conventional natural concrete mixes. Furthermore, the results showed that the bond strengths were conservative with several descriptive and code design equations, as well as fitting into the current ACI 408 database for conventional concrete. Finally, a new descriptive model equation was proposed and validated using the experimental results.

## **LAY SUMMARY**

Common practices of cost reduction in home remedial works and DIY jobs, such as driveway filling and erosion protection, may require reusing demolished waste concrete if available. On the otherhand, if the volume of waste concrete is large, the waste concrete will be disposed off at a landfill site. The demolished waste concrete is inert (does not decompose) and occupies large spaces and cover at landfill sites. The waste concrete can be recycled by crushing and removing most of the mortar which gives off another gravel and sand as raw materials and can be reused in new buildings. Though this is a departure from the norm of using new gravel and sand, several research works are advancing the cause that reusing the new recycled concrete is acceptable. In addition, this thesis supports that it can bind well with steel rebars when the gravel and sand are well processed to produce quality recycled concrete following the current code practices. Finally, the current building code guidelines for providing rebar joints/laps in say beams and slabs are still applicable when the quality recycled gravel and sand are used for concrete.

## **PREFACE**

This thesis is based on an original experimental work completed by the author in the Applied Laboratory for Advanced Materials & Structures (ALAMS), School of Engineering at the University of British Columbia (UBC)'s Okanagan campus. The author was responsible for completing all the literature review, material acquisition, experimental work, data collection, data analysis, modelling and thesis writing. Guidance and supervision throughout the work was contributed by Dr. Shahria Alam and Dr. Ahmad Rteil.

### **Summary of works**

- Rockson, C, Alam, M.S. and Rteil, A. "Bond Strength and Bond Behavior of Using Recycled Coarse and Fine Aggregates as Concrete on Deformed Rebars", Research Report, School of Engineering, UBC, Kelowna, October 2017.
- Rockson, C. "Effect of Cover on Bond Performance of Recycled Coarse and Fine Aggregates Concrete", ACI Fall Convention, Las Vegas, USA, August 2018.
- Rockson, C, Alam, M.S. and Rteil, A. 2019. "Effect of Cover on Bond Performance of Recycled Coarse and Fine Aggregates Concrete", CSCE Conference, Montreal, June 2019.
- Rockson, C, Alam, Tammana, K., Alam, M.S. and Rteil, A. " Effect of cover on bond strength of structural concrete using commercially produced recycled coarse and fine aggregates", Construction and Building Materials, April 2020. (Published)
- Rockson, C, Alam, Tammana, K., Alam, M.S. and Rteil, A. " Effect of Rebar Embedment Length on the Bond Behavior of Commercially Produced Recycled Concrete

Using Beam-end Specimens", (Under Review Construction and Building Materials, 2020)

- Rockson, C, Alam, Tammana, K., Alam, M.S. and Rteil, A. 2020. " Effect Effect of Anchorage Bond Strength and Behavior of Top-Cast Deformed bars in Commercially Produced Recycled Structural Concrete Using Beam-end Specimens", (Yet to submit, Cement and Concrete Composites, 2020)

# TABLE OF CONTENTS

ABSTRACT .....	iii
LAY SUMMARY.....	iv
PREFACE .....	v
TABLE OF CONTENTS.....	vii
LIST OF TABLES .....	xiv
LIST OF FIGURES .....	xv
LIST OF ABBREVIATIONS AND SYMBOLS .....	xviii
ACKNOWLEDGEMENTS .....	xx
DEDICATION .....	xxi
CHAPTER 1: INTRODUCTION.....	1
1.1 Background.....	1
1.2 Steel-concrete bond .....	3
1.3 Research objectives and scope.....	4
1.4 Thesis methodology and organization .....	4
CHAPTER 2: LITERATURE REVIEW .....	7
2.1 Concrete-steel bond .....	7
2.1.1 Mechanics of bond.....	7

2.1.2	Bond failure modes.....	8
2.1.3	Factors affecting bond .....	8
2.1.4	Bond test methods .....	9
2.1.5	Summary of research.....	10
2.2	Recycled aggregates, recycled concrete production methods, and quality .....	11
2.2.1	Recycled aggregates and recycled concrete .....	12
2.2.2	Successful recycling aggregates production methodologies .....	13
2.2.3	Successful recycled concrete production methodologies .....	14
2.2.4	Quality and durability of recycled concrete .....	14
2.3	Concrete properties affecting bond.....	16
2.3.1	Effect of compressive strength on bond .....	16
2.3.2	Effect of concrete density on bond .....	16
2.3.3	Effect of aggregates type on bond.....	17
2.4	Structural characteristics affecting bond .....	18
2.4.1	Effect of concrete cover and bar spacing.....	18
2.4.2	Effect of bond length using recycled concrete .....	19
2.4.3	Effect of transverse reinforcement .....	22
2.4.4	Effect of bar cast position (top location) .....	22

2.5	Bar properties affecting bond .....	24
2.5.1	Effect of bar size.....	24
2.5.2	Effect of rebar geometry (patterns) .....	24
2.5.3	Effect of rebar surface coating.....	25
2.6	Research needs.....	26
CHAPTER 3: EXPERIMENTAL METHODOLOGY .....		28
3.1	Test program.....	28
3.2	Test specimen .....	30
3.2.1	Structural details of test beam specimens.....	31
3.3	Test specimen fabrication.....	34
3.3.1	Recycled concrete mixing and pouring of test specimens.....	37
3.3.2	Specimen placement procedure .....	39
3.4	Materials and properties .....	40
3.4.1	Recycled aggregates production for concrete.....	40
3.4.2	Aggregates properties .....	42
3.4.3	Concrete and rebar materials .....	42
3.5	Instrumentation and data acquisition system.....	44
3.6	Specimen preparation for testing .....	45
3.6.1	Experimental Test Set-up .....	47

3.7	Test Procedure .....	48
CHAPTER 4: EXPERIMENTAL RESULTS AND DISCUSSION .....		51
4.1	General.....	51
4.2	Failure modes.....	55
4.3	Effect of concrete cover on bond (Groups 1 and 3).....	55
4.3.1	Effect of concrete cover on bond force (Groups 1 and 3) .....	55
4.3.2	Effect of concrete cover on normalized bond strength.....	56
4.3.3	Effect of concrete cover on first crack load and load vs slip curves .....	59
4.4	Effect of bond length on the bond capacity (Groups 1 & 5) .....	66
4.4.1	Effect of bond length increase on bond force and rebar yielding.....	66
4.4.2	Effect of bond length increase on bond strength .....	68
4.4.3	Effect of bond length increase on normalized bond strength .....	69
4.4.4	Effect of bond length increase on the Load vs Slip curves .....	71
4.5	Effect of bar size on bond (Groups 1 and 6).....	76
4.5.1	Effect of bar size on normalized bond strengths .....	78
4.5.2	Effect of bar size on cracking behavior .....	79
4.5.3	Effect of bar size on bond force vs slip curve .....	81
4.6	Effect of bar position on bond (Groups 1 and 7) .....	83

4.6.1	Effect of bar position on normalized bond strengths.....	84
4.6.2	Effect of bar position on bond force and slip .....	85
4.6.3	Effect of first crack load on bar position .....	86
4.7	Effect of transverse reinforcement on bond force (Groups 1, 2 and 4) .....	89
4.7.1	Effect of transverse reinforcement (stirrups) on bond contribution .....	91
4.7.2	Effect of transverse reinforcement on cracking load and cracking behavior ..	92
4.7.3	Effect of stirrups spacing on bond force (load) and slip curve.....	95
CHAPTER 5: EMPIRICAL EQUATIONS AND STATISTICAL MODELLING .....		99
5.1	Background.....	99
5.2	Descriptive Equations .....	100
5.2.1	Summary discussions on descriptive equations.....	103
5.3	Design Equations .....	103
5.3.1	Design equation using ACI 318M-11 and CSA A23.3-14.....	108
5.3.2	Design equation using BS8100.....	108
5.3.3	Design equation using Eurocode-2 and AASHTO.....	109
5.3.4	Summary discussion of design equation compliance .....	110
5.4	Proposed code provisions .....	111
5.5	Statistical analysis and modelling.....	112

5.6	Bond behaviour and ACI 408 database comparison.....	115
5.6.1	Background on bond behavior.....	115
5.6.2	ACI 408 database comparison.....	118
CHAPTER 6: CONCLUSIONS, LIMITATIONS, RECOMMENDATIONS FOR FUTURE RESEARCH AND NOVELTY .....		
		121
6.1	Conclusions on studied effect on bond variables .....	121
6.1.1	Effect of rebar cover on bond Group 1 and 3).....	121
6.1.2	Effect of embedment length on bond (Group1 and Group5).....	121
6.1.3	Effect of bar size on bond (Group6).....	122
6.1.4	Effect of bar position on bond (Group 7) .....	123
6.1.5	Effect of transverse reinforcement and spacing on bond (Groups 2 and 4) ..	124
6.2	Conclusions on effect of bond strength on bond equations and modelling .....	125
6.2.1	Effect of descriptive equations .....	125
6.2.2	Effect of design equations .....	125
6.2.3	Proposed descriptive model and ACI Database .....	126
6.3	Limitations of this study .....	126
6.4	Recommendations for future research .....	127
6.5	Novelty of this study.....	128

REFERENCES .....	130	
Appendix A	Summary of recycled coarse and fine aggregates applications..... 143	
Appendix B	Summary table of pullout bond test method and conclusions ..... 144	
Appendix C	Summary table of beam bond test with varied experimental settings and conclusions .....	145
Appendix D	Strain gage and adhesive installation..... 148	
Appendix E	Bending schedule for test beam specimens..... 150	
Appendix F	Recycled concrete products and stages of crushing..... 151	
Appendix G	Descriptive and design equations..... 152	
Appendix H	Bond failure in specimens..... 153	
Appendix I	Group 1 Test specimens R15-L200-C25 ..... 154	
Appendix J	Group 2 Test specimens R15-L200-C25-S1 ..... 157	
Appendix K	Group 3 Test Specimens R15-L200-C40..... 161	
Appendix L	Group 4 Test Specimens R15-L200-C25-S2 ..... 163	
Appendix M	Group 5 Test specimens R15-L300-C25 ..... 165	
Appendix N	Group 6 Test specimens R25-L300-C40 ..... 167	
Appendix O	Group 7 Test specimens R15-L200-C25-Top..... 170	

## LIST OF TABLES

Table 2.1 Factors affecting bond characteristics between concrete and rebar.....	9
Table 3.1 Experimental test matrix.....	29
Table 3.2 Mix design for 35 MPa structural concrete .....	43
Table 3.3 Compressive strength and density test results from cored specimens.....	44
Table 3.4 Test bar engineering design data .....	44
Table 3.5 Test bar chemical composition in steel rebar.....	44
Table 4.1 Specimens groups and pairings.....	52
Table 4.2 Table of experimental results and failure modes.....	53
Table 4.3 Percent variation of normalized bond strength (NBS) when cover increased.....	58
Table 4.4 Summary results of first crack load, maximum slip and strain in test specimens .....	61
Table 4.5 Effect of increasing bond length on rebar “yield” stresses.....	67
Table 4.6 Group1 and 5 bond strength and normalized bond strength variations .....	69
Table 4.7 Effect of bar size (Group 1 and 6) normalized bond strength .....	79
Table 4.8 Group 1 and 7 normalized bond strength.....	85
Table 4.9 Groups 1, 2 and 4 normalized bond strength effect of using stirrups.....	90
Table 4.10 Group 1, 2 and 4 bond strength contribution from stirrups .....	92
Table 5.1 Regression and ANOVA results of average (normalized) bond strength.....	113
Table 5.2 Regression and ANOVA results of raw (non-normalized bond strength).....	113
Table 5.3 Root mean square error (RMSE) of experimental and descriptive model.....	114
Table 5.4 Regression and ANOVA results of combined 100% RCA from literature .....	115

## LIST OF FIGURES

Figure 1.1 Thesis Organization.....	6
Figure 2.1 Bond forces along rebar, adapted (ACI Committee 408, 2003).....	7
Figure 2.2 Bond test methods, adapted (ACI Committee 408, 2003).....	10
Figure 2.3 Crack propagation paths and concrete cover.....	19
Figure 3.1 Free body diagram of beam end specimen.....	30
Figure 3.2 3-D Model of test specimen adapted per ASTM A944-15.....	31
Figure 3.3 Longitudinal and cross sectional details of typical test beam specimen.....	32
Figure 3.4 Modified test beam specimen with transverse reinforcement spacing at 200mm c/c .	32
Figure 3.5 Modified test beam specimen with transverse reinforcement spacing at 100mm c/c .	33
Figure 3.6 Longitudinal and cross sectional details of typical top position test beam.....	33
Figure 3.7 Prepared set of formwork with partitions.....	35
Figure 3.8 Formwork with flexural rebars and prepared stirrups.....	36
Figure 3.9 Completed formwork with test bars and embedded in PVC and sealed.....	36
Figure 3.10 Completed interior test specimen with stirrups, flexural rebars and bond area.....	37
Figure 3.11 Concrete pour, vibration and beam specimen curing.....	39
Figure 3.12 Recycling aggregates processing and stage products at Lock-Block Limited.....	41
Figure 3.13 Test bar outline design configuration (provided by supplier Nucour Steel).....	44
Figure 3.14 Test data acquisition (DAQ) set-up.....	45
Figure 3.15 Removed specimens from formwork and prepared specimens for testing.....	46

Figure 3.16 Strain gage pretesting from specimen lead wires .....	46
Figure 3.17 Schematic experimental test rig with test beam .....	49
Figure 3.18 Detail experimental test set-up with of beam specimens .....	49
Figure 3.19 Experimental mechanical assemblies at the loaded and unloaded end .....	50
Figure 4.1 Effect of cover increase on the bond forces and mix variation .....	56
Figure 4.2 Effect of cover increase on normalized bond strength with square root function.....	57
Figure 4.3 Normalized bond strength vs compressive strength with $\frac{1}{2}$ and $\frac{1}{4}$ roots .....	59
Figure 4.4 Plot of first crack and maximum splitting load cover=25mm and 40mm vs mix variation .....	62
Figure 4.5 Load-slip curves of loaded and unloaded specimens of various mixes.....	65
Figure 4.6 Bond strength effect and variation after length increase (200 to 300)mm.....	68
Figure 4.7 Normalized bond strength with square root function ( $\sqrt{f_c}$ ) .....	70
Figure 4.8 Trend line of maximum bar slip and mix variations with increased bond length .....	72
Figure 4.9 Typical load-slip curves of loaded (A&B) and unloaded (C&D) specimens of various mixes .....	73
Figure 4.10 First crack and failure load of L200 and L300 vs mix variation .....	74
Figure 4.11 Bond strength effect on changing bar size (15M to 25M).....	77
Figure 4.12 Normalized bond strength effect on changing bar size (15M to 25M) .....	79
Figure 4.13 Trendline of first crack and splitting loads for Group 1 & 6 (Effect of bar size).....	80
Figure 4.14 Load-slip and mix variations on effect on changing bar size (15M to 25M) .....	82
Figure 4.15 Bond force effect and variation on bar position (200 to 300)mm .....	83

Figure 4.16 Normalized bond strength effect and variation on bar position (200 to 300)mm .....	84
Figure 4.17 Typical load-slip curves (A to D) showing bar position of various specimens and mixes.....	88
Figure 4.18 Trendline of first crack and splitting loads for Group 1 & 7 (Effect of bar position)	87
Figure 4.19 Bond force effect on transverse reinforcement and spacing (100mm to 200mm) ....	90
Figure 4.20 Splitting failure of concrete cover with stirrups .....	94
Figure 4.21 Trendline of first crack and splitting loads for Group 1, 2 & 4 (Effect of stirrups/spacing).....	94
Figure 4.22 Bond slip effect on transverse reinforcement and spacing on concrete mixes.....	98
Figure 5.1 Bond efficiency of descriptive equations compared with recycled concrete mixes..	102
Figure 5.2 Bond efficiency of design equations compared with recycled concrete mixes.....	107
Figure 5.3 Experimental crack/separation and crushing failure of specimens .....	116
Figure 5.4 Reinforced beam section and stress distribution .....	117
Figure 5.5 ACI 408 Database comparisons for 200 mm bond length for 15M (c=25mm & 40mm) .....	119
Figure 5.6 ACI 408 Database comparisons for 300 mm bond length (15M and 25M).....	119
Figure 5.7 ACI 408 Database comparison for top rebar positions .....	120

## LIST OF ABBREVIATIONS AND SYMBOLS

### ABBREVIATIONS

AASHTO	American Association of State Highway and Transportation Officials
ACI	American Concrete Institute
BS	British Standard
CSA	Canadian Standard Association
EC	Euro Code
LVDT	Linear Variable Differential Transformer
NBS	Normalized Bond Strength
RCA	Recycled Coarse Aggregates
RFA	Recycled Fine Aggregates (FRA)
RILEM	International Union Of Laboratories And Experts In Construction Materials, Systems And Structures
RMSE	Root Mean Square Error

### SYMBOLS

$A_b$	= nominal area of rebar
$A_{tr}$	= area of transverse rebar
$c_b$	= smallest side or bottom concrete cover

- $c_{\max}$  = maximum cover
- $c_{\min}$  = minimum cover
- $d_b$  = nominal diameter of rebar
- $d_{cs}$  = center-to-center spacing of rebars
- $f'_c$  = cylinder compressive strength of concrete
- $f_{cu}$  = cubic compressive strength of concrete =  $0.8 f'_c$
- $f_{ctd}$  = design value concrete tensile strength
- $f_s$  = rebar stress
- $f_y$  = yield steel stress
- $f_{ytr}$  = yield steel stress of transverse reinforcement
- $k_1$  = rebar location factor (=1.0 for bottom placed rebars)
- $k_2$  = rebar coating factor (=1.0 for uncoated rebars)
- $k_3$  = concrete density factor (=1.0 for normal density and same for sustainable concrete)
- $k_4$  = rebar size factor (=0.8 for  $d_b \leq 20M$ , or 1.0 for  $d_b \geq 25M$ )
- $k_{tr}$  = contribution of confining transverse reinforcement across splitting planes
- $l_d$  = bond length/development length
- $\tau_b$  = mean bond stress/strength
- $T_c$  = total bond force due to concrete contribution
- $T_s$  = total bond force due to steel stirrup contribution
- $\psi_t$  = rebar location factor (=1.0 for bottom placed rebars)
- $\psi_e$  = rebar coating factor (=1.0 for uncoated rebars)
- $\psi_s$  = rebar size factor (=0.8 for  $d_b \leq 20M$ , or 1.0 for  $d_b \geq 25M$ )
- $\lambda$  = concrete density factor (=1.0 for normal density and same for sustainable concrete)
- $\eta_1$  = bond quality coefficient (=1.0 for good quality)
- $\eta_2$  = bar size factor (=1.0 for  $d_b \leq 32mm$ )

## ACKNOWLEDGEMENTS

This research was conducted in ALAMS at UBC's Okanagan campus with research funds from the Natural Sciences and Engineering Research Council of Canada (NSERC) and Industrial partner Lock-Block Limited.

The experimental investigation was under the diligent guidance of Dr. Shahria Alam, Professor, School of Engineering; Director, Green Construction Research & Training Center (GCRTC) and Chair, Engineering Mechanics and Materials Division of Canadian Society for Civil Engineering (CSCE), and Dr. Ahmad Rteil, Assistant Professor in Structural Engineering in the School of Engineering at UBC's Okanagan campus.

I will also like to thank the following who supported this work in diverse ways when the need arose; Messrs. Brent Wallace and Alvin Hathaway from Lock-Block, Charles Kyle from ALAMS, UBC and Kim Nordstrom and all the Technicians in the School of Engineering at UBC and Jeff Janson from Nucour Steel.

Particular thanks to all the past and present students at ALAMS, especially, Ms. Kishoare Tamanna for her diverse support and inputs into the thesis editing.

## **DEDICATION**

This thesis is dedicated to the glory of Almighty God (SDG- Father, I know that all my life is portioned out for me-MHB602) for making this possible, and to my Mum and the entire Rockson Family especially Maa-Abena who permitted me to be out of home when she needed me most. Also not forgetting T.M.K. Aggrey-Fynn Snr, Late Cdr (Rtd) K.T. Bedu-Addo and the Late K. K. Mercer Esq. (Snr Partner of KMP Chartered Engineers) for their lifetime support in my career. Finally, to all my faithful friends and faculty members and staff of UBC's School of Engineering especially my Professor Dr. M. Shahria Alam and Co-Professor Dr. Ahmad Retil for their support during my studies.

# CHAPTER 1: INTRODUCTION

## 1.1 Background

Four of the seventeen United Nations' Sustainable Development Goals (SDGs) highlight the need to optimize and conserve the earth and its resources. These are the SDG 7 (Affordable and Clean Energy), SDG 9 (Industry, Innovation, and Infrastructure), SDG 11 (Sustainable Cities and Communities), and SDG 12 (Responsible Consumption and Production).

In a concerted effort to reduce the consumption of natural resources by several industries including the construction industry, the high rate of extraction of natural resources and its availability has become ever critical. It is reported that about 50% of the raw materials used by the construction industry are taken from nature, and the construction industry also consumes 40% of the world's total energy demand whilst creating 50% of total waste in landfill sites (Oikonomou, 2005)

In Canada, the Infrastructure Report Card has determined that about 50% of Canada's infrastructure is rated "very poor to fair" with an estimated remedial cost of \$168 Billion (The Canadian Infrastructure Report Card, 2016). The infrastructure covered in the study ranged from building, bridges, and roads to transits, water treatment, and drainage where concrete is known to constitute a major proportion. The remedial works would create large volumes of concrete waste, while concrete production for new and replacement structures would require huge demand for new concrete aggregates. On the other hand, identifying new sources of natural aggregates for concrete is becoming challenging in terms of ecological considerations, high haulage cost, and increasing total cost of construction works (Bhattacharyya, 2011; Tam, 2008).

One solution to this challenging problem that is being studied is the use of crushed concrete as aggregates in new construction.

The use of recycled aggregates, which is obtained from demolished concrete and using it for new construction works is gaining notoriety, in addition to its incorporation into several standards (See Appendix A) including the Canadian Standards Association, 2014 (Gonçalves & Brito, 2010). Hitherto, recycled aggregates among other aggregate types have been identified in the American Concrete Institute Report, ACI Committee 701 (2016), for use in concrete and advancing the cause of the four SDGs.

Concrete generally contains 75% by volume coarse and fine aggregates fraction. Hence the aggregates' quality is of utmost significance in determining the performance of concrete (Neville & Brooks, 2010). Inherently, conventional aggregates are porous and the amount of voids is a determining factor on the strength and durability of concrete. When concrete is prepared from recycled aggregates, several researchers have confirmed the existence of the attached mortar which is highly porous and efforts to eliminate all the mortar has not been successful (Behera, Bhattacharyya, Minocha, Deoliya, & Maiti, 2014a; Katz, 2003). On the other hand, the residual mortar also contains unhydrated cement which has an added advantage of contributing to the total cement content and reducing the total amount of pore sizes when recycled aggregates hydrated for concrete (Behera et al., 2014a; Katz, 2003).

Though using recycled aggregates for non-structural concrete in construction application has not been largely criticized, rather safety concerns are likely to be raised when used as structural concrete due to the effect of reduced density, reduced compressive strength, reduced elastic

modulus and splitting tensile strength and increased water absorption (Evangelista & Brito, 2007; Katz, 2003).

The current construction state of the art knowledge and practices does not encourage the use of recycled structural concrete as an alternative to conventional structural concrete mixes whereas the looming construction and demolition waste, and over-exploitation of natural resources persists. However, efforts to encourage its use has resulted in proportionate mixes (of recycled with conventional aggregates) coupled with stringent compressive strength requirements (Gonçalves & Brito, 2010; Katz, 2003).

The use of quality recycled aggregates for structural concrete cannot be overemphasized since similar demands are required compared to conventional structural concrete to meet the strength and durability properties of concrete. Though quality recycled aggregates are recommended for structural concrete per the Japanese Standard, JIS A 5021, research to support that the bond between recycled structural concrete and rebar is adequate and conform to the current code provision to develop the required stress in the rebars is nonexistence.

## **1.2 Steel-concrete bond**

The rebar-concrete interface which acts as a medium of force transfer thus dictating the reinforced concrete performance is attributed to the anchorage of the rebars in the concrete, and its adequacy is achieved through several factors such as increased bond length, increased cover, and installing stirrups (transverse reinforcement) among others, which can increase the stress in the rebar to yield. Several tests have also demonstrated that brittle bond failures in structures could take place before steel yields (ACI Committee 408, 2003), and hence it is paramount to address the question of bond when rebars are anchored in recycled structural concrete.

### **1.3 Research objectives and scope**

This study presented will help to increase the use of quality recycled aggregate in structural concrete, which in turn would add to the range of alternatives of utilizing recycled aggregates in promoting the construction industry sustainability objectives.

This study aims at the following:

- a. Understanding the bond behaviour between quality recycled structural concrete and steel rebars and
- b. Use the obtained results to propose design recommendations in structural concrete elements made of quality recycled concrete.

In order to achieve the set objectives, the following parameters will be studied:

- The effect of cover on the bond
- The effect of bond length on bond
- The effect of bar size on bond
- The effect of bar position on bond
- The effect of transverse reinforcement on bond

### **1.4 Thesis methodology and organization**

This thesis has been organized into seven chapters and shown in Figure 1.1 including this Chapter.

In Chapter 2, the author reviews the available literature on the study of bond between RCA and deformed rebars with emphasis on the test methods employed by various researchers while

pointing out the sources of RCA and RFA (quality of recycled aggregates used), proportions of aggregates used, and the conclusion drawn based on the test method used. It also reviews the state of the art in producing quality recycled aggregates with emphasis on its use in concrete.

In Chapter 3, the proposed test method was detailed and discussed as per ASTM A944-09 together with the presentation of a summary of the experimental matrix.

Chapter 4, discusses the test results from the context of the effect of the five studied variables (cover, bond length, bar size, transverse reinforcement, and bar position) critical to propose design recommendations.

Chapter 5 compares the test results with five descriptive and five design equations from the literature. It evaluates the models therein based on the experimental test results. The chapter also uses the results and demonstrates with ANOVA and regression analysis and proposes a new empirical model similar to the descriptive equation of Orangun, Jirsa, & Breen, (1975). It further compares the results from other experimental data using only 100% RCA and discusses the ANOVA and regression results. The chapter further compares the test results with the ACI 408 database to qualitatively assess its good fit with conventional concrete mixes.

Finally, Chapter 6 presents the summary of the study including its novelty, recommendations for future research, and the limitations in this research.

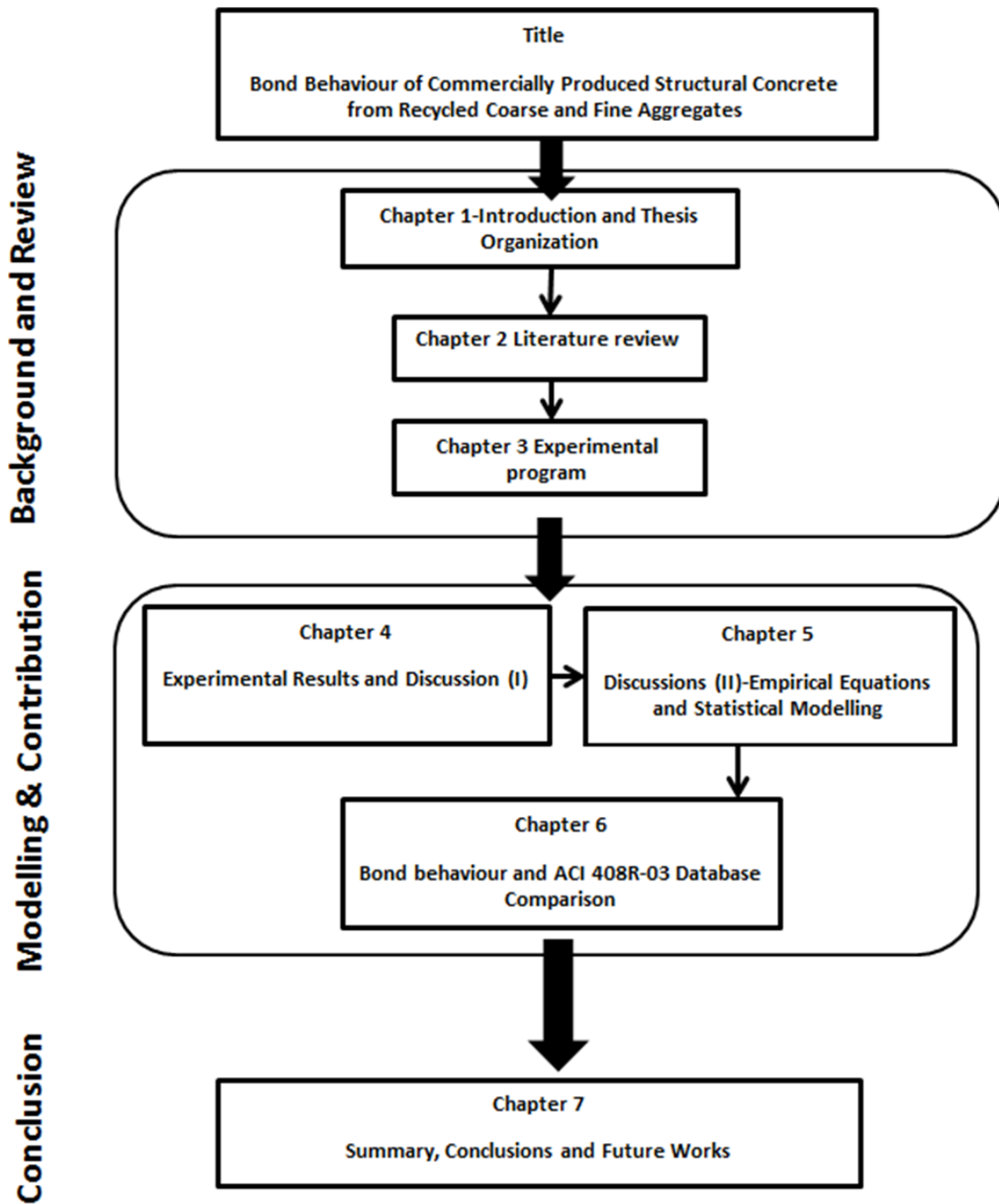


Figure 1.1 Thesis Organization

## CHAPTER 2: LITERATURE REVIEW

### 2.1 Concrete-steel bond

#### 2.1.1 Mechanics of bond

The bond between concrete and steel rebars plays a significant role in the mechanical performance and deformation of structures. When two or more materials co-join to form a unit, the dissimilar materials (in this case, concrete and steel) at their interfaces tend to form a structural bond. Bond also can be thought of as the shearing force between a bar and the surrounding concrete or the transfer mechanism between the bar and the concrete. In reinforced concrete, the force transfer is by three forces, adhesion forces, frictional forces, and mechanical interlocking forces as illustrated in Figure 2.1

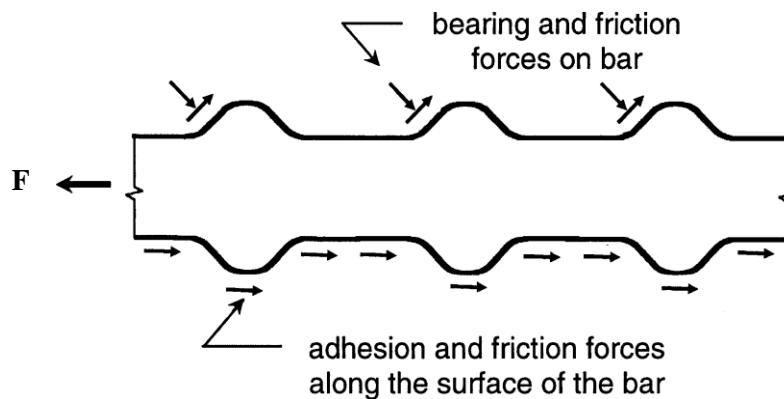


Figure 2.1 Bond forces along rebar, adapted (ACI Committee 408, 2003)

When a tensile force  $F$  is applied on a rebar as in Figure 2.1, the bond adhesion forces are lost first, which leaves the frictional forces and the mechanical interlocking forces to transfer the tensile forces. When the rebar is further tensioned, the frictional forces along the rebar are also lost quickly, leaving behind only the mechanical interlocking forces from the ribs, which act

against the concrete surface. At this stage, the rebar slips at a micro-level, and the ribs begin to crush the concrete in front of them.

The mechanical interlocking forces consist of bearing and frictional forces along the rib surface which plays a significant role in the bond between the concrete and the rebar as shown in Figure 2.1. For conventional concrete, adhesion strengths were 2-4 MPa (280-600 psi) and 1.3-1.7 MPa (190-240 psi) for shear and tensile bond tests, respectively (Lutz & Gergely, 1967). It is also estimated from other research work, that the adhesion and frictional forces contribute about 18% of the total bond force while the remaining 82% is from the mechanical interlocking forces (Xing, Zhou, Wu, & Liu, 2015). These lower metrics for the adhesion and frictional forces, emphasizes the importance of the mechanical interlocking through the design of the ribs as critical and rehashes the earlier studies by Wernisch, (1937) and subsequently by Clark, (1949).

### ***2.1.2 Bond failure modes***

There are two types of bond failure modes a) pullout failure and b) splitting failure. The pullout failure is best described as brittle whereas the splitting failure mode as ductile (ACI Committee 408, 2003).

### ***2.1.3 Factors affecting bond***

A myriad of factors affects the bond between concrete and steel rebars and has been reviewed extensively in ACI Committee 408, (2003) where the influencing variables are presented in a summary in Table 2.1 to show both the primary and secondary factors affecting bond. The primary factors have been quantified and culminated into the development length equation found in ACI 318, (2011) and the Canadian Standards Association, (2004). An in-depth review can be found in sections 2.3, 2.4, and 2.5 in this Chapter.

Table 2.1 Factors affecting bond characteristics between concrete and rebar

	<b>Concrete properties</b>	<b>Structural characteristics</b>	<b>Bar properties</b>
<b>Primary factors</b>	Compressive strength	Concrete cover	Bar size
	Aggregates type/quality	Bar spacing	Bar surface condition
		Bond length	Yield strength
		Transverse Reinforcement	
		Bar cast position	
<b>Secondary factors</b>	Fracture energy		Bar geometry
	Slump/Workability	Lap splices	Bar stress
	Admixtures		
	Degree of compaction		

#### **2.1.4 Bond test methods**

There are two broad categories of bond test methods, a) Pullout test method, and b) Beam bond testing found in the literature (see Figure 2.2). The test methods, in general, are governed by design principles that are underpinned by a mock-up representative of an actual field specimen. In the literature, bond testing was started by Abrams in 1913 using the pullout test and beam test method and thereafter, several other researchers have replicated similar specimens (Mains, 1951; Watsteint, 1941; Wernisch, 1937). In addition, a third test method known as the eccentric pullout test method was introduced by Perry and Thompson (1966) which did not gain popularity till to date. However, the ACI 408 versions of 1963 and 2003 have highlighted only the two-prong testing approach of using either a) the pullout test specimens and b) the beam test specimens to be used for bond testing (ACI Committee 408, 2003). The Committee further recommended that the pullout test specimens are not to be used since it does not mimic the

tensile stress state of concrete around the rebar in practice. The downside of the pullout test method is again enumerated in ACI 408-63 as:

- a. The pullout specimens give a reasonable measure of the anchorage bar length and vaguely represent what happens to the bond adjacent to any flexural crack in a beam.
- b. The surrounding concrete in compression adjacent to the rebar eliminates the transverse tension cracking compared to the beam specimens.

The different test specimens are schematically shown in Figure 2.2 (ACI Committee 408, 2003).

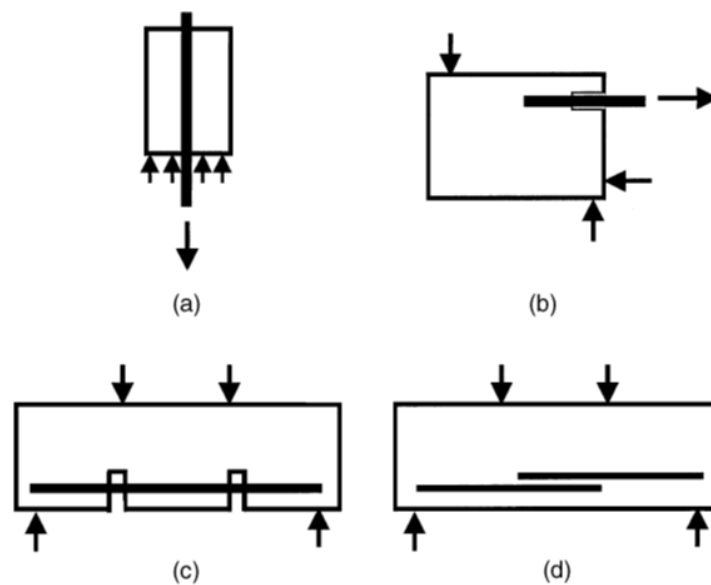


Figure 2.2 Bond test methods, adapted (ACI Committee 408, 2003)

### 2.1.5 Summary of research

The bond between recycled concrete and steel rebar is critical since the produced recycled concrete may not necessarily have an inherent concrete quality similar to the conventional concrete. In the summary of various studies listed in Appendix B and Appendix C, only eight

researchers were found in the literature using the beam test method whereas several others not listed apart from the 12 shown used pullout test method in determining the bond between recycled concrete and rebars ( Kim, Park, Jang, Jang, & Yun, 2017; Lima et al., 2013; Wang, 2019; Zhao, Lin, Wu, & Jin, 2013).

In addition, several researchers used coarse recycled aggregates generated from laboratory compared to commercially produced recycled aggregates whilst the use of recycled fine aggregates was generally excluded in the concrete mixes. Again, the bond parameters studied excluded critical variables such as the effect of transverse reinforcement, bar position, bond length, and bar size effect among others.

## **2.2 Recycled aggregates, recycled concrete production methods, and quality**

Concrete in its raw form is a composite material consisting of coarse aggregates and mortar (a mixture of fine aggregates, cement, and water) and in some instances with added mineral or chemical admixtures. In the case of recycled concrete, the coarse and fine aggregates are obtained from demolished concrete which is crushed into similar conventional sizes as in natural aggregates and used as a replacement for the coarse and fine fractions in the concrete mix. The wet and hardened properties of concrete are an antecedent to the final performance of any structural concrete members. Notable among them are the compressive strength, density, slump, water absorption, splitting tensile strength, flexural strength, modulus of elasticity, and the durability properties.

The use of recycled aggregates in concrete instead of natural aggregates in concrete structures requires similar properties. These have been critically demonstrated and reviewed in several studies (Behera, et al., 2014; Lotfy & Al-Fayez, 2015; McNeil & Kang, 2013; Sagoe-

Crentsil, Brown, & Taylor, 2001; Xiao, Li, Tam, & Li, 2014). A summary/overview of these cited studies and reviews shows that recycled concrete generally has a reduced compressive strength, concrete density, modulus of elasticity, durability, splitting tensile strength, and flexural strength, whereas its water absorption generally increases. On the other hand, comparable or other enhanced properties can be found in some studies with an emphasis of using quality recycled aggregates or by adding fibers, silica fume or other mineral and chemical admixtures to the concrete mix (Guo et al., 2018; Senaratne, Lambrousis, Mirza, Tam, & Kang, 2017).

Alternatively, the mixing of recycled concrete in order to obtain similar properties as conventional concrete has been studied beyond the conventional mixing methods, and may produce good quality recycled concrete (see **section 2.2.3**). Other studies beyond the mixing methodology are the use of improved recycling methods to obtain different grades and quality of recycled aggregates (see **section 2.2.2**).

### ***2.2.1 Recycled aggregates and recycled concrete***

The ACI E701 defines recycled aggregates as a process involving breaking of old concrete (typically pavement or structures), removing the reinforcement where applicable, and crushing the resulting material to a specified size and gradation (ACI Committee 701, 2016). It further states that though 100% recycled coarse aggregates may be used, up to 20% recycled fine aggregates in combination with natural fines are recommended to be used in concrete. However, the quality compliance and testing of both the recycled aggregates and concrete is a prerequisite (Behera et al., 2014; Evangelista, 2013; McNeil & Kang, 2013)

### ***2.2.2 Successful recycling aggregates production methodologies***

ACI E701 report, ACI Committee 701, (2016), cites that recycled aggregates “may be of better quality than natural aggregates” and hence the obtained form through processing is critical in determining the quality. In practice, conventional crushers are used to produce recycled aggregates and these processes and methodologies are applicable for recycled aggregate recovery which is increasingly becoming scientific and well documented. In addition, there are several methods and new approaches which have proven to yield quality recycled coarse and fine aggregates, and are enumerated below:

- a. Repeated crushing and screening (ACI Committee 555R-01, 2002; Dosho, 2007; Huda & Alam, 2014; Silva, Brito, & Dhir, 2017)
- b. High media separation (HMS) using magnetite solution (Kang & Kee, 2017)
- c. A novel dry classification (ADR) obtained by using mechanical separation and densities of the aggregates. (Lotfi, Eggimann, Wagner, Mróz, & Deja, 2015)
- d. ‘BauCycle’ process developed by Franhouver Research Institute, used to obtain quality recycled fines up to 1mm and based on using physical properties such as color and chemical composition (Agg-Net, 2018).
- e. Wet screening of recycled fines (ACI Committee 555R-01, 2002).
- f. Graded quality of aggregates based on repeated recycling processes for structural and non-structural applications per specifications of JIS A 5021, 5022 5023 (Noguchi, 2010)

In general, recycled aggregates obtained after applying innovative processing still has residual mortar (which is less dense) clinging to the original natural aggregates and can affect the physical and mechanical properties of the recycled aggregates and the resulting concrete.

### ***2.2.3 Successful recycled concrete production methodologies***

The concrete properties are a critical success factor because it is the single most important material which acts as a bonding agent around the rebar. Some known successful mixing methods to produce quality recycled concrete are the Equivalent Mortar Volume (EMV), Two-Stage Mixing Approach (TSMA) and Densified Mixture Design Algorithm (DMDA), which have been demonstrated in experiments (Fathifazl et al., 2009; Tam, Tam, & Wang, 2007; Tu, Chen, & Hwang, 2006).

### ***2.2.4 Quality and durability of recycled concrete***

The quality and durability of recycled concrete are of concern since the attached mortar which sticks on the recycled aggregates is generally reported to be detrimental to the aggregates or concretes' physical and mechanical properties. Despite these reported detriments, improved quality and durability of recycled aggregates and concrete (especially obtained through quality processing) has been demonstrated in research (Behera et al., 2014; Lotfy & Al-Fayez, 2015; Sagoe-Crentsil et al., 2001; Silva et al., 2017; Xiao et al., 2014). In another study by Matias, Brito, Rosa, & Pedro, (2014), it was demonstrated that using superplasticizers with RCA improved the durability and it was reasoned that the use of superplasticizers can address the durability defects in RCA including reduced carbonation and chloride ion resistance. The research by Matias et al., (2014) further asserted that the use of 100% RCA reduces the slump and the reduced slump however may help with improving the bonding of rebars.

As listed in Table 2.1, compressive strength and aggregate type & quality are among the primary factors influencing the bond between concrete and the steel rebar. These two will be discussed in the context of previous works undertaken by other researchers and the test methods

used. In addition, the use of recycled aggregates for concrete is gradually being admitted into standards and practice guidelines, and an overview summary can be found in the literature (CSA A23.1, 2014; Gonçalves & Brito, 2010; Marco, 2015; McNeil & Kang, 2013).

Recycled concrete has been described as “potentially inferior” and thus its mechanical properties vary widely (Behera et al., 2014). In various studies, the compressive strengths are reported to be generally lower based on the proportional content of RCA used (Behera et al., 2014; McNeil & Kang, 2013). The reported reduction in compressive strength ranged from 12% to as high as 76% and has been attributed to the presence of the porous mortar attached to the recycled aggregates (Behera et al., 2014).

On the contrary, similar or marginal reduction in strength may be obtained when a prescribed mix design methodology is adopted. These include proportionate mixes of recycled aggregates of say 30%, or reducing the water/cement content, selecting a quality source of recycled concrete, or adopting a modified mixing approach (Behera et al., 2014). New research suggests that improving the microstructure of recycled aggregates can produce high-performance concrete of 97 MPa (Pedro, Guedes, De-Brito, & Evangelista, 2019). In support of this research, an earlier work by Manzi, Mazzotti, & Bignozzi, (2013) argued that properly sorting the particle sizes of both RCA and RFA can result in a high compressive strength, complemented by good engineering properties such as flexural strength, elastic modulus, density, and water absorption.

Though several reported studies have used recycled coarse aggregates in combination with natural fine aggregates for recycled structural concrete, other researchers have used recycled fines as a replacement where a similar range of reduction or improved compressive strengths has been concluded (Evangelista, 2013; Pedro, Brito, & Evangelista, 2017). The foregoing is an

indication that the source and quality of the recycled aggregates are extremely crucial to forming a critical mass for recycled structural concrete applications.

## **2.3 Concrete properties affecting bond**

### ***2.3.1 Effect of compressive strength on bond***

As demonstrated in the preceding section on the divergent performance of compressive strength, opposing findings are also reported on bond strength performance using recycled concrete (Behera et al., 2014). With regards to improved bond, the causes were the addition of fly ash in the concrete mixes, increased internal curing effect from recycled aggregates due to additional hydration of cement paste and improved pore structure formation through new and secondary C–S–H gel formations (Behera et al., 2014). It is worth noting that the reported and tested effects used the pullout test method compared to the other bond testing methods. In addition and from Appendix B (showing the list of pullout tests and summary of bond effect), several researchers reported similar bond strength to conventional concrete mix even though there was reduced compressive strength while using high proportions up to 100% RCA. On the contrary, reduced bond strength which was attributed to reduced tensile strength, and increased normalized bond strength with the increase of RCA up to 100% RCA was also reported (Huang & Wang, 2011; Prince & Singh, 2014). Similar contrary findings are also shown in Appendix C (list of bond tests using beam specimens with summary conclusions of bond effect).

### ***2.3.2 Effect of concrete density on bond***

No study was found in the literature investigating the bond development and its effect from the reduced density when using recycled concrete. However, it can generally be inferred from the several works listed in Appendix B that reduced densities as a result of increasing the RCA

proportions in the concrete mix did not affect the bond strength when using the pullout test method. However, in the work of Ajdukiewicz & Kliszczewicz, (2002) when using pullout test specimens, there was reported reduced wet concrete densities of about 5% when using RCA and RFA and concluded that there was a reduced bond strength by a maximum of 20%. Similarly, while using a modified mixing approach known as the equivalent mortar mix volume (EMV) and the beam end test method by Fathifazl et al., (2012), a reported 2% reduction in wet concrete density was obtained and concluded that similar bond strength was observed. However, with the conventional mixing approach, the bond strength could reduce up to a maximum of 18% due to the unaccounted presence of mortar. Thus accounting for the residual mortar through the proposed mixing method (EMV) is critical and helps address the bond strength reduction. The foregoing leaves a research gap in terms of the known lower densities of RCA and RFA due to the clinging mortar and its impact on bond properties. In addition, the reduced concrete density from recycled structural concrete may impact the structural performance and requires to be evaluated when recycled coarse and fine aggregates are combined.

### ***2.3.3 Effect of aggregates type on bond***

Aggregates for concrete are naturally occurring and require several blasting, crushing, and screening processes to enable grading into coarse (>5 mm) and fine (<5 mm) fractions before using them in concrete. A similar processing paradigm is needed to obtain recycled aggregates for concrete and would even be more difficult since the concrete rubbles would be from different sources and hence the aggregates obtained thereof. Studies contained in the ACI Committee 408, (2003) confirmed that using unconfined concrete from natural aggregates of basalt and limestone can have a 13% variation in bond force emanating from the concrete component, though both are natural aggregates of different densities. Few studies have been conducted identifying the type of

aggregates obtained as recycled (as they are usually heterogeneous) and secondly on the effect of aggregate type and used as recycled concrete on bond strength. The single study found was by Ajdukiewicz & Kliszczewicz, (2002), and demonstrated that aggregate origins of granite or basalt are advantageous for recycled concrete and can result in high performance recycled concrete (80MPa). However, no research was found while using recycled fines of different aggregate origins on the bond performance. Furthermore, the work of Kim, Sim, & Park, (2012) and Kim & Yun, (2014) included up to 60% RFA (of unstated aggregate origins) where there were contrary conclusions of 18% reduction and similar bond strength performance, respectively. Thus studies on bond demarcating the aggregate origins and the density effect can be helpful if the inherent natural aggregate origins and types are clearly classified, which is lacking in the literature.

## **2.4 Structural characteristics affecting bond**

The characteristics affecting the bond behavior are discussed in the literature for natural aggregate concrete including the cover, rebar spacing, bond length, transverse reinforcement and bar cast position (ACI Committee 408, 2003). The following sections are reviewed with respect to using recycled concrete as a material.

### ***2.4.1 Effect of concrete cover and bar spacing***

There are two types of concrete cover, side cover and bottom cover (shown in Figure 2.3), and the minimum of these two provides the critical stress path for surface crack propagation. Providing cover and spacing is fundamental in construction practice and helps in protecting the rebars from corrosion and allows the coarse aggregates in the concrete to freely flow around the rebars. Essentially, a reduced cover increases the probability of bond splitting failure, while

increasing the cover reduces the internal moment arm. In various researches using the pullout test method, (see Appendix B) there is no opportunity to practically vary the rebar cover since the rebars are placed centrally in the test specimens as shown earlier in Figure 2.2(a).

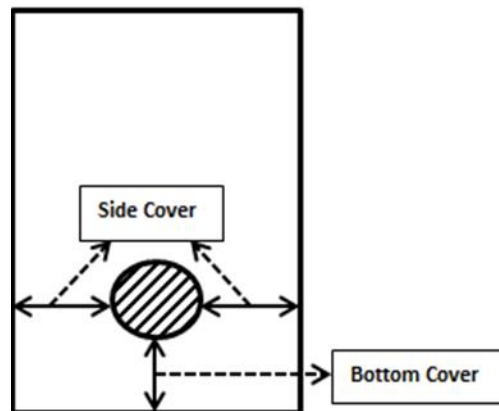


Figure 2.3 Crack propagation paths and concrete cover

Contrary to the pullout specimens, the beam-end and spliced beam specimens offer the opportunity to adjust and monitor the effect of rebar cover in an experimental test. While using the spliced beam test method, Robert, Gaurav, & Singh, (2017) tested using a 15 mm and 25 mm cover and proposed a descriptive equation taking into consideration the effect of the increase in cover. Robert et al., (2017) concluded that when using 100% RCA, the effect on bond strength is marginal and further suggested that when more experimental data become available, a robust descriptive equation can be proposed. This underscores the need for more research when using recycled structural concrete during bond testing.

#### ***2.4.2 Effect of bond length using recycled concrete***

Increasing the bond length increases the bond capacity (though not proportional) and hence more bond energy is required to form a crack and fail a member in bond (ACI Committee 408, 2003).

#### ***2.4.2.1 Effect of bond length on bond strength using pullout test method***

A large number of studies in the literature have examined the bond behaviour and performance of recycled structural concrete and deformed bars using the pullout test method (Ajdukiewicz & Kliszczewicz, 2002; Breccolotti & Materazzi, 2013; Choi & Kang, 2008; Duan, Kou, & Poon, 2013; Eiras-López, Seara-Paz, González-Fonteboa, Martínez-Abella, 2017; Seara-Paz, González-Fonteboa, Eiras-López, & Herrador, 2013; Xiao & Falkner, 2007).

The Table in Appendix B shows a summary of various experimental variables including bond length, bar sizes, aggregate proportions. The reported findings on the effect of bond in various studies were divergent in opinions. Several of the studies reported similar bond strengths between recycled concrete and deformed rebars, except (Ajdukiewicz & Kliszczewicz, 2002; Kim, Yun, Park, & Jang, 2015a; Kim et al., 2012) where a reduction in bond strength was reported. In these studies, the concrete mix included recycled fine aggregates and/or increased content of recycled coarse aggregates. In addition, several of the studies used aggregates crushed in the laboratory compared to using commercially processed or high-quality recycled aggregates. It is important to note that the work of Malešev, Radonjanin, & Marinković, (2010) though used laboratory-processed recycled aggregates, they concluded a similar bond strength for conventional and recycled concrete. They emphasized the use of quality recycled aggregates for concrete. Furthermore, Kim et al., (2015) concluded from their experiment that the bond strength, when compared with the code equations, were conservative and explained that the code equations were based on splice beam test specimen with low cover/diameter ratio and splitting tensile strength compared to pullout tests.

In Appendix B, except the study by Huang & Wang, (2011) and Guerra, Ceia, De Brito, & Júlio, (2014), all other studies focused on using a single bond length in addition to recycled aggregates from the laboratory and thus insufficient studies exist in varying the embedment lengths while observing the effect of the bond using quality recycled aggregates as concrete. However, the literature on using commercially produced recycled aggregates for structural concrete has yielded positive results, thus highlighting the need for producing quality controlled recycled aggregates for concrete (Brown & Taylor, 2001; Lotfy & Al-fayez, 2015; Pedro et al., 2017).

#### ***2.4.2.2 Effect of bond strength on bond length using beam test method***

In comparison to the pullout test method, Appendix C shows a summary of the recommended beam test specimens (ACI Committee 408, 2003). It can be inferred that limited studies exist when comparing the beam test method and the pullout test method, to understand conclusively the bond between recycled structural concrete and rebar. Once again, most researchers used laboratory-processed/generated recycled concrete except Sadati, Arezoumandi, Khayat, & Volz, (2017) where the 50% RCA concrete was obtained and used from the industry. However, Hamad, Dawi, Daou, & Chehab, (2018) used a commercially produced RCA from laboratory concrete waste and concluded that the bond strength of RCA was (2 to 16)% greater than conventional concrete. It can also be noted from Appendix C that most of the researchers excluded the use of RFA from the concrete mix and maintained proportions of RCA up to 100%. Though rebar sizes and bond length were varied across individual studies in Appendix C, the effect of bond length change on bond strength prediction and capacity has not been adequately addressed except in the study by Butler, West, & Tighe, (2015). Though the study by Butler et al. (2015) reported a 21% reduction in bond strength, it was inconclusive on the effect of bond

length variation and its impact on design provisions such as in CSA A23.3 or ACI 318M-11. However, the study correlated the aggregate strength (ACV-aggregate crushing value) and the development length and concluded that a (50 to 60)% short in development length was observed. In comparison, there was reported reductions of 18-33% by Fathifazl et al., (2012) based on the conventional mixing methodology which was significant in relation to a marginal reduction of 4 and 10% by Pandurangan, Dayanithy, & Prakash, (2016) where the residual mortar removed by acid or mechanical means was only 2 and 5%, respectively.

#### ***2.4.3 Effect of transverse reinforcement***

Transverse reinforcement generally helps reduce splitting cracks and increases the bond strength as the transverse rebars intercept the crack propagation while providing additional confinement around the tensile rebars. Due to this, the transverse reinforcement may convert splitting failure to pullout failure or flexural failure (ACI Committee 408, 2003).

Many researchers conducted bond tests on recycled concrete; however, none investigated the effect of transverse reinforcement on the bond behavior of recycled concrete. However, testing by Pandurangan et al., (2016), used the RILEM RC5 hinge beam test method on bond, the test bars are encased in stirrups within the bonded length. The effect of transverse reinforcement was not considered in this experiment and such a study is needed when considering the bond between recycled structural concrete and deformed rebars.

#### ***2.4.4 Effect of bar cast position (top location)***

Several research studies have been conducted showing the significant reduction of bond strength when rebar positions have more than 300 mm of concrete underneath, dating to the work

of Abrams in 1913 and led to its incorporation in ACI 318-1951 code (ACI Committee 408, 2003; Jeanty, Mitchell, & Mirza, 1988).

The North American codes on reinforced concrete structures, CSA A23.3 and ACI 318, has proposed that rebars positioned with 300 mm of concrete below the bottom cast have lower bond strength when conventional structural concrete is used. The reason for the reduced bond strength is that the top bars have bleeding concrete water and trapped air around them, due to bleeding, settlement, and segregation resulting in a lower contact area between the concrete and rebar (ACI Committee 408, 2003). In the same technical report, similar bond strengths of bottom-placed and top-placed rebars were also reported, though the rebars were placed above 300mm.

However, while using 150 mm square pullout specimens with high-quality RCA and RFA, top rebars located at 300 mm and 775 mm, were not significantly affected when a maximum of 60% RFA was used (Kim, Yun, Park, & Jang, 2015b). Equally worth noting is the work by Sadati et al., (2017), when using spliced beams with 50% RCA and fly ash, where the rebars were located at about 400 mm; it was reported that there was “no sign of top-bar effect observed”. The researchers stated that the addition of air-entrained admixture to the concrete could be the cause of the similarity as it removes most of the voids around the top rebars as hypothesized. Though it is known that the use of RCA and RFA (which is a less dense material) has higher water absorption compared to NCA and NFA, its impact on the bond properties has not been studied extensively. The reason is that the high water absorption of the recycled aggregates may be responsible for absorbing the bleeding concrete and may be worth a hypothesis and a critical parameter to study during any experimental investigation. Thus, further work is needed to validate these research findings while using 100% quality commercially

processed recycled aggregate concrete compared to laboratory manufactured recycled aggregates concrete.

## **2.5 Bar properties affecting bond**

### ***2.5.1 Effect of bar size***

Researchers such as, Robert, Prince & Singh, (2013) in using the pullout test method with recycled concrete generated from the laboratory, they concluded that for design purposes when using bar sizes of 12, 16, 20 and 25 mm there was no bond strength effect, as major code provision (such as ACI 318-08, Australian AS3600 and the CEP-FIP Model code) comparisons were conservative. Thus, a research gap exists in studying the bar size effect if other test methods such as beam end or splice specimens were used. Research has shown that smaller bar sizes results in a larger bond stress and vice versa when larger rebars are used. The effect of bar size and the appropriate factors to quantify its bond effect when using natural aggregates are found in standards CSA A23.3 and ACI 318-11.

### ***2.5.2 Effect of rebar geometry (patterns)***

There are generally two types of rebar patterns (smooth and deformed) used in construction practice and guided by codes and standards. In the case of deformed rebars, several patterns have been examined and are reported to influence the measure of bond capacity (ACI Committee 408, 2003; Clark, 1949).

Rebars are expected to bond to the concrete and aid maintain the structural integrity while reducing the deformations/slips in a member. Several researchers have pointed different bar shapes or geometry (patterns) and its effect on bond performance. However, these have been

standardized in ASTM A615 to help unify various mill production variabilities. Apart from nominal rebar sizes, other parameters such as the rib height, rib angle, rib face angle, and relative rib area can be found to affect the bond strength when considering the interaction between concrete and rebar (ACI Committee 408, 2003).

In the studies summarized in Appendix B and Appendix C, all the researchers used deformed rebars except for Xiao & Falkner, (2007) where smooth rebars were used in pullout test and concluded that the bond strength between recycled concrete and smooth rebars reduced by 12% and 6% when 50% and 100% RCA was used, respectively. However, when the smooth rebars were compared with deformed rebars, a 100% increase was observed when using 100% RCA and thus confirming the improved bond performance when using deformed rebars. No study was found using recycled fines with smooth rebars and thus indicating a research gap if smooth rebars are to be used even for stirrups as recommended in the CSA A23.3.

### ***2.5.3 Effect of rebar surface coating***

Coated rebars are used in construction to protect the steel surface from corrosion which tends to reduce the tensile capacity of the rebars. The coated surface reduces the interface surface friction between the concrete and rebar. The commonly used coated rebars are galvanized and epoxy coated, and the ACI Committee 318, (2011) and CSA A23.3, (2014) requires an additional 20% of bonded length for epoxy coated, and an additional 50% of bonded length for both epoxy and galvanized rebars placed with a clear cover and clear spacing of less than  $3d_b$  and  $6d_b$  respectively.

In the case of using recycled aggregates for structural concretes no research findings were identified investigating the bond behavior with any coated rebars and would be worth investigating further.

## **2.6 Research needs**

The foregoing literature review (in sections 2.2 to 2.5) has identified missing gaps in various studies which include but not limited to:

1. Using commercially processed and quality recycled aggregates to produce concrete and to undertake bond testing since this would largely reflect the aggregate and concrete quality to the end-user in the construction industry.
2. The use of both recycled coarse and fine aggregates as structural concrete and its effect on bond
3. Using the appropriate beam test method to understand the bond between recycled concrete and deformed rebars.
4. Several test variables based on the literature have not been conclusively investigated. These variables are, cover and spacing, bond length, bar size, bar position/location, and transverse reinforcement) in a single study to comprehensively evaluate the effect of bond behavior when using structural concrete produced from quality recycled aggregates.
5. Bond testing of smooth and deformed rebars using epoxy coated and galvanized rebars using deformed or smooth rebars with quality recycled concrete from commercial or laboratory sources.

Thus, to address the large research gap and to unearth the effect of bond strength when considering:

- a. The use of commercially produced high quality recycled aggregates
- b. The use of both recycled coarse and fine aggregates as structural concrete
- c. The effect of bond and the impact of the variables identified when using 100%RCA and up to 100%RFA to help understand the need for structural detailing requirements, and
- d. Using a recommended beam test method to determine conclusively the bond strength.

This thesis experimental portion would consider investigating the bond behavior and bond strength addressing all the four missing gaps by using the appropriate beam specimens proposed in the (ACI Committee 408, 2003).

The study will help to understand the bond behavior, both qualitative and quantitative, and provide the needed design recommendations if needed.

## CHAPTER 3: EXPERIMENTAL METHODOLOGY

### 3.1 Test program

To adopt a concrete mix which would complement the full range of a “softer” concrete (processed recycled concrete with the maximum amount of voids) when using recycled concrete, five mixes comprising a control mix of natural coarse and fine aggregates and four other mixes had 100% recycled coarse aggregates where the recycled fines were substituted at 25%, 50%, 75% and 100% by weight.

The test program was designed to address the identified gaps in the literature. Variables include cover (25 mm and 40 mm), bond length (200 mm and 300 mm), bar size (15M=16 mm and 25M=25 mm), transverse reinforcement, and spacing (10M at 100 mm and 200 mm spacing, and rebar position-top and bottom). This resulted in seven specimen groups, (Group 1 to Group 7) and for five concrete mix proportions and two replicates, a total of 70 specimens were realized. The experimental test matrix for the considered variables is shown in Table 3.1 and indicates the group number, specimen label, mix proportions, and specimen details such as  $l_d/d_b$ ,  $c/d_b$ , stirrup spacing, and bar position. Two replicates were chosen to confirm the validity of the test results, which is similar to beam test replicates conducted by (Butler et al., 2015; Hamad et al., 2018; Robert et al., 2017).

The specimens were labeled as  $M_a-R_d-L_c-C_b-S_e-T$ , where M stands for the concrete mix and subscript “a” is the mix proportion number, R represents a letter for the reinforcement bar size and subscript “d” is the nominal bar diameter number, L represents a letter for bond length and subscript “c” is the bond length dimension in millimeters, C represents a letter for cover and

subscript “b” is the rebar cover dimension in millimeter, S represents the letter for the stirrups and subscript “e” is the stirrup spacing, and T is for the bar position at the top and more than 300mm of concrete beneath the rebar.

Table 3.1 Experimental test matrix

Specimen group#	Specimen name-label	Mix proportion	Bar dia ( $d_b$ )	Bond length ( $l_d$ )	$l_d/d_b$	cover(c)	$c/d_b$	Stirrup spacing	Bar position
G1	M1-R15-L200-C25	NCA+NFA=M0/0	M15	200	12.5	25	1.56	N/A	Bottom
G1	M2-R15-L200-C25	100RCA+25RFA=M25/75	M15	200	12.5	25	1.56	N/A	Bottom
G1	M3-R15-L200-C25	100RCA+50RFA=M50/50	M15	200	12.5	25	1.56	N/A	Bottom
G1	M4-R15-L200-C25	100RCA+75RFA=M75/25	M15	200	12.5	25	1.56	N/A	Bottom
G1	M5-R15-L200-C25	100RCA+100RFA=M100/100	M15	200	12.5	25	1.56	N/A	Bottom
G2	M1-R15-L200-C25-S1	NCA+NFA=M0/0	M15	200	12.5	25	1.56	100	Bottom
G2	M2-R15-L200-C25-S1	100RCA+25RFA=M25/75	M15	200	12.5	25	1.56	100	Bottom
G2	M3-R15-L200-C25-S1	100RCA+50RFA=M50/50	M15	200	12.5	25	1.56	100	Bottom
G2	M4-R15-L200-C25-S1	100RCA+75RFA=M75/25	M15	200	12.5	25	1.56	100	Bottom
G2	M5-R15-L200-C25-S1	100RCA+100RFA=M100/100	M15	200	12.5	25	1.56	100	Bottom
G3	M1-R15-L200-C40	NCA+NFA=M0/0	M15	200	12.5	40	2.5	N/A	Bottom
G3	M2-R15-L200-C40	100RCA+25RFA=M25/75	M15	200	12.5	40	2.5	N/A	Bottom
G3	M3-R15-L200-C40	100RCA+50RFA=M50/50	M15	200	12.5	40	2.5	N/A	Bottom
G3	M4-R15-L200-C40	100RCA+75RFA=M75/25	M15	200	12.5	40	2.5	N/A	Bottom
G3	M5-R15-L200-C40	100RCA+100RFA=M100/100	M15	200	12.5	40	2.5	N/A	Bottom
G4	M1-R15-L200-C25-S2	NCA+NFA=M0/0	M15	200	12.5	25	1.56	200	Bottom
G4	M2-R15-L200-C25-S2	100RCA+25RFA=M25/75	M15	200	12.5	25	1.56	200	Bottom
G4	M3-R15-L200-C25-S2	100RCA+50RFA=M50/50	M15	200	12.5	25	1.56	200	Bottom
G4	M4-R15-L200-C25-S2	100RCA+50RFA=M75/25	M15	200	12.5	25	1.56	200	Bottom
G4	M5-R15-L200-C25-S2	100RCA+100RFA=M100/100	M15	200	12.5	25	1.56	200	Bottom
G5	M1-R15-L300-C25	NCA+NFA=M0/0	M15	300	18.8	25	1.56	N/A	Bottom
G5	M2-R15-L300-C25	100RCA+25RFA=M25/75	M15	300	18.8	25	1.56	N/A	Bottom
G5	M3-R15-L300-C25	100RCA+50RFA=M50/50	M15	300	18.8	25	1.56	N/A	Bottom
G5	M4-R15-L300-C25	100RCA+75RFA=M75/25	M15	300	18.8	25	1.56	N/A	Bottom
G5	M5-R15-L300-C25	100RCA+100RFA=M100/100	M15	300	18.8	25	1.56	N/A	Bottom
G6	M1-R25-L300-C40	NCA+NFA=M0/0	M25	300	12	40	1.6	N/A	Bottom
G6	M2-R25-L300-C40	100RCA+25RFA=M25/75	M25	300	12	40	1.6	N/A	Bottom
G6	M3-R25-L300-C40	100RCA+50RFA=M50/50	M25	300	12	40	1.6	N/A	Bottom
G6	M4-R25-L300-C40	100RCA+75RFA=M75/25	M25	300	12	40	1.6	N/A	Bottom
G6	M5-R25-L300-C40	100RCA+100RFA=M100/100	M25	300	12	40	1.6	N/A	Bottom
G7	M1-R15-L200-C25-T	NCA+NFA=M0/0	M15	200	12.5	25	1.56	N/A	Top
G7	M2-R15-L200-C25-T	100RCA+25RFA=M25/75	M15	200	12.5	25	1.56	N/A	Top
G7	M3-R15-L200-C25-T	100RCA+50RFA=M50/50	M15	200	12.5	25	1.56	N/A	Top
G7	M4-R15-L200-C25-T	100RCA+75RFA=M75/25	M15	200	12.5	25	1.56	N/A	Top
G7	M5-R15-L200-C25-T	100RCA+100RFA=M100/100	M15	200	12.5	25	1.56	N/A	Top

Total # of specimens=5 concrete mix batches\*2 replicates (A&B) \*7specimen groups = **70 Specimens**

### 3.2 Test specimen

To mimic a realistic bond behaviour where the stress state around the concrete and test rebar are both in tension, a beam end specimen was selected for this study. This test specimen represents half of a full simply supported beam and is economical compared to a full splice or anchorage beam, and also the test set up is at only one end. The free body diagram with tension (T) and compression (C) forces of a half beam is shown in Figure 3.1.

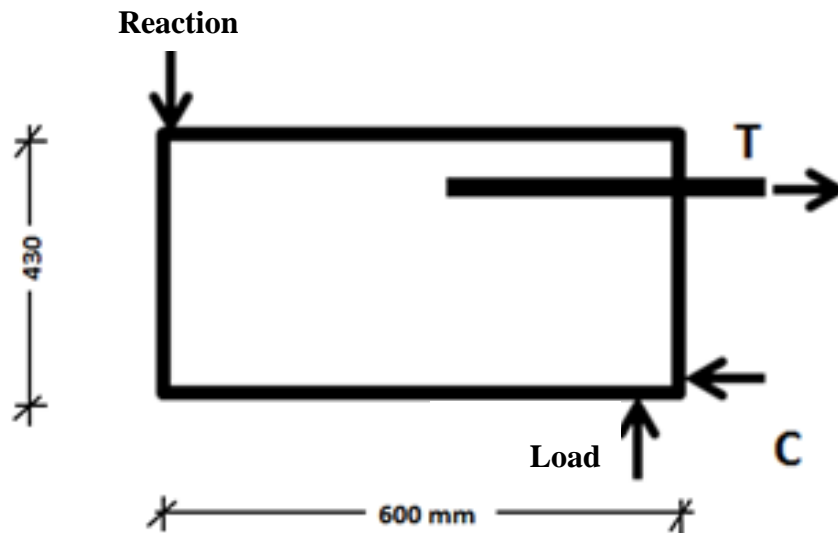


Figure 3.1 Free body diagram of the beam-end specimen

The proposed beam size used was (230\*430\*600)mm and conforms to (ASTM-A944, 2015) requirements. A 3-D test specimen model is shown in Figure 3.2.

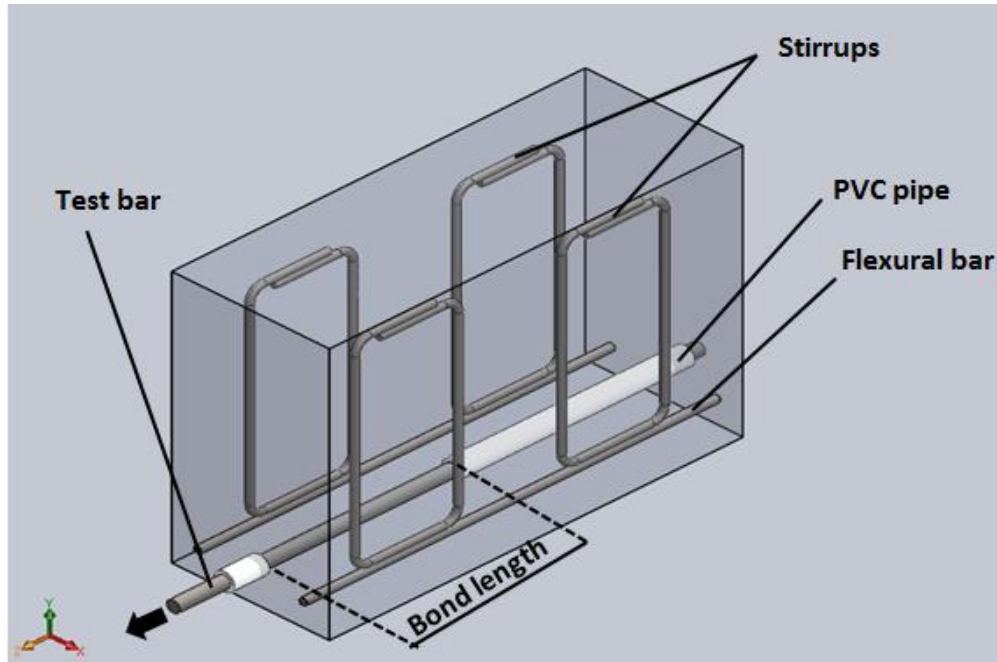


Figure 3.2 Three-D Model of test specimen adapted per ASTM A944-15

### 3.2.1 Structural details of test beam specimens

The reinforced structural beam drawings (longitudinal and cross-sections) of typical specimens are shown in Figure 3.3, Figure 3.4, Figure 3.5, and Figure 3.6. Figure 3.3 is typically for Groups 1, 3, 5, and 6, whereas Figure 3.4 and Figure 3.5 are for Groups 2 and 4, respectively, and Figure 3.6 is for Group 7 specimens only. Group 7 specimens are the inverted version of Group 1 where the flexural rebars and the test bars are at the top. For the test specimens with transverse reinforcement within the bond length, the reinforcement arrangements were adapted as per (Darwin & Graham, 1993).

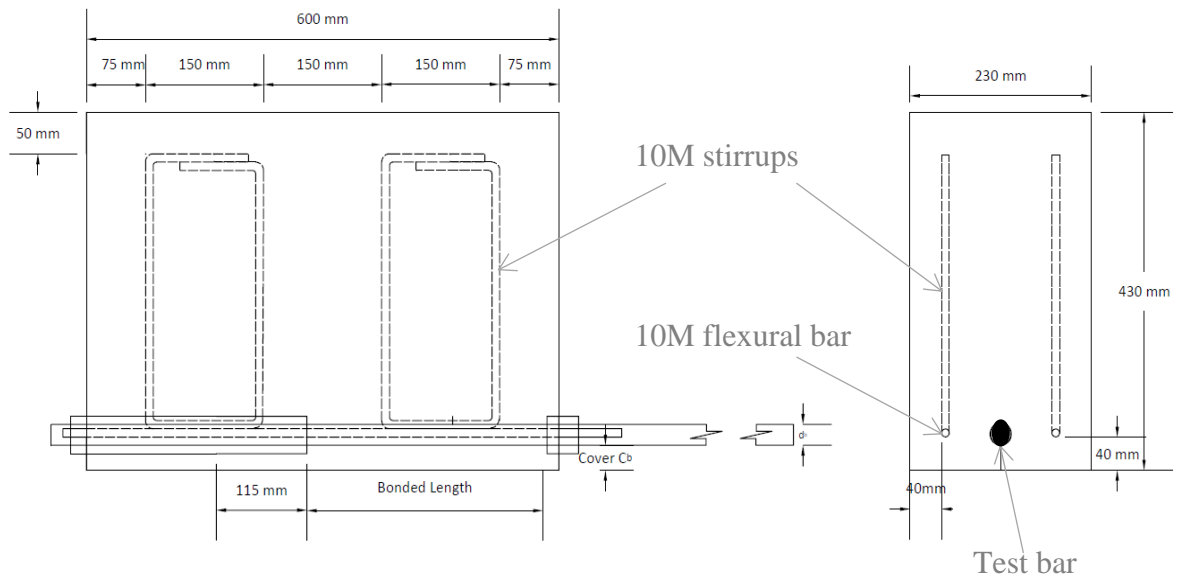


Figure 3.3 Longitudinal and cross-sectional details of typical test beam specimen (Group 1, 2, 5 and 6)

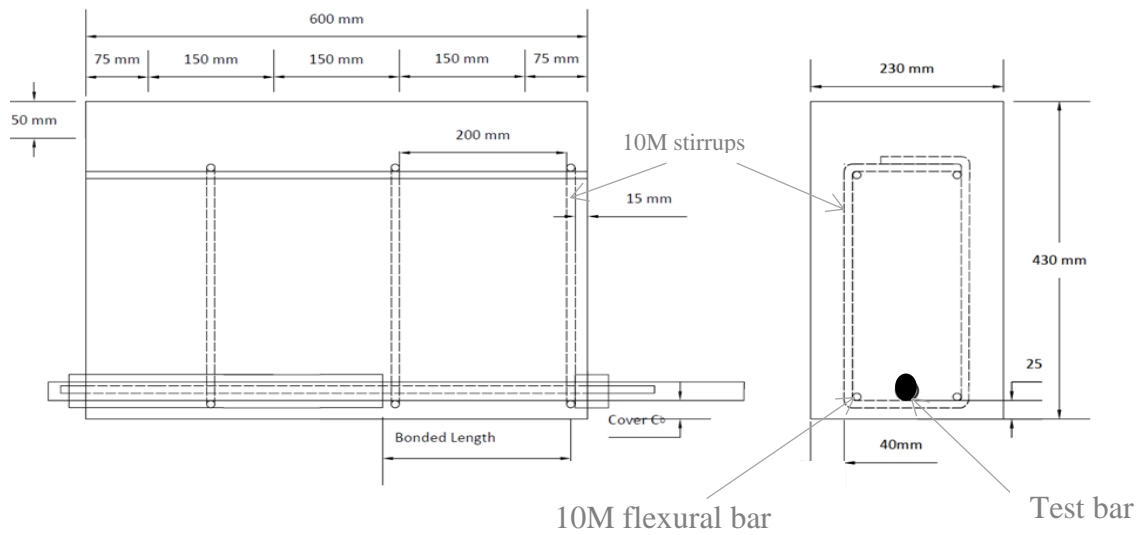


Figure 3.4 Modified test beam specimen with transverse reinforcement spacing at 200mm c/c (Group 2)

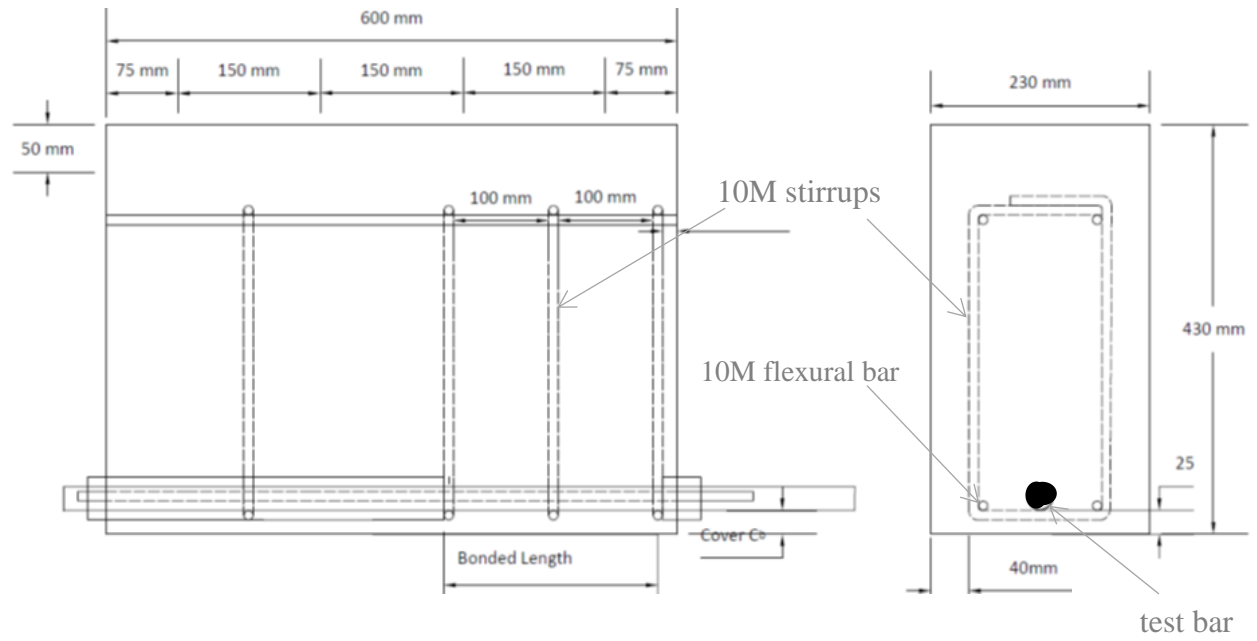


Figure 3.5 Modified test beam specimen with transverse reinforcement spacing at 100mm c/c (Group 4)

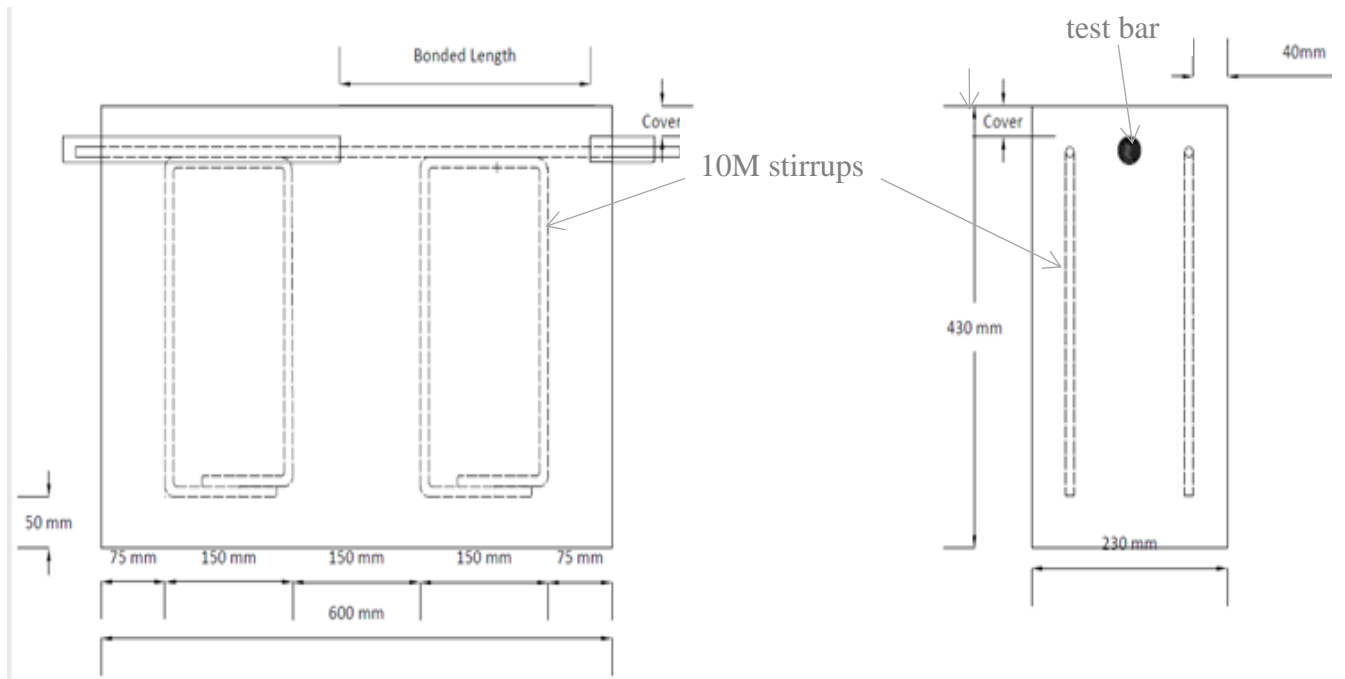


Figure 3.6 Longitudinal and cross-sectional details of typical top position test beam (Group 7)

In general, the specimen design for Groups # 1, 3, 5, 6, and 7 was similar except for Group 7 where the test bar and the flexural rebars were inverted upwards. Groups 1, 3, 5, 6, and 7 were provided with two straight flexural rebars of size 10M and four pieces of 10M closed loop stirrups. Two of the stirrups were spaced equally and tied to one of the flexural bars and placed on the side to the specimen formwork. The stirrups and the flexural bars were provided with a 30-40 mm cover (made from mortar blocks) and placed at the sides of the specimen to prevent the beam from failing in shear and also to prevent any steel stirrups within the bond length.

Groups # 2 and 4 specimen designs were adapted per Darwin & Graham, (1993). Four 10M flexural rebars (two each at the top and bottom) were used while the side 10M stirrups were now placed along the bond length and spaced at 200 mm for Group 2 and 100 mm for respectively. The stirrups and flexural rebars were shaped as per the ASTM A944 test standard. The test bars (made up of 15M or 25M) are also placed longitudinally and centrally within the specimen with enough length to run across the specimen. In this study, the test bars for each specimen was provided with an adequate length of about twice the length of the beam to aid in the pullout testing as well as measuring the slips at the loaded and unloaded ends. The bending schedule for the entire experimental program is shown in Appendix E.

### **3.3 Test specimen fabrication**

A total of 15 formworks were prepared where each had formwork was moulded for 5 beams. The test specimens were prepared in a set of 15 (5x3) for each batch of concrete pour which includes one dummy specimen to aid pre-testing, accurate experimental adjustments, and instrumentation. The forms were constructed using 19mm and 10mm thick plywood on the exterior and internal partitions, respectively as shown in Figure 3.7. They were screwed together

on all sides and as well as having an undercarriage for handling. Circular holes were drilled on the central portions of the 230mm width end of the formwork (on two sides) of each specimen portion in the formwork. This was to allow a two short 19mm (for 15M rebars) or 38mm (for 25M rebar) PVC pipe (serving as bond breakers) to be inserted on each opening side of the forms followed by the test bars positioning along the 600mm specimen length (Figure 3.7, Figure 3.8, and Figure 3.9)



Figure 3.7 Prepared set of formwork with partitions

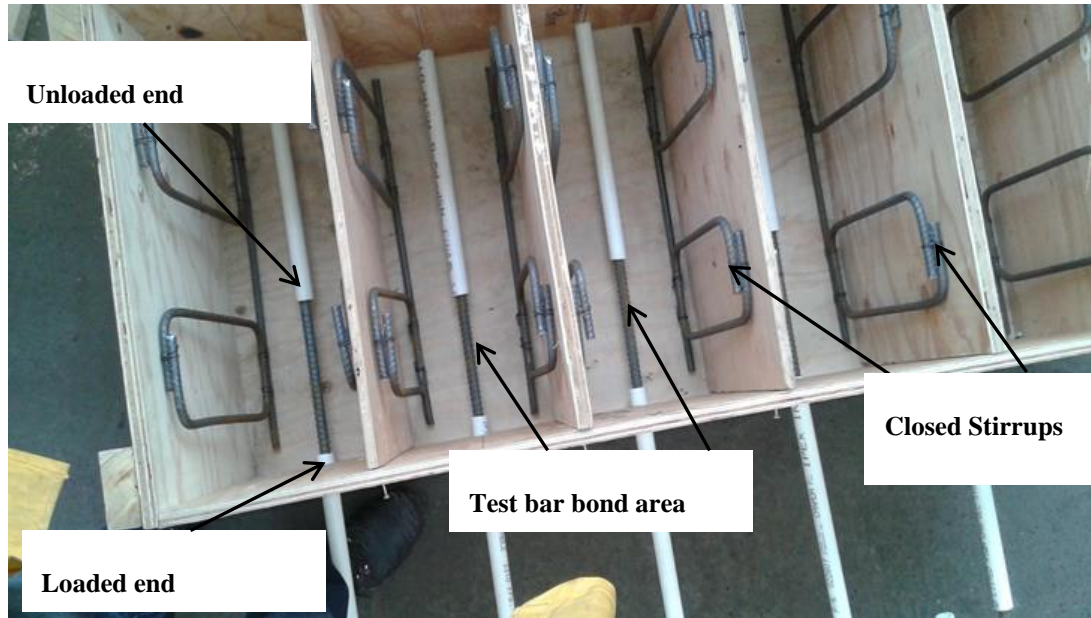


Figure 3.8 Formwork with flexural rebars and prepared stirrups



Figure 3.9 Completed formwork with test bars and embedded in PVC and sealed

The drilled holes and sizes were guided by the cover to be provided, whereas the PVC lengths were guided by the bond length to be provided per specimen (Figure 3.9). The internal

and external joints were sealed using a Wet Grab (“no more nail”) sealants to prevent mortar grout leakages during the concreting process and provide bond integrity. Prior to installing the test bars, the rebars were wire brushed and the midpoints of the bonded area were marked and grinded to degrease and expose the grey steel surface. The exposed steel surface was cleaned with Acetone to remove any steel grits and grease, before applying the strain gage (Appendix D).

Form oil was applied to the interior wood surfaces while protecting the exposed rebars (bonded length) with plastic covering, after which the 10M ready bent stirrups and the tied straight flexural rebars were placed in the forms before concrete pouring. Accessories such as 30-40mm mortar blocks were used as stirrups cover, binding wires to tie and hold in place the stirrups, and U-shaped hooks used as sling hooks on the specimen were used as appurtenances.

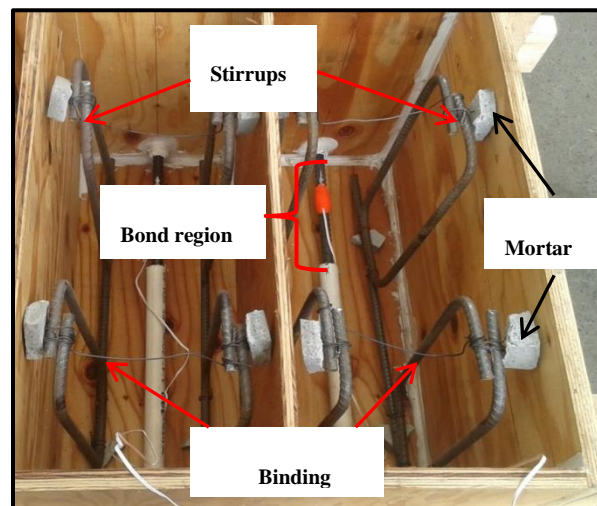


Figure 3.10 Completed interior test specimen with stirrups, flexural rebars and bond area

### 3.3.1 *Recycled concrete mixing and pouring of test specimens*

The concrete mix design was an in-house mix design batched by using the Marcotte batching plant software which synchronically compensates for any material weights in the final mix. The

batching plant has computer moisture probes at the inlet and controls the water addition based on inlet aggregates moisture content, and hence contributing to the overall concrete batch quality.

The specimens were cast in five different batches per mix design and each pour was done in two layers and vibrated internally using a poker vibrator after every layer. The exposed concrete face was finished off with a metal trowel and covered with burlap to prevent evaporation. The ASTM A944-15 standard recommends that the test beam shall be cured in the forms until a minimum strength of 14MPa is achieved. This was adhered to in addition to burlap covering and daily water ponding on the exposed specimen surfaces till finally the forms were removed after 90 days. Figure 3.11 shows the concrete pouring into the specimen forms, concrete vibration, and curing process during the specimen preparation at the batching plant.

Upon completion of the curing, the removed specimens from the formwork are stored in the laboratory for preparation prior to testing.



A-Concrete pour and vibration



B-Beam specimen curing

Figure 3.11 Concrete pour, vibration and beam specimen curing

### 3.3.2 Specimen placement procedure

The beam specimens were placed in five mix batches where each batch consisted of fourteen (14) specimens made up of a pair of companion specimens to form a pair of a group of specimens. Thus seven groups of specimens were made where each groups' specimens were of the same experimental setup details as shown in Table 3.1. The Group details are listed below for clarity.

- Group 1- Ten (10) beam specimens were made of 15M bar with 200mm bond length, 25mm cover, and labelled as “R15-L200-C25-B” for all the mixes used.
- Group 2- Ten (10) beam specimens were made of 15M bar with 200mm bond length, 25mm cover with 10M transverse reinforcement spaced at 100mm within the bonded length. It was labelled as “R15-L200-C25-B-S1” for all the mixes used.
- Group 3- Ten (10) beam specimens were made of 15M bar with 200mm bond length, 40 mm cover, and labelled as “R15-L200-C40-B” for all the mixes used.
- Group 4- Ten (10) beam specimens were made of 15M bar with 200mm bond length, 25mm cover with 10M transverse reinforcement spaced at 200mm within the bonded length. It was labelled “R15-L200-C25-B-S2” for all the mixes used.
- Group 5- Ten (10) beam specimens were made of 15M bar with 300mm bond length, 25mm cover, and labelled as “R15-L300-C25-B-S0” for all mixes used.
- Group 6- Ten (10) beam specimens were made of 25M bar with 300mm bond length, 40mm cover, and labelled as “R25-L300-C40-B” for all mixes used.

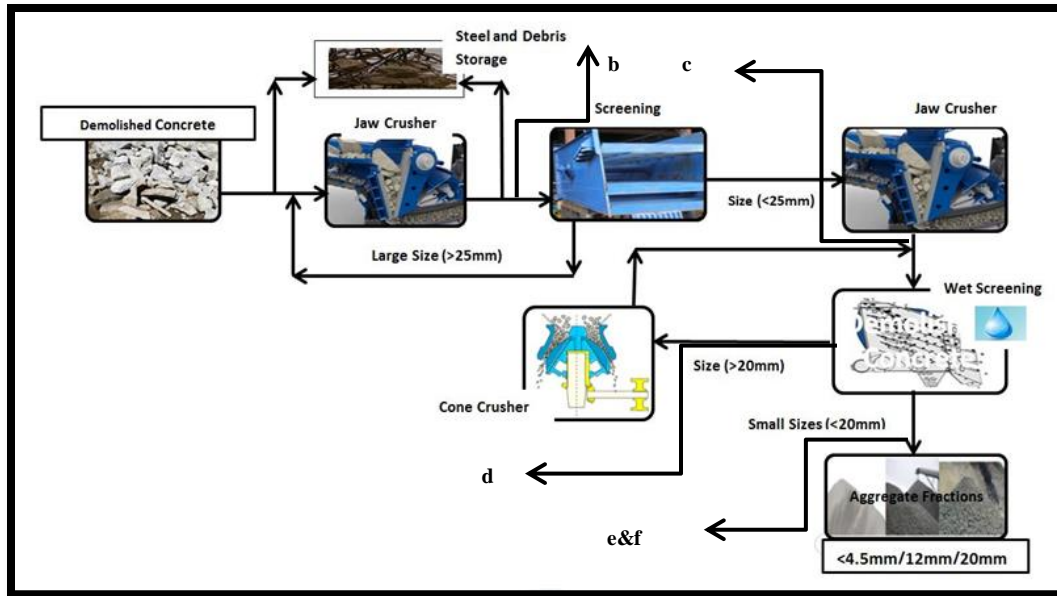
Group 7- Ten (10) beam specimens were made of 15M bars positioned above 300mm of the concrete specimen, 25mm cover, and labelled as “R15-L200-C25-T” for all the mixes used.

### **3.4 Materials and properties**

#### ***3.4.1 Recycled aggregates production for concrete***

In order to achieve the first two objectives, Lock Block Limited, a company with several years of concrete recycling, located in Vancouver, was identified to provide the needed quality recycled aggregates for the recycled concrete. The selected aggregates recycling processing and recycle concrete production plant was Lock-Block Ltd located in Vancouver. The processing used in this research is outlined in (ii)

Figure 3.12 to demonstrate the three-tiered crushing process of aggregates at the production plant. The process involves using two jaw crushers and one cone crusher coupled with extensive intermediary sieving, washing, and removal of organic and foreign materials such as debris, wood, and steel (with self-cleaning magnets). The aggregates' quality is improved further at storage since the two coarse fractions (20mm and 10mm clear) and the fine aggregates are separately stockpiled in open-air to avoid cross-contamination. The output aggregates are shown in Appendix F after each stage of processing. The aggregates processing is analogous to the processing method for obtaining coarse and fine recycled aggregates for structural concrete in Japan with stringent quality control (Dosho, 2007).



(i)



b

c

d

e

f

(ii)

Figure 3.12 Recycling aggregates processing (i) and stage products (ii) at Lock-Block Limited

Legend- a) Recycling production process b) Recycled products from the 1<sup>st</sup> Jaw Crusher; b) Recycled products from the 2<sup>nd</sup> Jaw Crusher; c) Recycled products from the Cone Crusher before wet screening; d) Coarse recycled aggregates from the wet screening deck; and e) Recycled fine aggregates from the wet screening deck

### 3.4.2 Aggregates properties

The aggregates after production undergo periodic testing by the British Columbia Provincial Metro Materials Testing Department. Critical physical testing of the aggregates material testing results as provided by Lock-Block Limited are presented in Table 3.2

Table 3.2 Raw aggregates' properties used in concrete production

Aggregates	Bulk Dry SG	Water Absorption (%)	Moisture Content(%)	Fineness Modulus
<b>Recycled</b>				
19mm Clear RCA	2.46	3.36	-	-
10mm Clear RCA	2.35	4.78	-	-
Combined 19 mm and 10 mm RCA	2.50	4.79	1.91	
5mm RFA	2.13	8.71	1.82	3.28
<b>Natural</b>				
Combined 19 mm and 10 mm NCA	2.70	0.70	1.31	
5mm NFA	2.59	1.90	1.70	3.12

### 3.4.3 Concrete and rebar materials

The concrete and rebar materials (cement, aggregates, admixture, and water) were all stored at the manufacturers recommended conditions. The cement was the general use (GU) type which is stored in silos and dispensed into batch mixes as described in section 3.6. The five concrete mix proportions are shown in Table 3.3 which includes the two types of medium-range admixtures (Eucon AEA-92S and Plastol 341) which was added to each batch. The compressive strengths were obtained through (110x230) mm drilled core specimen and the results are shown in Table 3.4. The drilled core cylinders were adapted using ASTM C42 test method which is a departure from regular concrete cylinders per ASTM A944 and storing them beside the test beams. The ASTM C42 cored cylinders were used since the test beams were prepared off the

laboratory testing site, 400km, at a commercial concrete recycling and production plant, and the likelihood of damaged cylinders during the transportation process. Drilled cores are accepted per ACI 318-11M clause 5.6.4 to confirm that the load-carrying capacities of concrete strengths are not significantly impaired. The measured slumps and air content are also similarly shown in Table 3.3. The 10M, 15M & 25M deformed bars in this study were all Grade 400 and conform to the CSA G30.18.09 with nominal yield strength of 420MPa. The mill production geometric data, chemical composition and the rebar design for test bars 15M and 25M are shown in Table 3.5, Table 3.6, and Figure 3.13 respectively.

The reinforcement rib designs were crescent-shaped on opposite sides of the rebars' barrel and merge towards the core. Nucour Steel Mill in Seattle through Harris Rebar, Vancouver supplied all the rebars. The chemical composition with heat numbers (SE17100669/ SE17100094 for 15M) and (SE17100848/SE17100843 for 25M) was used in this experiment.

Table 3.3 Mix design for 35 MPa structural concrete

Material	Control-M0/0	M25/75	M50/50	M25/75	M100/100
	Quantity (kg/m <sup>3</sup> )				
Recycled Fine Aggs, RFA	700	196	335	575	641
Natural Fine Aggs, NFA	0	592	335	188	0
Ratio by weight(RFA:NFA)	0:100	25:75	50:50	75:25	100:0
Coarse Aggregates (NCA/RCA)	1018	1023	1023	1023	1023
Cement (General Use)			375		
Cold Water			145 litres		
Admixture AEA 92S			12 ml/100kg		
Admixture 341 Mid-Range			350 ml/100kg		
Water/Cement			0.39		
Slump			80-100mm		
Air Content			4-5%		

Table 3.4 Compressive strength and density test results from cored specimens

	Control-M0/0	M25/75	M50/50	M25/75	M100/100
Hardened Density (kg/m <sup>3</sup> )	2406	2141	2121	2120	2150
Mean strength (MPa)	55.52	36.31	30.40	37.58	30.22
Std. Deviation	2.00	1.58	1.58	2.35	1.92

Table 3.5 Test bar engineering design data

Rebar Grade (Test Bars)	Rebar Designation	Bar Size (mm)	Rib Spacing (mm), Cs	Rib Height (mm)	Rib Angle, (β)	Nominal Weight (Kg/m)	Ultimate Tensile Strength (MPa)	Yield Strength (MPa)
CSA Gr 400W	M15	16	11.2	1.14	69°	1.57	633	432
CSA Gr 400W	M25	25	14.1	1.65	69°	3.93	671	471

Table 3.6 Test bar chemical composition in steel rebar

Elements in Steel	C	Mn	P	Si	Cu	Ni	Cr	V	Cb
Proportion (%) -15M, 25M	0.28	1.29	0.013	0.037	0.11	0.09	0.02	0.024	0.002

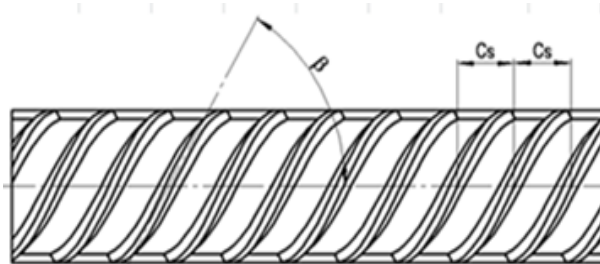


Figure 3.13 Test bar outline design configuration (provided by supplier Nucour Steel)

### 3.5 Instrumentation and data acquisition system

The experimental data acquisition and instrumentation comprised of using and National Instruments (NI) DAQ instrumentation set up (to obtain the test bar strain and slip) and an MTS actuator to obtain the applied load.

The NI-DAQ instrumentation set-up is shown in Figure 3.14 and connected to a computer display monitoring graphically the instantaneous test results. Two Linear Variable Differential Transformers, (LVDTs) were used to measure the test bar slips at the loaded and unloaded ends.

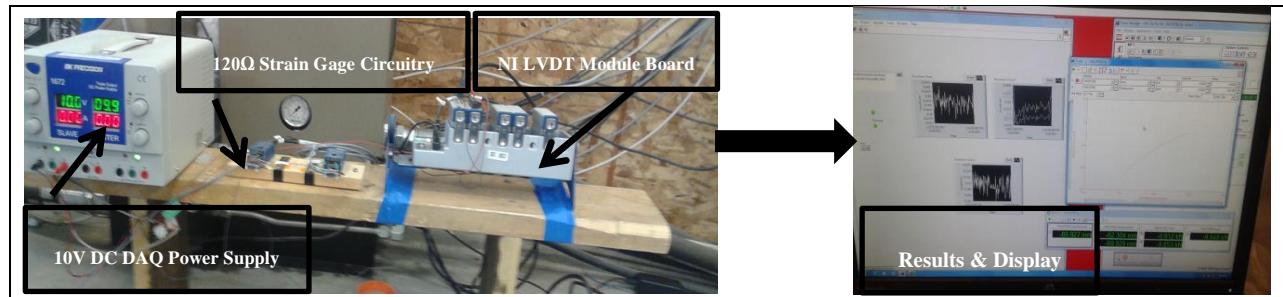


Figure 3.14 Test data acquisition (DAQ) set-up

The test bars were fitted with 5mm strain gages at their mid-points and were pretested for Ohmic values readings of  $120 \pm 5$  Ohms. Each specimen (placed in the test set up, discussed in section 3.6.1) with its attached LVDT's and strain gages was connected to the NI DAQ instrumentation system,  $120\Omega$  circuitry, and 10V DAQ power supply. The DAQ software sampling rate was set at 20 readings per second for both the LVDT and the strain gage. The set up was calibrated for each test specimen and the instrumentation allowed instant test data to be collected and stored in the computer, while the test was being concurrently undertaken. The test data was stored on a Notepad and retrieved, which was subsequently transferred into an excel spreadsheet for analysis upon test completion.

### 3.6 Specimen preparation for testing

After the 90-day period, the specimens were carefully de-molded from the formwork. All the bottom-placed test bar specimens were inverted carefully in position and the testing surface was sprayed with white paint within the bonded length area to help mark and map out any visible crack during the testing.

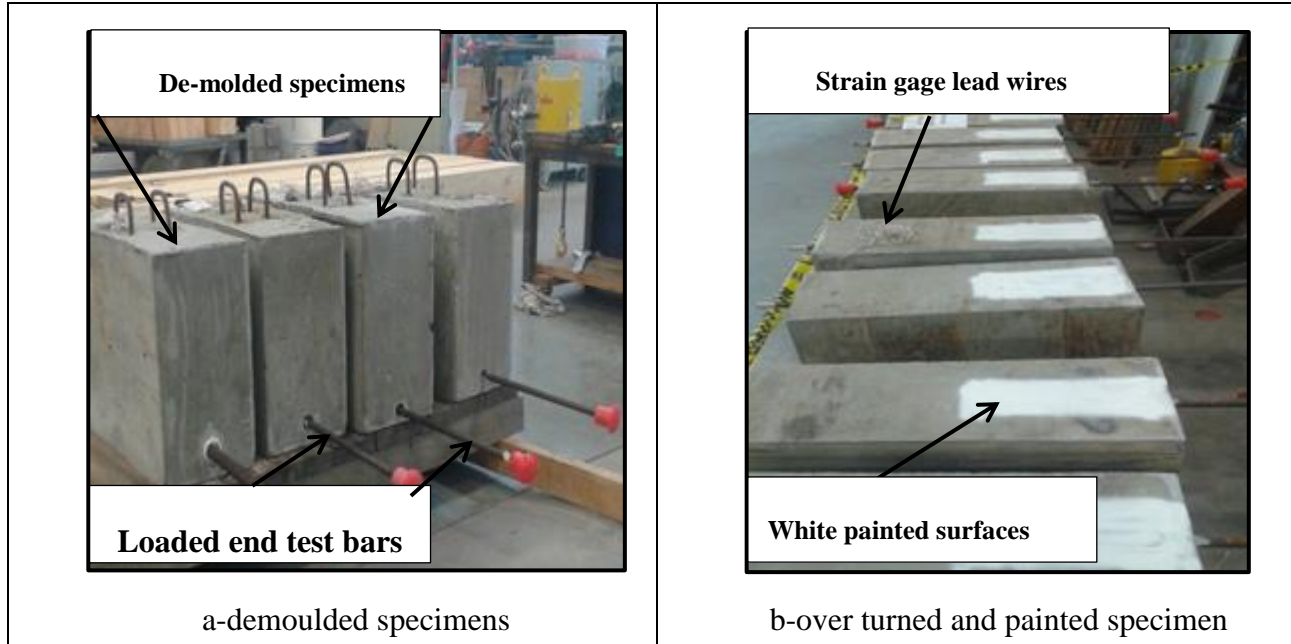


Figure 3.15 Removed specimens from formwork and prepared specimens for testing

Though the strain gage was installed and tested before concrete pouring it was again pretested to ensure that gage lead wires which were embedded in the concrete specimens were undamaged and continuous as shown in Figure 3.16.



Figure 3.16 Strain gage pretesting from specimen lead wires

### 3.6.1 Experimental Test Set-up

In order to accurately test the specimens and determine the pullout load, slip and strain, a test set up at the Applied Laboratory for Advanced Materials & Structures (ALAMS) was used where the MTS Actuator was attached to a reaction frame, and the specimen mounted in a steel braced frame attached to a floor mounted on a post-tensioned stanchion pedestal. A schematic outline of the test set-up is shown in Figure 3.17. The physical and completed test set up is similarly shown in Figure 3.18 whereas the mechanical mounting assembly details (at the loaded and unloaded ends) including the rebar coupler and LVDT installation are shown in

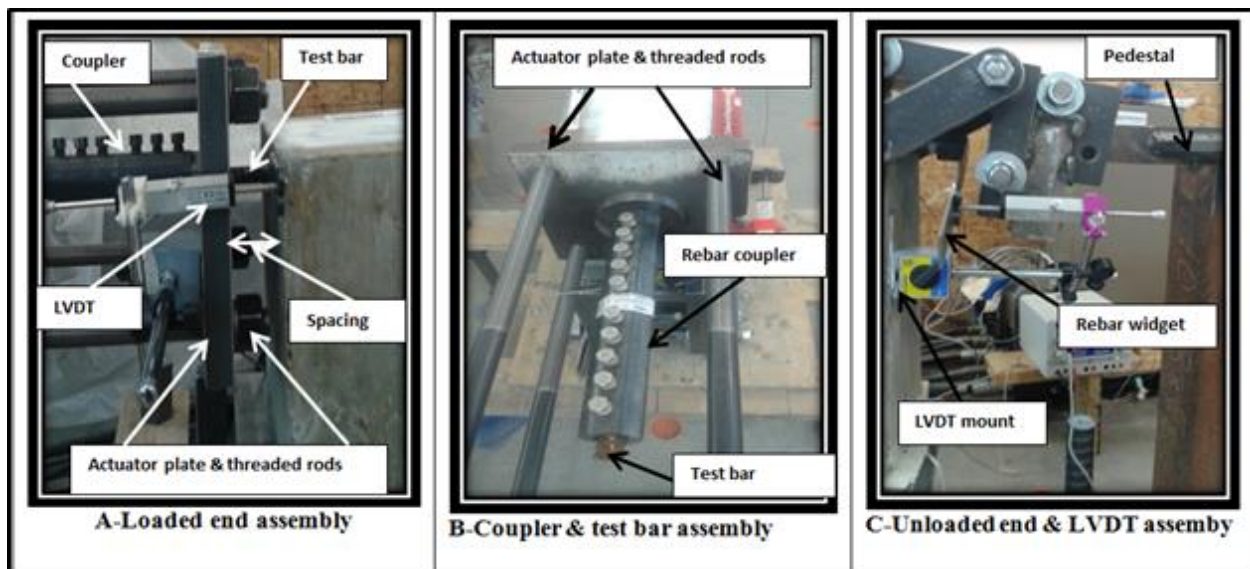


Figure 3.19. The actuator head which was fitted with long threaded rods and a hollow reaction plate made it feasible to fit the test bar with a coupler. The coupler was torqued to the test bar to prevent slip and fitted close to the specimen face and shown in Figure 3.19 A and B. The spacing between the test specimen and the actuator head was needed to ensure that the compression plate did not affect the tension stress field in the concrete during the pullout which is contrary to the

pullout test specimen shown in Figure 2.2 (a), where the compression plate is attached to the specimen face.

As a requirement in the ASTM A944, and shown in Figure 3.19 (A) and (C), the loaded and unloaded end slips were fitted with an LVDT to measure the relative slip and the rebar lengthening during the testing process. However, the unloaded end is less effective in transferring the bond forces (ACI Committee 408, 2003), but this unloaded end LVDT will be used to supplement the primary loaded end LVDT for data collection of the test bar slip.

### **3.7 Test Procedure**

The beam testing procedure was based on the test standard ASTM-A944, (2015) with modifications where needed as proposed by (ACI Committee 408, 2003). The specimens were tested using a monotonic axial load from a 250KN capacity MTS actuator having a 250mm stroke length. The relative slip of the rebars with respect to the surrounding concrete was measured using a Transtech LVDT which had a 100mm mechanical travel range. A displacement control load setting of 2.0mm/min was applied from the actuator until failure. Failure was defined as when the specimen lost 10% of its peak load capacity.

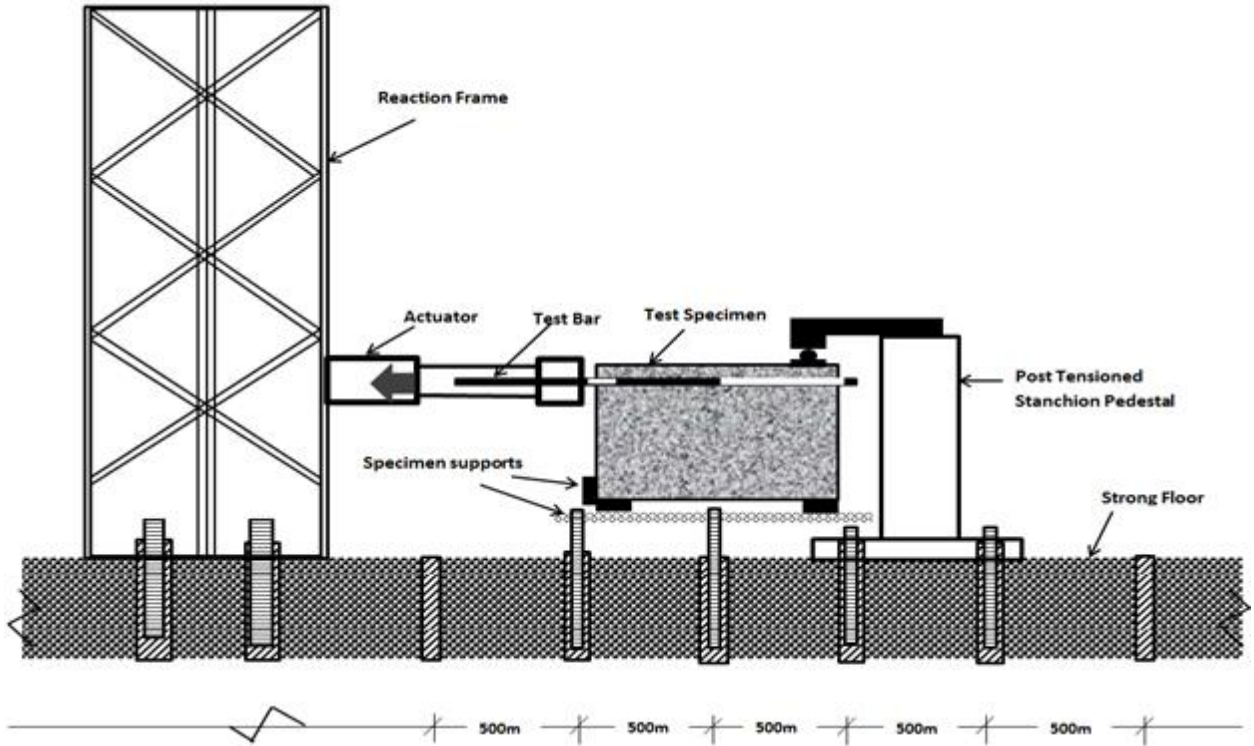


Figure 3.17 Schematic experimental test rig with a test beam

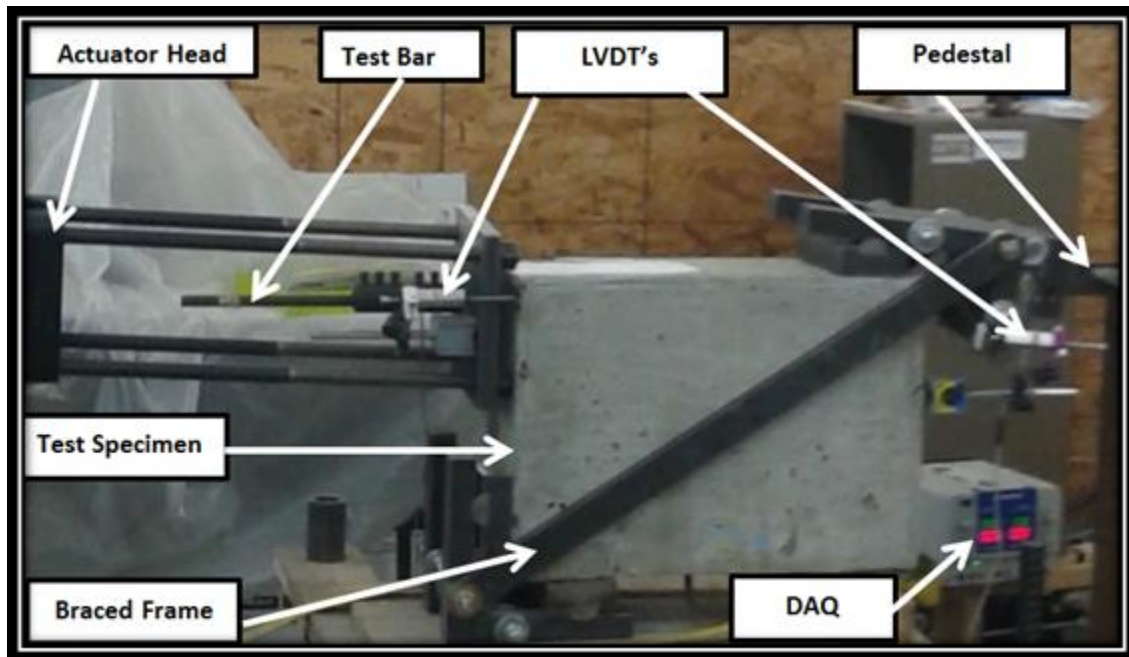


Figure 3.18 Detail experimental test set-up with of beam specimens

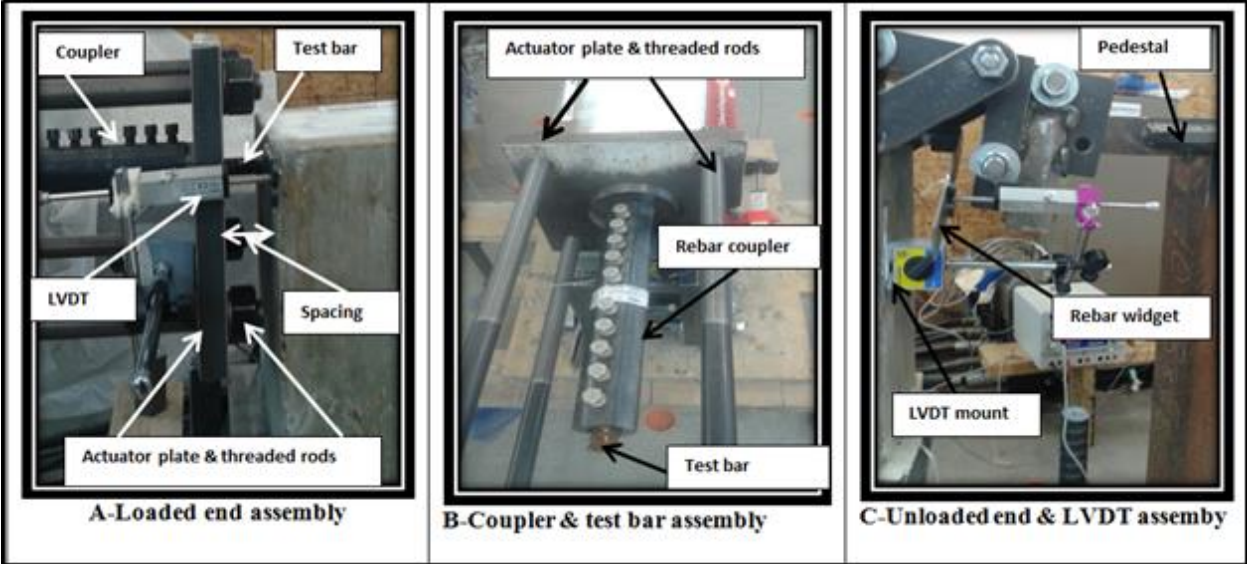


Figure 3.19 Experimental mechanical assemblies at the loaded and unloaded end

## CHAPTER 4: EXPERIMENTAL RESULTS AND DISCUSSION

### 4.1 General

The determination of the bond between concrete and rebars has been historically not only difficult but complex due to its nonlinearity and the variable nature of the interaction process as well as the stress distribution along the concrete and rebar interface. Given these setbacks, the ACI 408 Committee and the CEB task group VI reports have resorted to quantitatively determine the bond by consolidating a database for which bond experiments and performance are stored and updated for comparison. This chapter discusses the bond performance results of the seven groups of specimens with five different mixes (M0/0, M25/75 up to M100/100) shown in the test matrix in Table 3.1. Seventy beam end specimens were tested monotonically to determine the bond capacity after which the specimens were evaluated for the failure load, failure mode, relative slips of the rebar, crack widths, and patterns. The test results of the bond behavior and performance are presented, evaluated, and discussed with respect to the conventional concrete mix M0/0.

The discussion on the bond capacity and behavior will focus on the bond forces and normalized bond strengths, the load vs slip at the loaded and unloaded ends, as well as the failure mode crack widths and crack formations. The loads corresponding to the observed crack formation on the white painted beam surfaces were marked out manually as generally done in concrete beam load vs deflection testing (Malešev et al., 2010). Measured bar forces and strains will also be compared with theoretical values to ascertain the yielding of steel, and to determine the brittleness and behavior of beam specimens, whereas any experimental anomaly will also be reported and discussed. In general, the results and discussion will be centered on each of the

specimen groups (G1-Group 1 to G7-Group 7) and between (a pair or more) groups as indicated in the test matrix, to unearth the effect of the variable under study.

In this wake, and to orderly present and discuss the test results, the Table 4.1 shows how the groups and pairs of specimen mixes would be used to compare the effect of the variables and to enable easier comprehension and comparison of the bond performance while drawing conclusive evidence from the experiments therein.

Table 4.1 Specimens groups and pairings

<b>Groups and pairs</b>	<b>Test results to compare</b>
Group 1	Reference specimen (Control)
<i>Odd numbers</i>	
Groups 1 and 3	Effect of cover
Groups 1 and 5	Effect of bond length
Groups 1 and 7	Effect of bar position
<i>Even numbers</i>	
Groups 1 and 6	Effect of bar size
Groups 1 and 2	Effect of stirrups
Groups 2 and 4	Effect of stirrups spacing

The complete results are shown in Table 4.2. The average bond stress concept,  $\tau_b$  will be used in determining the bond strength for the two replicate samples and will be computed based on the average peak load, F and given by:

$$\tau_b = \frac{F}{\pi d_b l_d} \text{----- Equation (1)}$$

where  $d_b$  and  $l_d$  represent the bar diameter(mm) and bonded length (mm) respectively. Though there is a variation of force along the rebar, the use of average bond stress and behaviour of an embedded rebar in concrete has been demonstrated to produce similar quantitative results (ACI Committee 408, 2003; Kayali & Yeomans, 2000). The standard deviation and coefficient

Table 4.2 Experimental results and failure modes

Beam Group #	Specimen name	Mix name	Concrete Strength, $f'_c$ -MPa	Force KN	Mean	Std Dev	CoV	Ave. Bond Stress MPa	Mean Normalized Bond Str. MPa	Failure mode
Gp 1	M1-R15-L200-C25-A	M0/0	55.52	90.38	88.53	2.62	2.96%	8.81	1.18	Splitting
	M1-R15-L200-C25-B	M0/0	55.52	86.68						Splitting
	M2-R15-L200-C25-A	M25/75	36.31	72.21	75.26	4.31	5.72%	7.49	1.24	Splitting
	M2-R15-L200-C25-B	M25/75	36.31	78.3						Splitting
	M3-R15-L200-C25-A	M50/50	30.40	62.12	63.93	2.55	3.99%	6.36	1.15	Splitting
	M3-R15-L200-C25-B	M50/50	30.40	65.73						Splitting
	M4-R15-L200-C25-A	M75/25	37.58	74.06	71.96	2.98	4.14%	7.16	1.17	Splitting
	M4-R15-L200-C25-B	M75/25	37.58	69.85						Splitting
	M4-R15-L200-C25-A	M100/100	30.22	67.85	66.56	1.83	2.75%	6.62	1.20	Splitting
	M5-R15-L200-C25-B	M100/100	30.22	65.26						Splitting
Gp 2	M1-R15-L200-C25-S1-A	M0/0	55.52	119.04	112.17	9.72	8.66%	11.16	1.50	Splitting
	M1-R15-L200-C25-S2-B	M0/0	55.52	105.3						Splitting
	M2-R15-L200-C25-S1-A	M25/75	36.31	97.68	102.83	7.28	7.08%	10.23	1.70	Splitting
	M2-R15-L200-C25-S1-B	M25/75	36.31	107.97						Splitting
	M3-R15-L200-C25-S1-A	M50/50	30.40	102.8	102.65	0.21	0.21%	10.22	1.85	Splitting
	M3-R15-L200-C25-S1-B	M50/50	30.40	102.5						Splitting
	M4-R15-L200-C25-S1-A	M75/25	37.58	103.8	100.90	4.10	4.06%	10.04	1.64	Splitting
	M4-R15-L200-C25-S1-B	M75/25	37.58	98.00						Splitting
	M5-R15-L200-C25-S1-A	M100/100	30.22	103.19	107.05	5.46	5.10%	10.65	1.94	Splitting
	M5-R15-L200-C25-S1-B	M100/100	30.22	110.91						Splitting
Gp 3	M1-R15-L200-C40-A	M0/0	55.52	107.33	104.18	4.45	4.28%	10.37	1.39	Splitting
	M1-R15-L200-C40-B	M0/0	55.52	101.03						Splitting
	M2-R15-L200-C40-A	M25/75	36.31	80.53	79.53	1.42	1.79%	7.91	1.31	Splitting
	M2-R15-L200-C40-B	M25/75	36.31	78.52						Splitting
	M3-R15-L200-C40-A	M50/50	30.40	72.98	70.45	3.59	5.09%	7.01	1.27	Splitting
	M3-R15-L200-C40-B	M50/50	30.40	67.91						Splitting
	M4-R15-L200-C40-A	M75/25	37.58	80.23	80.41	0.25	0.32%	8.00	1.31	Splitting
	M4-R15-L200-C40-B	M75/25	37.58	80.59						Splitting
	M5-R15-L200-C40-A	M100/100	30.22	73.75	71.39	3.34	4.68%	7.10	1.29	Splitting
	M5-R15-L200-C40-B	M100/100	30.22	69.03						Splitting
Gp 4	M1-R15-L200-C25-S2-A	M0/0	55.52	120.42	120.42			11.98	1.61	Splitting
	M1-R15-L200-C25-S2-B	M0/0	55.52	124.7*						Rebar fracture
	M2-R15-L200-C25-S2-A	M25/75	36.31	104.21	102.24	2.79	2.72%	10.18	1.69	Splitting
	M2-R15-L200-C25-S2-B	M25/75	36.31	100.27						Splitting
	M3-R15-L200-C25-S2-A	M50/50	30.40	94.65	89.19	7.72	8.66%	8.88	1.61	Splitting
	M3-R15-L200-C25-S2-B	M50/50	30.40	83.73						Splitting

Beam Group #	Specimen name	Mix mane	Concrete Strength, $f'_c$ -MPa	Force KN	Mean	Std Dev	CoV	Ave. Bond Stress MPa	Ave. Normalized Bond Str. MPa	Failure mode
Gp 4 Cont'd	M4-R15-L200-C25-S2-A	M75/25	37.58	92.85	95.60	3.89	4.07%	9.51	1.55	Splitting
	M4-R15-L200-C25-S2-B	M75/25	37.58	98.35						Splitting
	M5-R15-L200-C25-S2-A	M100/100	30.22	99.22	100.67	2.05	2.04%	10.02	1.82	Splitting
	M5-R15-L200-C25-S2-B	M100/100	30.22	102.12						Splitting
Gp 5	M1-R15-L300-C25-A	M0/0	55.52	104.42	104.42	0.59	0.57%	6.93	0.93	Splitting
	M1-R15-L300-C25-B	M0/0	55.52	105.26						Splitting
	M2-R15-L300-C25-A	M25/75	36.31	90.3	95.79	7.76	8.11%	6.36	1.05	Splitting
	M2-R15-L300-C25-B	M25/75	36.31	101.28						Splitting
	M3-R15-L300-C25-A	M50/50	30.40	92.17	90.90	1.80	1.98%	6.03	1.09	Splitting
	M3-R15-L300-C25-B	M50/50	30.40	89.63						Splitting
	M4-R15-L300-C25-A	M75/25	37.58	95.07	94.48	0.83	0.88%	6.27	1.02	Splitting
	M4-R15-L300-C25-B	M75/25	37.58	93.89						Splitting
	M5-R15-L300-C25-A	M100/100	30.22	88.92	90.90	2.80	3.08%	6.03	1.10	Splitting
	M5-R15-L300-C25-B	M100/100	30.22	92.88						Splitting
Gp 6	M1-R25-L300-C40-A	M0/0	55.52	170.74	170.74	1.33	0.78%	7.25	0.97	Splitting
	M1-R25-L300-C40-B	M0/0	55.52	168.86						Splitting
	M2-R25-L300-C40-A	M25/75	36.31	146.64	150.28	5.14	3.42%	6.38	1.06	Splitting
	M2-R25-L300-C40-B	M25/75	36.31	153.91						Splitting
	M3-R25-L300-C40-A	M50/50	30.40	105.97	117.14	15.79	13.48%	4.97	0.90	Splitting
	M3-R25-L300-C40-B	M50/50	30.40	128.30						Splitting
	M4-R25-L300-C40-A	M75/25	37.58	135.3	133.42	2.64	1.98%	5.67	0.92	Splitting/Shear failure
	M4-R25-L300-C40-B	M75/25	37.58	131.55						Splitting
	M5-R25-L300-C40-A	M100/100	30.22	128.97	125.20	5.33	4.26%	5.32	0.97	Splitting
	M5-R25-L300-C40-A	M100/100	30.22	121.43						Splitting
Gp 7	M1-R15-L200-C25-T-A	M0/0	55.52	90.09	90.09	11.70	12.99%	8.97	1.20	Splitting
	M1-R15-L200-C25-T-B	M0/0	55.52	73.54						Splitting
	M2-R15-L200-C25-T-A	M25/75	36.31	76.46	82.23	8.15	9.92%	8.18	1.36	Splitting
	M2-R15-L200-C25-T-B	M25/75	36.31	87.99						Splitting
	M3-R15-L200-C25-T-A	M50/50	30.40	71.21	66.14	7.18	10.85%	6.58	1.19	Splitting
	M3-R15-L200-C25-T-B	M50/50	30.40	61.06						Splitting
	M4-R15-L200-C25-T-A	M75/25	37.58	65.84	67.03	1.68	2.51%	6.67	1.09	Splitting
	M4-R15-L200-C25-T-B	M75/25	37.58	68.22						Splitting
	M5-R15-L200-C25-T-A	M100/100	30.22	60.89	62.73	2.60	4.15%	6.24	1.14	Splitting
	M5-R15-L200-C25-T-B	M100/100	30.22	64.57						Splitting

of the variance of the experimental results are also computed. Equations 7.1 to 7.10 in Appendix G, shows several empirical formulas which have guided structural bond determination in various engineering applications.

## **4.2 Failure modes**

The failure modes of the test specimens as listed in Table 4.2 were the splitting mode of failure, and was predominant in all the specimen groups except for two specimens. The two specimens were M1-R15-L200-S2-B and M4-R25-L300-C40-A where the failures were rebar fracture and a combined shear/splitting respectively.

## **4.3 Effect of concrete cover on bond (Groups 1 and 3)**

As generally required, structural elements are provided with adequate cover to protect the reinforcement from corrosion and ensure that the internal moment due to tension and compression is not compromised. In the experiment, the cover of 25 mm (Group 1) was chosen to fit for internal members whereas a 40mm cover (Group 3) for external members also usually suffices.

### ***4.3.1 Effect of concrete cover on bond force (Groups 1 and 3)***

Figure 4.1 shows the bond force variation of the two groups of specimens compared with the control specimen of the conventional concrete mix. As observed, the average bond force for the recycled concrete mixes were lesser compared to the conventional concrete mix. The bond force varied from (15 to 28)% for conventional concrete and (23 to 32)% for recycled concrete mixes, when the cover was increased from 25mm to 40mm respectively. It can be deduced from the same figure that the marginal gain in bond force was of 5-10% for the companion recycled concrete specimens when the cover was increased, but for the conventional concrete specimens there was an increase of 17%. This marginal increase can be attributed to the increased mass of concrete around the rebar due to increased cover, though a significant increase of 60% cover amount (25mm to 40mm) was provided. Furthermore, the marginal increase shows that though

the crack path from the bar surface lengthened when the clear cover was 25mm to 40mm, the crack formation at the rebar and concrete interface and its propagation till failure is very minimal. This observation confirms the brittle nature of both conventional and recycled concrete mixes.

It was also observed in Figure 4.1 that the substitution of RFA with NFA did not significantly affect the bond strength in recycled concrete mixes since the M25/75 and M75/25 vis-à-vis M50/50 and M100/100 did not record a trending departure in strength. The variation in results shown in the same Figure 4.1 can be attributed to the differences in concrete strengths between conventional concrete (55MPa-M0/0) and the recycled concrete in this experiment (37MPa-M75/25) shown in Table 4.3.

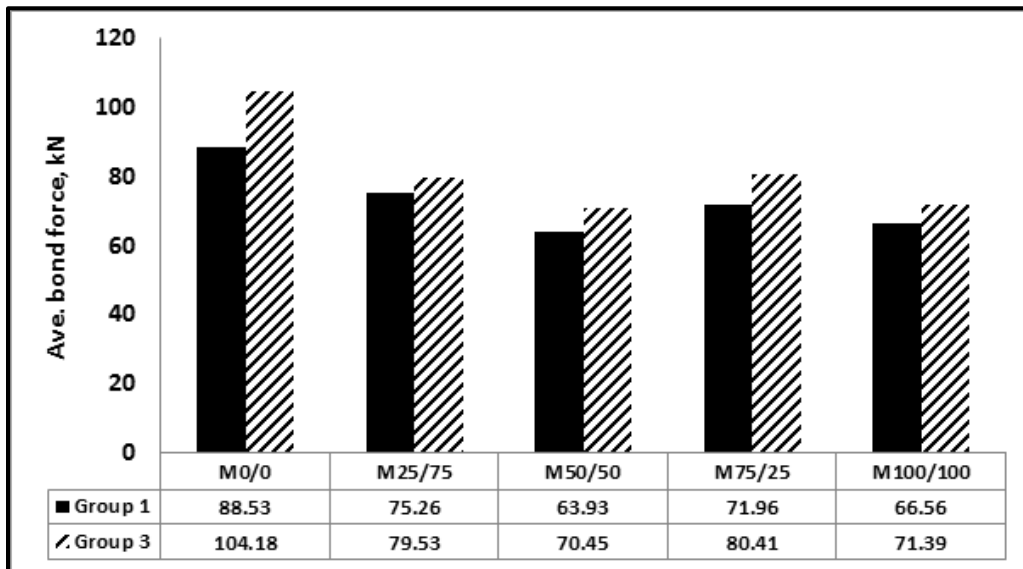


Figure 4.1 Effect of cover increase on the bond forces and mix variation

#### 4.3.2 Effect of concrete cover on normalized bond strength

Because of the variation in concrete strength across the test specimens, the average bond strength was calculated using equation (1), and the resulting data were normalized by  $\sqrt{f'_c}$ ,

thereby reducing the influence of compressive strength variation on the test results. Figure 4.2 shows the mean normalized bond strength data of the specimens.

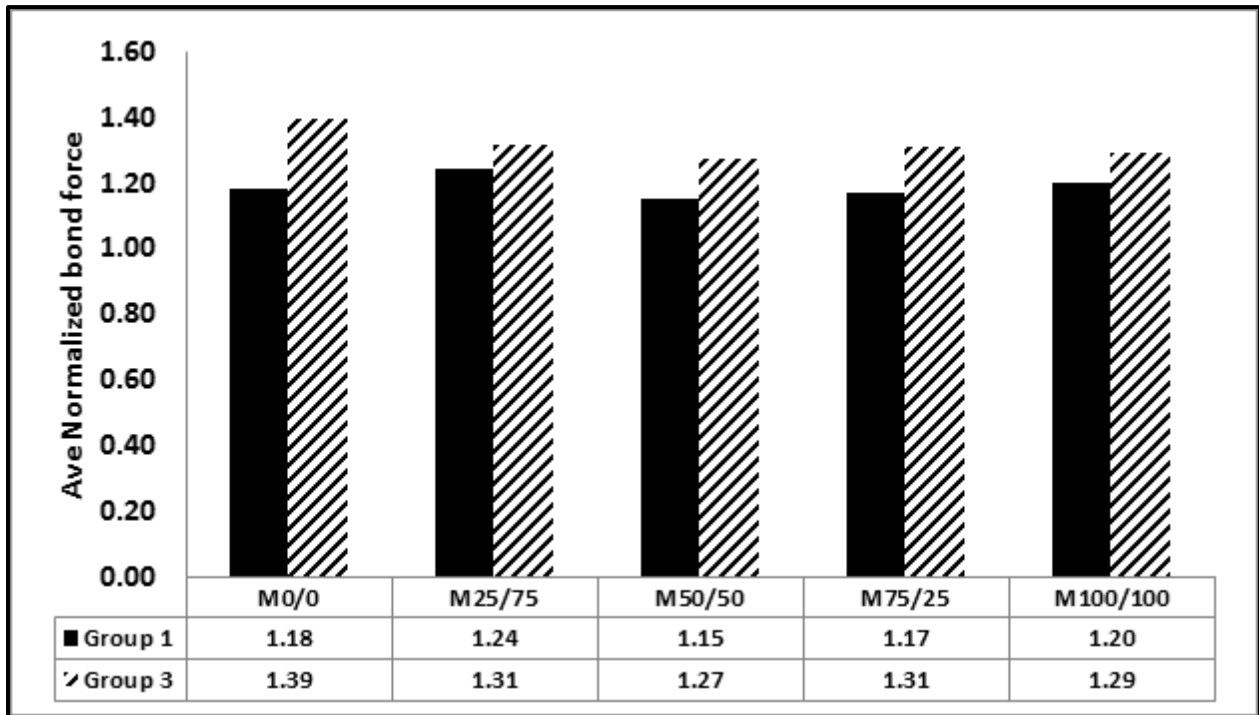


Figure 4.2 Effect of cover increase on normalized bond strength with square root function

The mean bond strength was normalized with the square root function ( $\sqrt{f'_c}$ ) as shown in Figure 4.2. It indicates that the cover size and variation of RFA in recycled concrete has a marginal effect on the normalized bond strength. When the recycled concrete mixes were compared with the conventional concrete, the normalized bond strength reduced by less than 3% for M50/50 and M75/25 whilst there was less than 5% increase for the M25/75 and M100/100. Table 4.3 summarizes the average percent variation of the normalized bond strength for the two groups of specimens when compared to the conventional concrete mix. The variation in bond

strength was (-3% to +5%) and (-6% to -9%) when the cover was 25mm and 40mm respectively across the recycled concrete specimens.

Table 4.3 Percent variation of normalized bond strength when cover increased

$f'_c$	<b>M0/0</b>	<b>M25/75</b>	<b>M50/50</b>	<b>M75/25</b>	<b>M100/100</b>
	55.52	36.32	30.39	37.59	30.22
<b>Group 1, cover=25mm</b>					
Sample A	1.21	1.19	1.12	1.20	1.23
Sample B	1.16	1.29	1.19	1.13	1.18
Average	1.18	1.24	1.15	1.17	1.20
% Difference in Ave.	-	+5.10%	-2.60%	-0.85%	+1.70%
<b>Group 3, cover=40mm</b>					
Sample A	1.43	1.33	1.32	1.30	1.34
Sample B	1.35	1.30	1.23	1.31	1.25
Average	1.39	1.31	1.27	1.31	1.29
% Difference in Ave.	-	-5.62%	-8.60%	-6.20%	-7.12%

The variations found were minimal (-9% to +5%) for the entire experimental setting compared to that reported by Butler, West, & Tighe, (2011), (-10% to -20%), though similar cover=30mm and  $f'_c=30\text{MPa}$  was used in a comparative beam experiment. The reduced variation could be due to the processing of aggregates and the quality of recycled concrete (commercial recycled aggregates), and hence using an improved quality recycled concrete source may help address any bond deficiencies and variations in bond strength.

Contrary to the work by Butler et al., (2015), where no relationship was found with the common root functions of ( $1/2$  and  $1/4$ ), a good correlation coefficient was observed using  $\sqrt[4]{f'_c}$  which supports some principal investigations found (ACI Committee 408, 2003; Canbay & Frosch, 2006). The graphical relationship is shown in Figure 4.3.

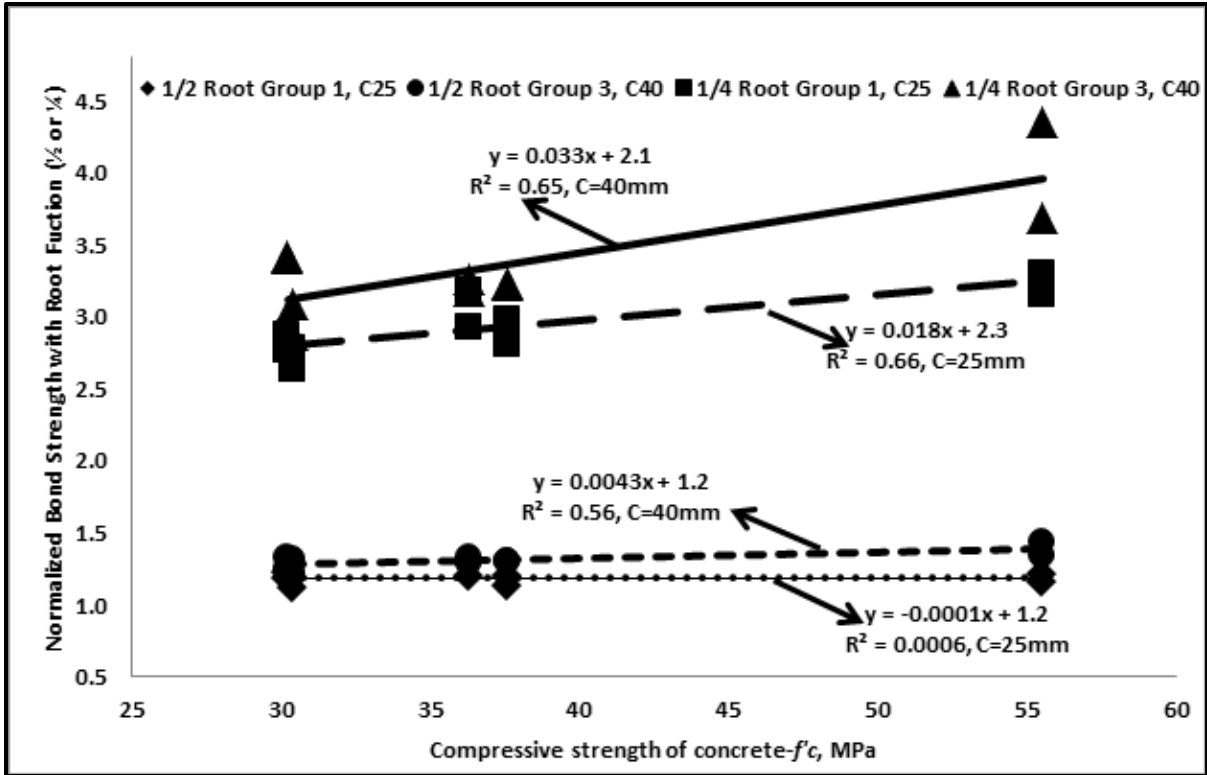


Figure 4.3 Normalized bond strength vs compressive strength with  $\frac{1}{2}$  and  $\frac{1}{4}$  roots

### 4.3.3 Effect of concrete cover on first crack load and load vs slip curves

In concrete structures, brittle failures are not preferred since it is important to maintain the structural integrity of every structural element. Though splitting failure behaviour is most preferred in a brittle concrete material, the crack formation and gradual crack propagation at the concrete surface is a good indication towards a final brittle behaviour when recycled structural concrete is used.

The load-slip curves shown in Figure 4.5 are indicative of the stiffnesses of the bond between concrete and deformed rebars. It can be observed from the graphical plots in Figure 4.5 (A to H) that M0/0 specimens were much stiffer with higher bond strength and greater slips than those of the recycled concrete mixes. The bond-slip curves generally showed no slip initially, followed by

a gradual slip of the rebar around the concrete, until it reaches the peak. The reported peak loads were comparable to those demonstrated by (Butler et al., 2015; Lin & Zhao, 2016; Pandurangan et al., 2016; Yang, Deng, & Ingham, 2016) when using either conventional and recycled concrete in beam test specimens. Though this experiment used commercially processed (quality RCA and RFA) in the concrete mixes, the comparable maximum loads show that there was no effect when compared to similar experiments while using NCA and NFA.

On the other hand, reported peak slips have varied considerably when using either recycled or conventional concrete test beam specimens as observed in the literature. Butler et al., (2011), showed a typical peak slip of 0.5mm for a cover of 30mm when using recycled concrete, whereas Pandurangan et al., (2016) reported the peak slip in the range of 0.55-1.44mm using recycled and conventional concrete with a cover of 10mm, and Darwin & Graham, (1993); Lin & Zhao, (2016) and Yang et al., (2016) reported a slip range of 4.2 to 5.0mm, 0.02 to 0.13mm and 1.25-2.50mm, respectively for only conventional concrete. These reported slips at the loaded ends are similar (0.2mm to 6.0mm) to the experimental results as shown in Table 4.4 and Figure 4.5 (A to H). Hence, it can be concluded that the bond-slip performance of recycled structural concrete is similar to conventional structural concrete. The similarity observed in this experiment can be attributed to the quality of the recycled coarse and fine aggregates, which contributed effectively to the mechanical interlocking mechanism between the rebar ribs and the surrounding recycled concrete.

In addition, as shown in Figure 4.4, it can be observed that the trend of the first crack load for the cover of 40mm is generally closer to the maximum splitting load than the case when the cover was 25mm. This occurrence is expected and conforms to the theoretical concept that increasing

the rebar cover is likely to cause a splitting failure accompanied by a pullout or a pure pullout failure, as observed in specimen M50/50-C40-A.

Table 4.4 Summary results of first crack load, maximum slip, and strain in test specimens

<b>Specimen Name and Label</b>	<b>First crack load, KN</b>	<b>Proportion for cracks,</b>	<b>Max. splitting load (KN)</b>	<b>Max loaded end slip (mm)</b>	<b>Max strain (micro-strain)</b>
<b>Group 1</b>					
M0/0-C25-A	43	48%	90.38	2.63	580
M0/0-C25-B	NV	N/A	86.68	0.20	SGD
M25/75-C25-A	35	48%	72.21	0.77	700
M25/75-C25-B	NV	N/A	78.30	-	SGD
M50/50-C25-A	36	58%	62.11	1.38	615
M50/50-C25-B	43	65%	65.73	0.28	2800
M75/25-C25-A	47	63%	74.06	0.78	2550
M75/25-C25-B	40	57%	69.72	1.30	1300
M100/100-C25-A	44	65%	67.85	1.58	515
M100/100-C25-B	45	72%	62.26	1.34	SGD
<b>Group 3</b>					
M0/0-C40-A	65	61%	107.30	5.12	750
M0/0-C40-B	87	86%	101.03	5.79	500
M25/75-C40-A	55	68%	80.53	-	SGD
M25/75-C40-B	55	70%	78.52	2.13	2220
M50/50-C40-A	70	96%	72.98	1.35	1640
M50/50-C40-B	60	88%	67.91	0.13*	500
M25/75-C40-A	71	88%	80.23	1.31	655
M25/75-C40-B	65	81%	80.59	1.87	2270
M100/100-C40-A	64	87%	73.25	0.60	1900
M100/100-C40-B	60	87%	69.03	0.89	1800

NV-Not visible (assumed same for companion specimen), N/A-Not applicable, SGD-Strain Gage Damaged, \*unloaded end-slip

Thus, a further increase in cover beyond say 50mm may have resulted in a pure pullout failure in the test specimens. The experimental crack formation and widths are similarly shown in Appendix I and Appendix K for Groups 1 and 3 respectively.

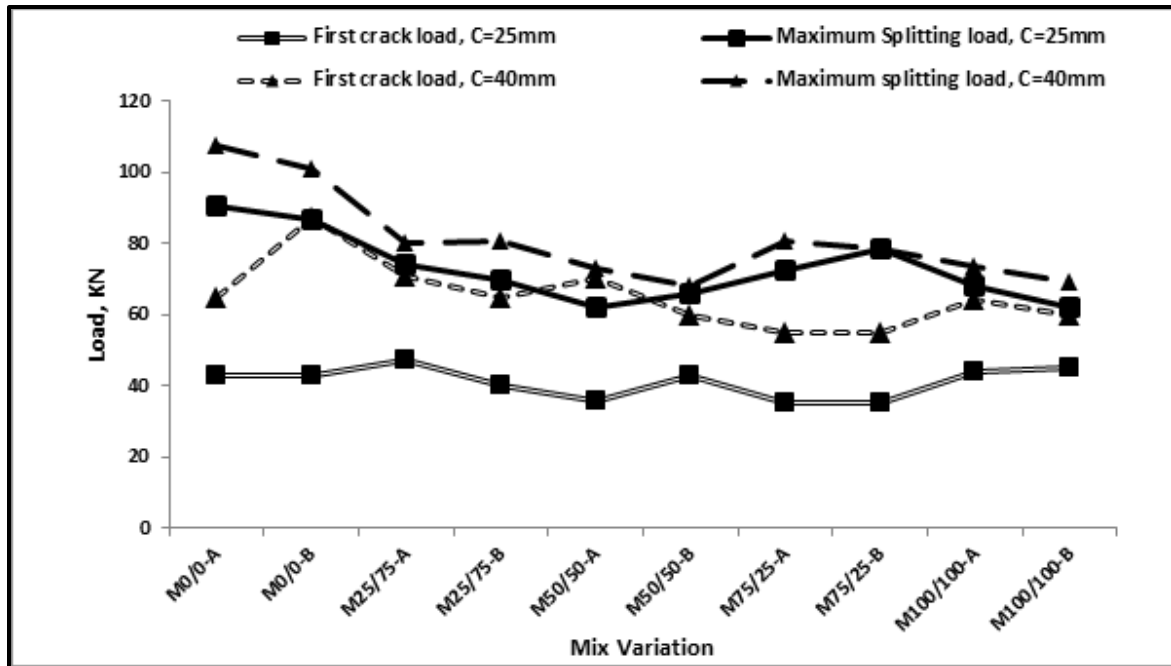


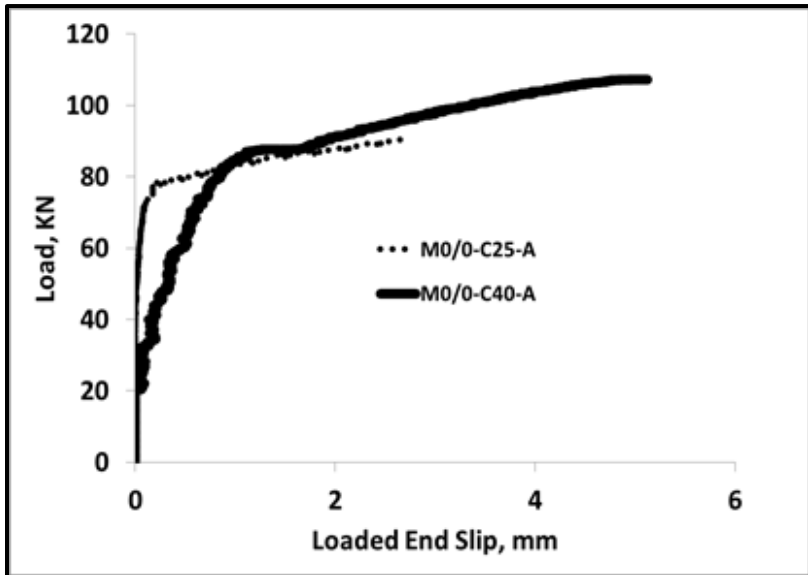
Figure 4.4 Plot of first crack and maximum splitting load cover=25mm and 40mm vs mix variation

#### 4.3.3.1 Loaded and unloaded end slips and strains in the test rebar

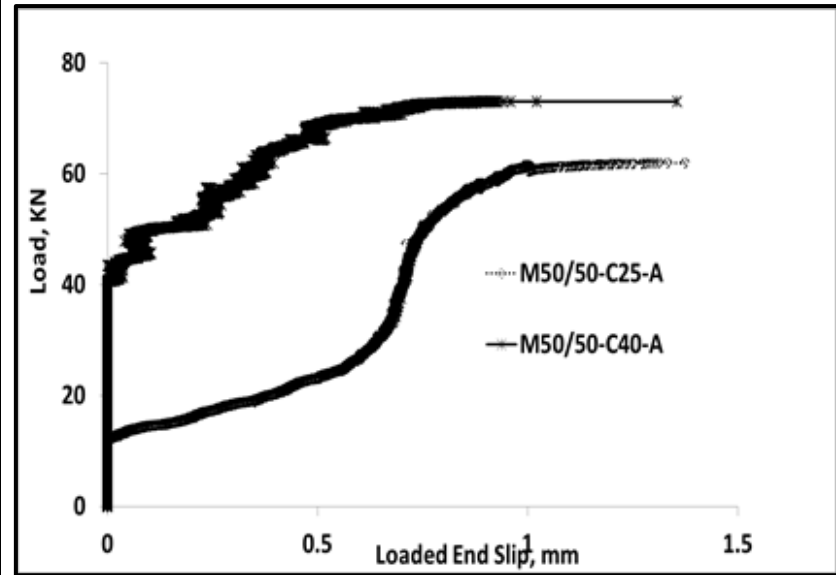
Generally from Table 4.4, it can be observed that all the test bars slipped at the loaded end based on the adapted ASTM A944 experimental set-up. Though the slips generally varied from specimen to specimen, there was no discernible trend when comparing the two groups of specimens when the concrete cover was increased. Similar non-discernible slip amount and behavior was observed by Martí-Vargas & García-Taengua, (2015) and thus makes the use the rebar slip amounts an unreliable source of depicting bond behavior, unless the slip is large enough at failure where there is no further increase in load. It must be noted that the difference in the slip at the loaded and unloaded ends represents the lengthening of the rebar (ACI Committee 408). However, for bars that did not yield, and where the strain is far less when considering 0.25% strain, the change in length is far less than slip amounts of say 2mm.

It can also be deduced from Table 4.4 that the NCA specimens in Groups 1 and 3 yielded at the loaded ends ( $>85\text{KN}$ ) whereas the RCA specimens did not yield the test bars. Thus a reduced bond capacity can be inferred through the concrete strengths varied in each case. On the contrary, the strain at the mid-point at ultimate load did not yield for the NCA specimens, whereas it yielded in some instances (M50/50 and M75/25 for the Group 1 specimens) and some strain gages also got damaged. Because of this, the strain gages were not accurate in readings due to the external influence of the concrete cracking process during the de-bonding process. In this wake, the ACI 408 recommends using rebars which have been cut, internally grooved for strain gage installation and welded back as test bars for detailed studies. Alternatively, strain gages installed in resealed grooves along the longitudinal ribs are equally acceptable as another option to obtain strain measurements on the test bars. To this end, the strain measurements were not reliable due to the influence of concrete cracking around the test bars and will not be used in further discussions.

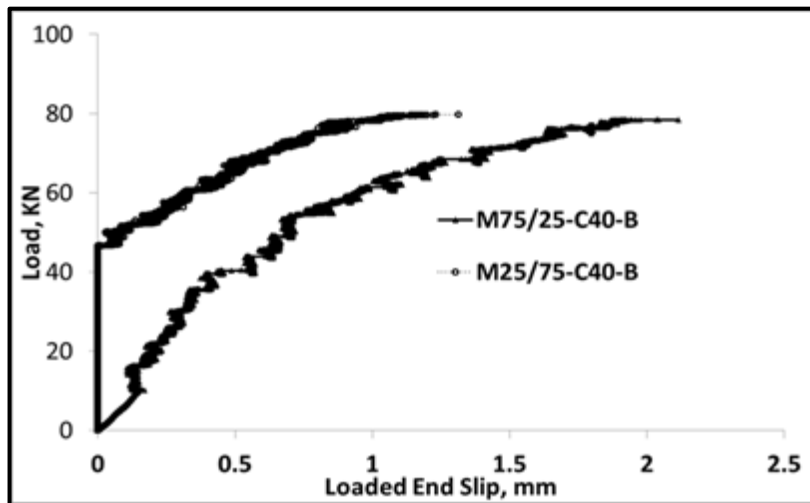
The area under the load slip curves shown in Figure 4.5 represents the energy expended (work done) in overcoming the bond between the concrete and rebar which may translate in the form of fracture energy and considered as a secondary factor as outlined in Table 2.1 per ACI Committee 408, (2003) report.



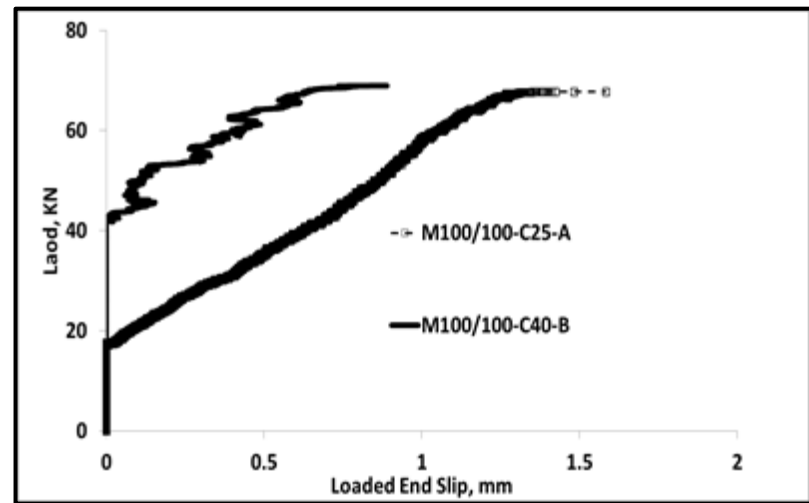
A-Load-slip curve when cover is increased (25 to 40mm) and using NCA and NFA



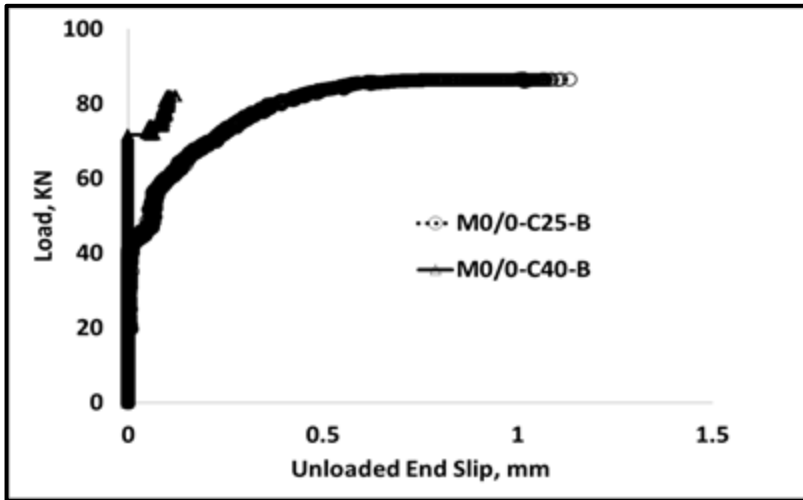
B-Load-slip curve when cover is increased (25 to 40mm) and using M50/50



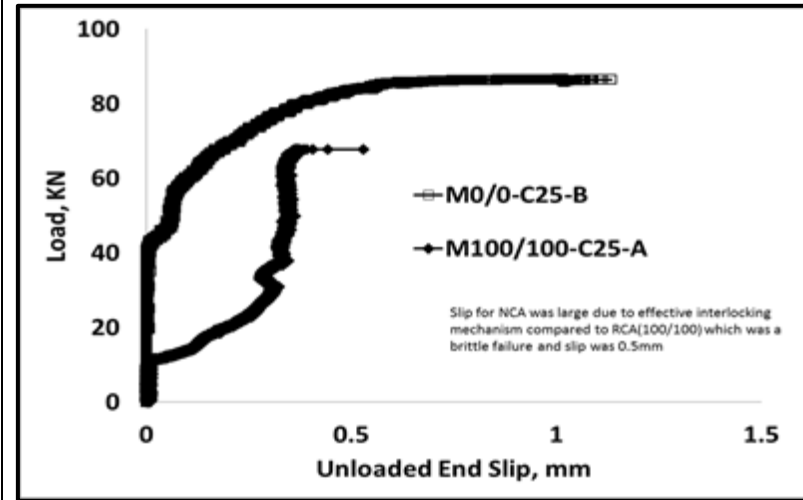
C-Load-slip curve using 40mm cover with M25/75 and M75/25



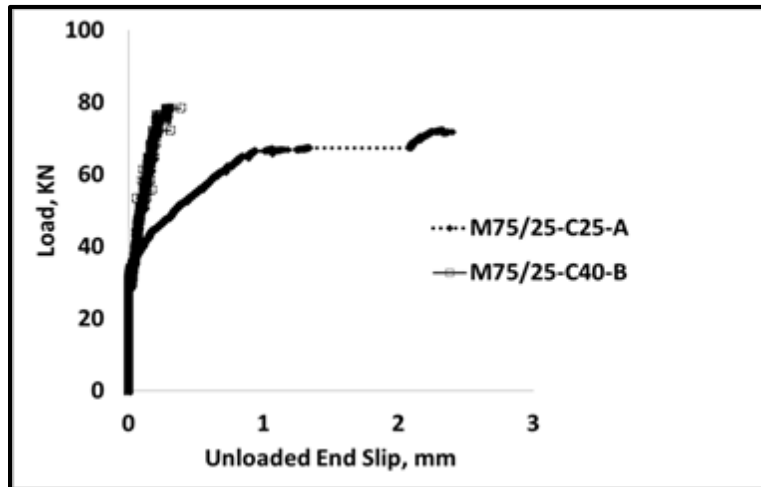
D-Load-slip curve with increased cover (25 to 40mm) and using M100/100



E-Load-slip curve when cover is increased (25 to 40mm) and using NCA and NFA only



F-Load-slip curve when cover is same (25mm) and comparing M0/0 and M100/100



G- Load-slip curve when cover was increased and using M75/72

Figure 4.5 Load-slip curves of loaded and unloaded specimens of various mixes

#### **4.4 Effect of bond length on the bond capacity (Groups 1 & 5)**

Bond lengths (embedment lengths) of rebars in concrete generally vary with the bond capacity but not proportionally since bond forces are greatest near where a crack exists and varies along the embedment length. Because of this phenomenon, the embedded rebar may either develop the required stress (yield) with large slip due to large bond forces, with a longer bond length, or the rebar may slip without yielding where the rebars are shorter in length (ACI Committee, 2003).

##### ***4.4.1 Effect of bond length increase on bond force and rebar yielding***

There was a general mean bond force reduction of (-15 to -28)% within Group 1 specimens compared to a reduction of (-9 to -13)% for Group 5 when comparing the recycled concrete mix specimens with the control. The wide difference could be attributed to the variation in concrete strength between the control and the recycled specimens. The reduced variance was expected within Group 5 specimens since the increased bond length implies an increase in bonded area and hence reducing the stress over the bond length. However, there was a minimal variance of -4% to +12% when comparing only the recycled concrete specimens with M100/100 in Group 1, whereas for the Group 5 specimens, the variation was between (0 to +5)% for a similar mix of M100/100. Thus for a longer embedment length, the mean bond force variation generally reduced across the specimens in Group 5 when compared to Group 1.

As observed in Table 4.5, the bond force generally increased across the specimens across Groups 1 and 5 when the bond length was increased for each companion concrete recipe. The increased force was 16% for the control specimen whereas the recycled concrete mixes varied

from 21% to 30% increase. Thus the proportion of bond force increased across specimens and was not negatively affected by the use of quality recycled aggregates for concrete.

Table 4.5 also shows the bar stresses ( $f_s$ ) within each pair of the specimens in Group 5 and can be concluded that the minimum development length of 300mm as required by CSA A23.3 and ACI 318M-11 resulted in yielding (exceeded stresses of 420MPa) the entire test bars. Hence, increasing the bond lengths due to the use of quality and commercially produced recycled aggregates and concrete may ensure yielding, and additional length of rebars may not be needed since the quality of the aggregates and concrete can provide the needed bond capacity.

Table 4.5 Effect of increasing bond length on rebar “yield” stresses

	<b>Bond force and rebar stresses</b>				
	<b>Concrete mix variation</b>				
	<b>M0/0</b>	<b>M25/75</b>	<b>M50/50</b>	<b>M75/25</b>	<b>M100/100</b>
<b><u>L-200-C25-Group 1</u></b>					
<b>Sample A</b>					
Bond/Bar Force, $F_b$ , KN	90.38	72.21	62.12	74.06	67.85
$f_s = F_b / \text{Bar Area}$ , MPa	451.90	361.05	310.60	370.30	339.25
<b>Sample B</b>					
Bond/Bar Force, $F_b$ , KN	86.68	78.3	65.73	69.85	65.26
$f_s = F_b / \text{Bar Area}$ , MPa	433.40	391.50	328.65	349.25	326.30
Mean bond strength	8.81	7.49	6.36	7.16	6.62
<b><u>L-300-C25-Group 5</u></b>					
<b>Sample A</b>					
Bond/Bar Force, $F_b$ , KN	104.42	90.30	92.17	95.07	88.92
$f_s = F_b / \text{Bar Area}$ , MPa	522.10	451.50	460.85	475.35	444.60
<b>Sample B</b>					
Bond/Bar Force, $F_b$ , KN	105.26	101.28	89.63	93.89	92.88
$f_s = F_b / \text{Bar Area}$ , MPa	526.30	506.40	448.15	469.45	464.40
Mean bond strength	6.96	6.36	6.03	6.27	6.03

#### 4.4.2 Effect of bond length increase on bond strength

The mean bond strength variation across the various mixes is shown in Table 4.5. As expected, the bond strength reduced when the length was increased which is due to the increased bonded area around the rebar. The strength reduction varied from (-15 to -28)% within specimens in Group 1 compared to (-9 to -13)% in Group 5 (see Table 4.6). However, for comparisons across specimens when the bond length was increased, the reduction in mean bond strength was (-5 to -15)% for the recycled concrete mixes whereas it was -21% for the conventional concrete mix. The observed variations of maximum bond strength reductions of -15% and -21% for the recycled and conventional concrete mixes respectively are not wide, it is important to confirm this and discount the effect of concrete strength by using the normalized bond strength when using  $\sqrt{f'_c}$ . The normalized bond strength is next discussed in section 4.4.3.

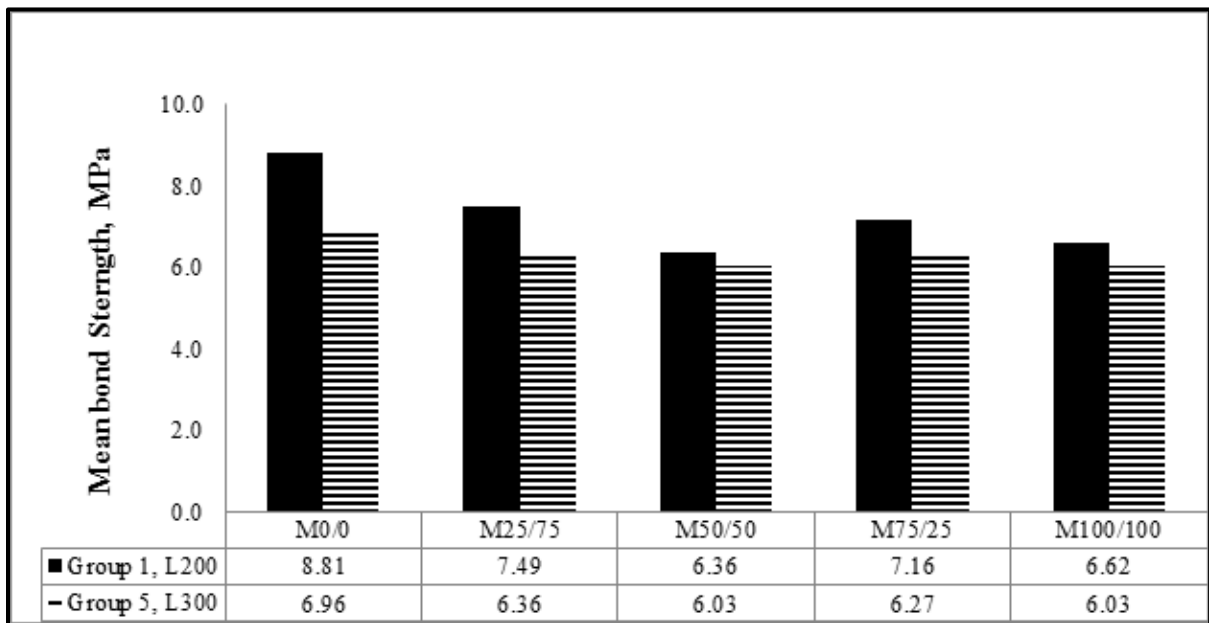


Figure 4.6 Bond strength effect after bonded length increase (200 to 300)mm

#### 4.4.3 Effect of bond length increase on normalized bond strength

The normalized bond strengths with the square root function of the compressive strength for the two groups of specimens are shown in Table 4.6 and Figure 4.7. It can be observed that while the normalized bond strength varied from (-1 to +5)% for Group1 specimens, Group5 specimens varied from (+10 to +18)% when compared with the conventional concrete mix. There was a general reduction in normalized bond strength across specimens but the bond capacity was increased correspondingly to achieve yielding. This can be re-confirmed in Table 4.5 when all the Group 5 specimens yielded (>85KN) when the minimum development length of 300mm was used as required by the CSA A23.3 and the ACI 318-14.

Table 4.6 Group1 and 5 bond strength and normalized bond strength variations

	<b>Bond strength and normalized bond strength</b>				
	<b>Concrete mix variation</b>				
	<b>M0/0</b>	<b>M25/75</b>	<b>M50/50</b>	<b>M75/25</b>	<b>M100/100</b>
<b><u>Bond strength (G1 and G5)</u></b>					
<b>Group 1-G1</b>	8.81	7.49	6.36	7.16	6.62
<i>BS Reduction (%) Within specimens-G1</i>		-15%	-28%	-19%	-25%
<b>Group 5-G5</b>	6.96	6.36	6.03	6.27	6.03
<i>Within specimens-G5</i>		-9%	-13%	-10%	-13%
<i>BS Reduction (%) Across specimens(G1 and G5)</i>	-21%	-15%	-5%	-12%	-9%
<b><u>Normalized bond strength (Gp1 and Gp5)</u></b>					
<b>Group 1-G1</b>	1.18	1.24	1.15	1.17	1.20
Variation within G1 specimens		5%	-2%	-1%	2%
<b>Group 5-G5</b>	0.93	1.05	1.09	1.02	1.10
Variation within G5 specimens		13%	17%	10%	18%
Variation across G1& G5 specimens	-21%	-15%	-5%	-12%	-9%

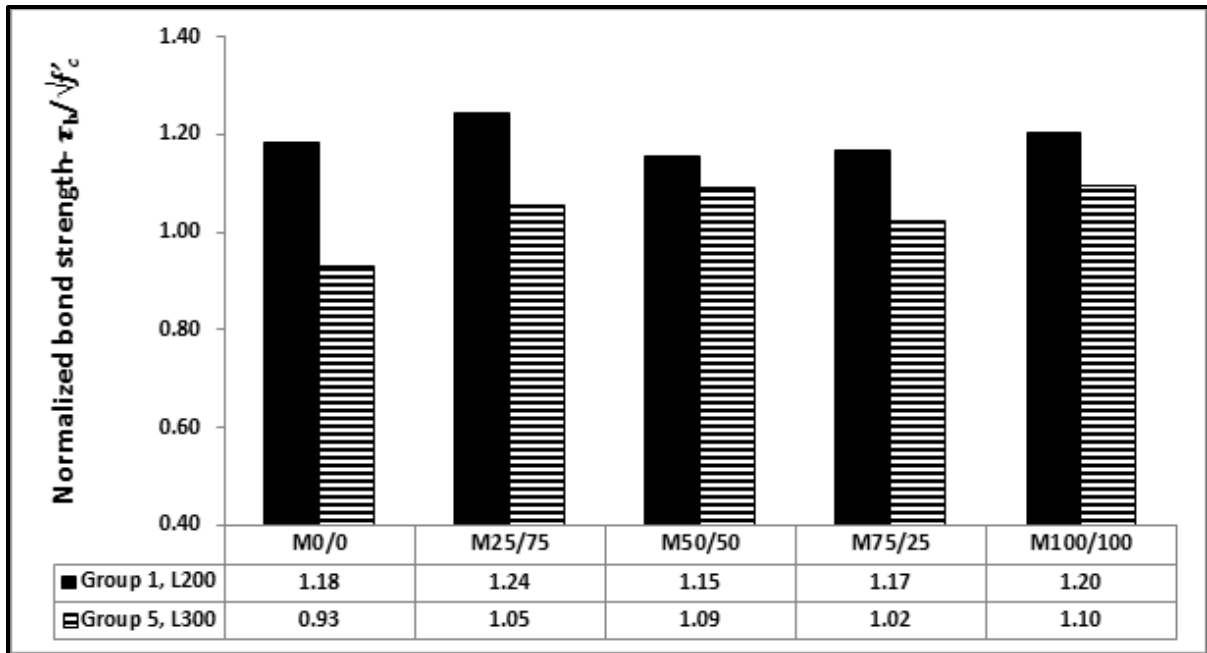


Figure 4.7 Normalized bond strength with square root function ( $\sqrt{f'_c}$ )

The general findings of the normalized bond strengths in this experiment were also similar to the experiment of Butler et al., (2015), where similar beams with  $l_d/d_b = 15$  and  $f'_c = 30-50\text{MPa}$  were used. The reported normalized bond strength for the conventional concrete (50MPa) was 0.81, whereas for the recycled concrete mix (30MPa) it was 0.83. However, in this experiment, normalized bond strength of 0.93 and (1.02 to 1.10) was observed for the conventional and recycled concrete, respectively which is close to unity.

In other experimental splice beams with similar  $l_d/d_b$  ratio of 18.95 compared to 18.80 in this experiment, Sadati et al., (2017) reported a 21% higher normalized steel stresses when using 50% recycled coarse aggregates and natural fines when compared to conventional concrete. Similarly, Fathifazl et al., (2012) reported a normalized bond strength increase of 13% and 16% when using 100% natural aggregates and recycled aggregates respectively. It must be emphasized that though the experimental works of Sadati et al., (2017) and Fathifazl et al.,

(2012) excluded the use of recycled fines, the use of fine recycled aggregates in this experiment, as well as 100% coarse recycled aggregates, did not negatively impact the bond strength.

However, in this experiment, a higher normalized bond strength of 1.1 was obtained when using 100% coarse and fine recycled aggregated compared to 0.93 when using the conventional concrete. Thus the increased normalized bond strength trend in Figure 4.7 for the Group 5-L300 specimens, when compared to the conventional concrete, is a confirmation that quality recycled concrete may perform similarly in bond as shown in this experiment.

#### ***4.4.4 Effect of bond length increase on the Load vs Slip curves***

Considering the effect of an increase in bond length being investigated (resulting in additional ribs being embedded in concrete), there was a general increase in the slip of all the Group 5 (L300) specimens compared to Group 1 (L200) specimens, as shown in Figure 4.8 since the bar length and rib interlocking mechanism was increased and would largely contribute to improving the structural safety.

The load-slip curves in Figure 4.9 are indicative of the bond response between the concrete and deformed rebars. The load-slip curves were generally similar in terms of having no slip initially, followed by a gradual slip of the bars in the concrete when the load increases until it reaches the peak and plateaus with an accompanying large slip. This behaviour was similarly observed and reported in (ACI Committee 408, 2003). It can be observed and concluded that slips for the conventional concrete mixes (M0/0 in Figure 4.9 A and B) were greater than that of the recycled concrete mixes (M100/100-Figure 4.9 B). On the other hand, the unloaded end slips (Figure 4.9 C and D) were generally less (0.4-1.2) mm compared to the loaded end specimens of (1.5-6) mm. The variance observed confirms the gradual slip at the loaded end while the unloaded end

remains relatively stationary. It must also be noted that the unloaded slips were generally greater than (M0/0-L200) compared to the recycled concrete mixes of M100/100-L300, though more ribs were engaged in the embedded concrete. This observation may be attributable to the general concrete weakness of the recycled mixes (30-37MPa) compared to the 55MPa for the conventional concrete mixes-M0/0. Thus, the ribs may not play a significant role at the unloaded end during the slipping process.

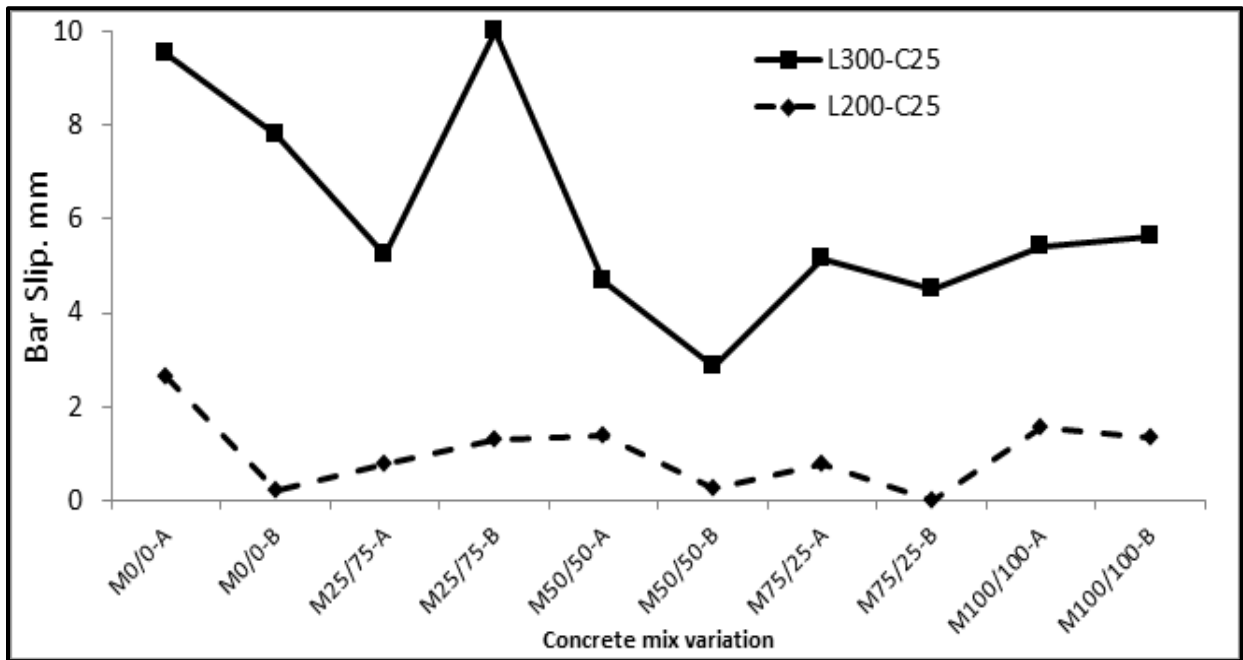


Figure 4.8 Trend line of maximum bar slip and mix variations with increased bond length

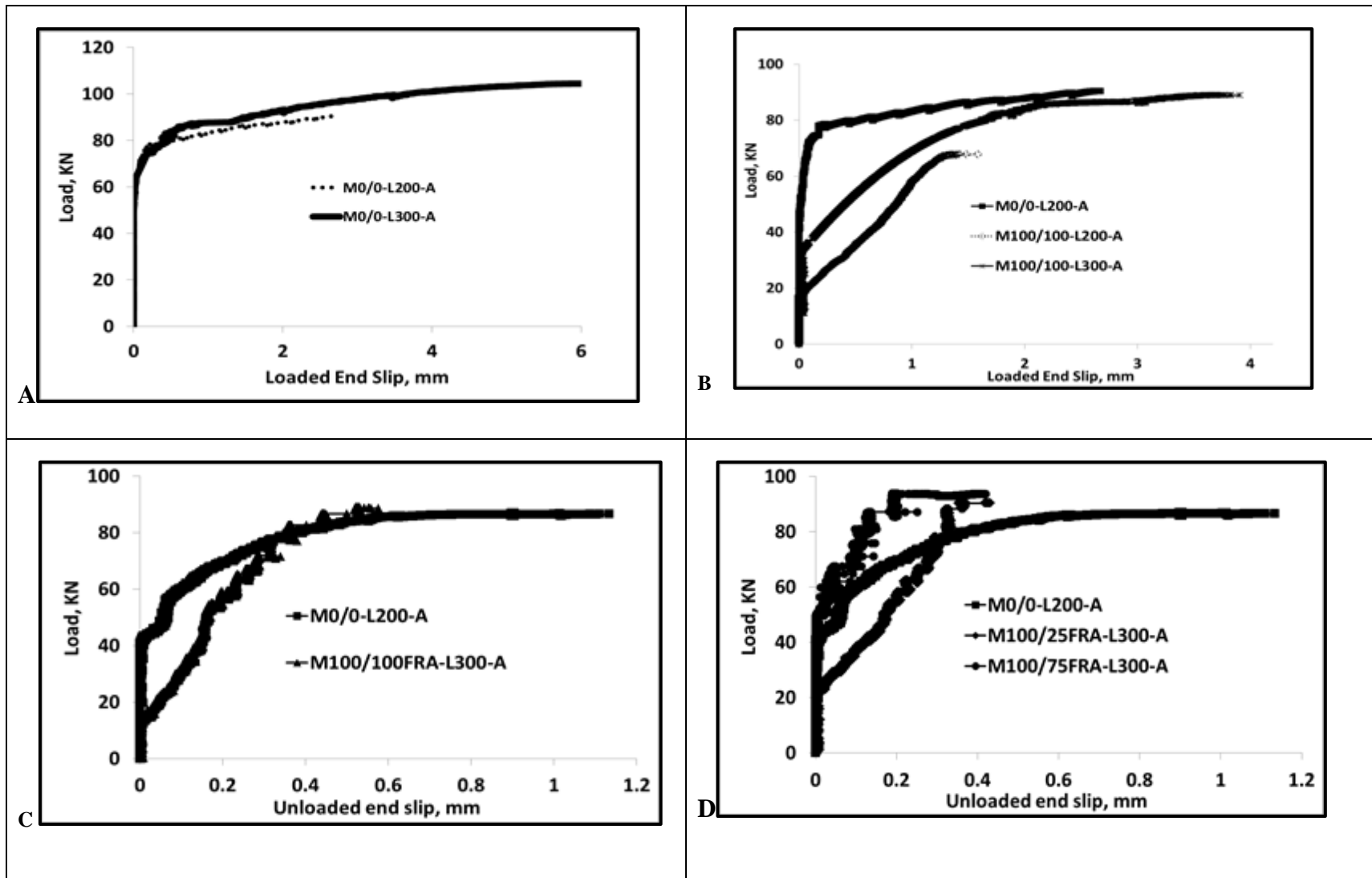


Figure 4.9 Typical load-slip curves of loaded (A&B) and unloaded (C&D) specimens of various mixes

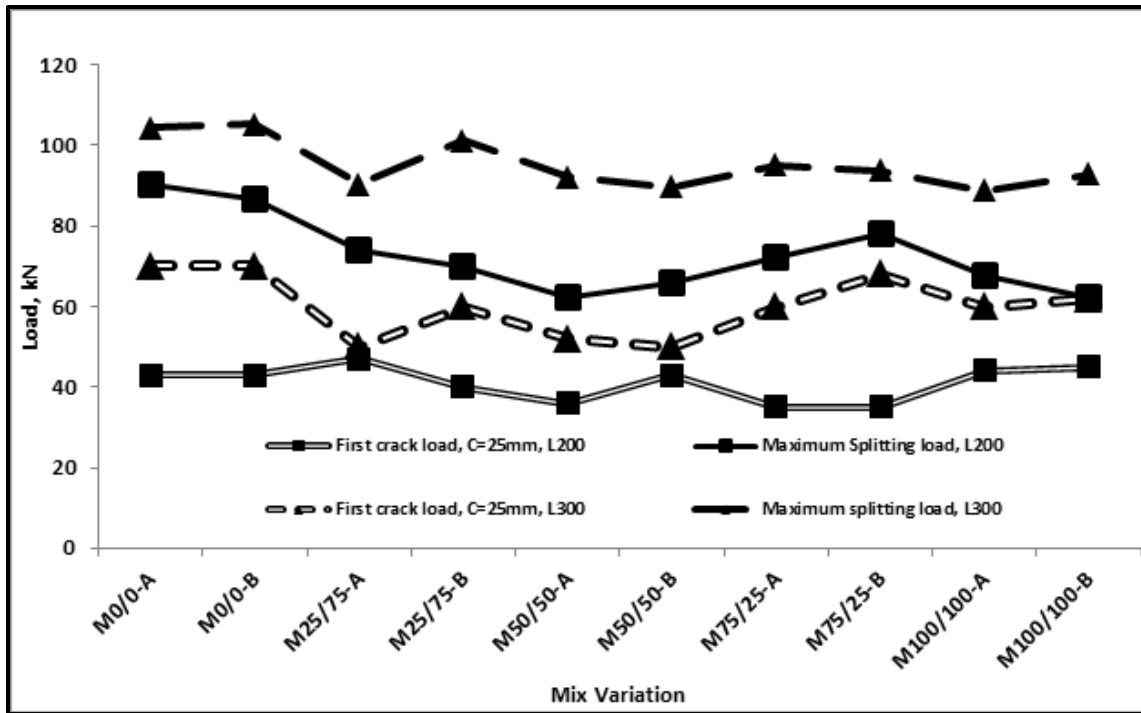


Figure 4.10 First crack and failure load of L200 and L300 vs mix variation

Effect of bond length increase on first crack load and splitting loads

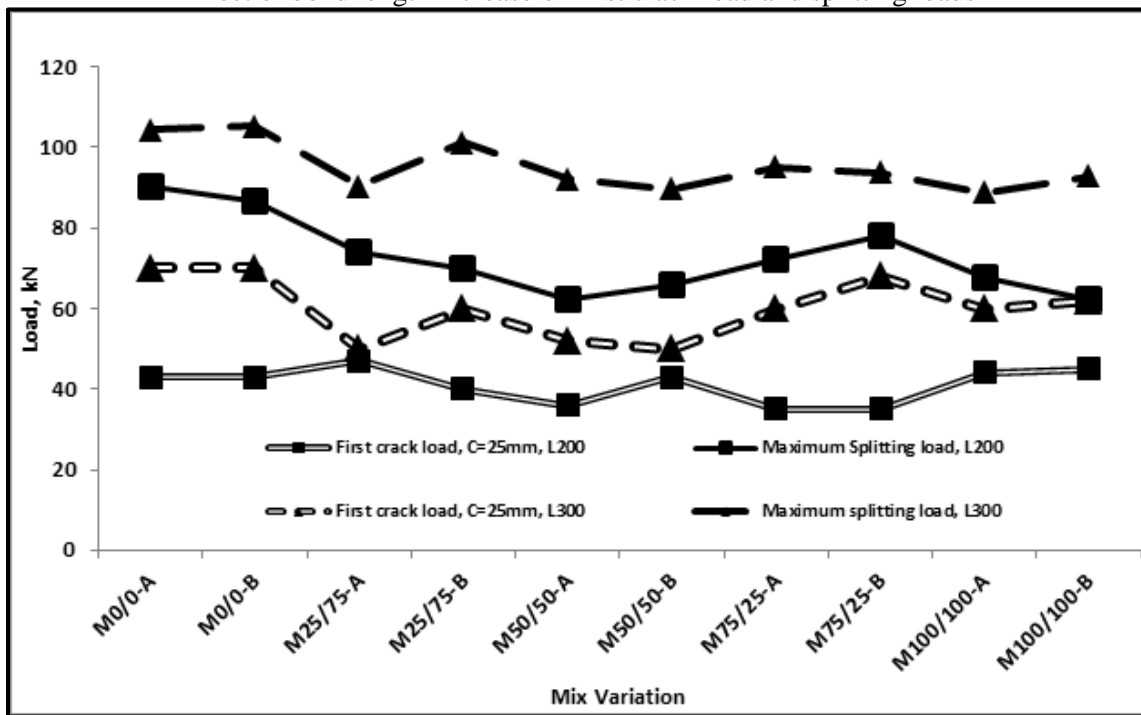


Figure 4.10 shows the first crack load for the conventional and recycled concrete in the range of (35 to 47KN) when the bond length is 200mm and (50 to 70KN) when increased to 300mm bond length. These first crack loads are greater than the experimental results reported by Kaarthik & Subramanian, (2014), (26 to 40KN) when concrete beams containing recycled fines and were improved with silica fume and fibers. In addition, the proportion of first crack load to the maximum is 50-70% in this experiment, an initial crack load of 70% for specimens which were reported for a more brittle high strength concrete by Ahmed, Siddiqi, Ashraf, & Ghaffar, (2008). The foregoing first crack load observations in this experiment reinforces the need to obtain quality recycled coarse and fine aggregates for structural concrete, which has similar physical properties and could result in similar beam behavior without adding fibers which are known to reduce crack formation in concrete. In addition, Malešev et al., (2010) and Mohamad, Khalifa, Samad, Mendis, & Goh, (2016), demonstrated that the first crack loads of quality recycled concrete beams performed similarly to conventional concrete beams and can be inferred that the bond in flexure is similar for both conventional and quality recycled concrete beams. The reduced trend of slips from M0/0 specimens to M100/100 specimens is an indication of a reduced bond capacity when compared to the conventional concrete and shown in Figure 4.8

The splitting cracks which represent a bond failure for Group 1 and Group 5 specimens were similar except for the extended length and crack area in Group 5 specimens. Commonly, it can be noted in the crack album in (Appendix I and Appendix M), that the cracks were wider at the loaded end and finer at the unloaded end where the bond forces are assumed to be equal to zero.

However, for the concrete mixes within each group, the cracks were generally wider for the recycled concrete mixes than for the conventional concrete mixes. These observations attest to

the inherent voids in the recycled aggregates used as structural concrete. However, its effect on bond and crack formation when using quality recycled aggregates as in this experiment were minimal as observed in the normalized bond strength comparisons. In a similar vein, when using recycled structural concrete in tested beam elements, the cracking behaviour was indifferent in the works of (Gonzalez-Fonteboa & Martinez-Abella, 2007; Sato, Maruyama, Sogabe, & Sogo, 2007).

#### **4.5 Effect of bar size on bond (Groups 1 and 6)**

The ten beams tested in Group 6 were used in determining the bond capacity and to observe the bond effect as when larger bar sizes are used with quality recycled structural concrete. The mean bond strength was used to first normalize the bonded area of concrete and rebar to allow a rational comparison of the effect of the bar size. In addition, the bond strength was normalized with the square root of the compressive strength as done previously.

As expected (and shown in Figure 4.11) and from the literature, the bond strengths reduced by -22% for M0/0 mix, whereas the recycled structural concrete mixes similarly reduced in a similar range of (-17 to 28)%. In a correlative beam end test using 15M and 30M rebars Fathifazl et al., (2012) reported a reduction of (-28 to -41)% when EMV mixing method of 100% RCA and no RFA was used. Though in this experiment similar ratios of  $c/d_b = 1.6$  and  $l_d/d_b = 12.5$  for 15M and 25M rebars, the total bonded area (shear area) of rebar to the concrete is about 234% more, which is significant to impact the bond strength reduction. However, the bond forces in this Group 6 experiment (121 to 154)kN when using recycled structural concrete is comparable to the splice beam (with  $l_d = 305$ mm, 25M rebar, and 140kN load) test by (Hamad & Machaka, 1999). The foregoing further demonstrates that structural recycled concrete can

perform similarly in bond to the conventional structural concrete where similar conditions prevail.

The bond forces in this experiment for all the 25M bottom positioned rebars were less than 206KN ( $f_y=420$  MPa) showing that the bars did not yield during the test. However, it is important to note that the minimum bond length of 300mm proposed in the ACI 318M-11 and the CSA A23.3 was used for this 25M Group 6 test, whereas the 15M Group 5 test yielded. Thus the minimum development length of 300mm may not be applicable in larger sized rebars as demonstrated in this experiment (section 4.4.1 ) and also confirmed in ACI Committee 408, (2003) in section 2.2.1.

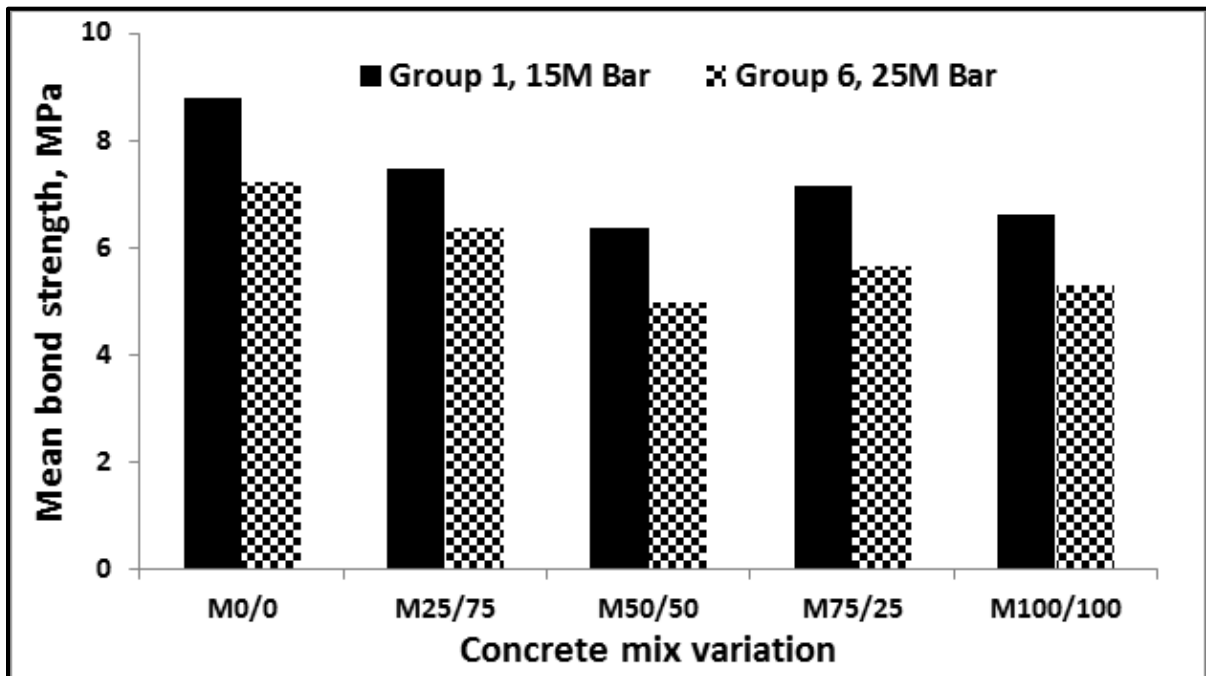


Figure 4.11 Bond strength effect on changing bar size (15M to 25M)

#### ***4.5.1 Effect of bar size on normalized bond strengths***

The effect of normalized bond strength is shown in Figure 4.12 **and** Table 4.7 where the variation in normalized bond strengths for Group 6 rebars was marginal (-4 to +9)% when compared with the conventional concrete mix.

A similar trend of marginal variation was observed when Group 6 specimens were compared across with Group 1 for the reduced normalized bond strength. Thus, an 18% reduction was observed for the conventional concrete mix, compared to the recycled structural concrete mixes which recorded a reduction in the range of (-15 to -22)%.

Thus a generalized reduction in normalized bond strength when the bar size increased with an increase in the bond surface area, forms a critical shear area. Though the normalized bond strength variation was similar, within the range, it confirms that the aggregate hardness, density, and interlocking matrix in the concrete mixes of recycled and conventional may be generally similar.

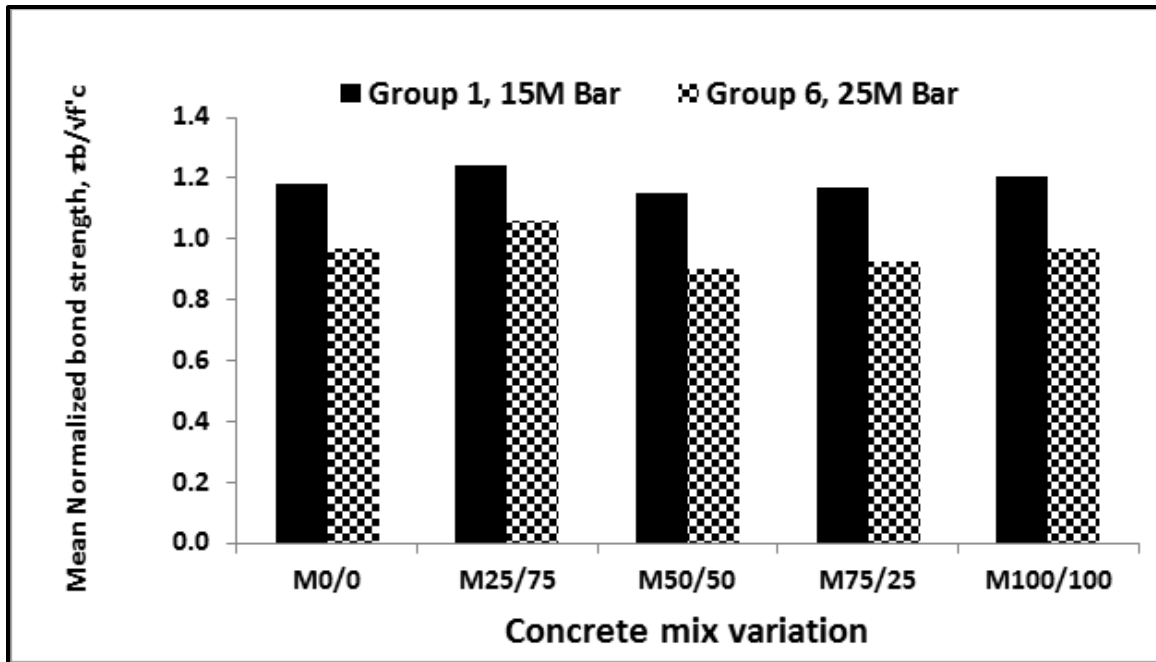


Figure 4.12 Normalized bond strength effect on changing bar size (15M to 25M)

Table 4.7 Effect of bar size (Group 1 and 6) normalized bond strength

	Normalized bond strength				
	Concrete mix variation				
	M0/0	M25/75	M50/50	M75/25	M100/100
<b>Group 1</b>	1.18	1.24	1.15	1.17	1.20
<i>Variation within mix specimens</i>		5%	-2%	-1%	2%
<b>Group 6</b>	0.97	1.06	0.90	0.92	0.97
<i>Variation within mix specimens</i>		9%	-7%	-4%	0%
<i>Variation across specimens (Effect of variable)</i>	-18%	-15%	-22%	-21%	-20%

#### 4.5.2 Effect of bar size on cracking behavior

The first cracks in all the beams occurred at the tip of the loaded end when the bar was under tension within the bonded length. As can be observed from the crack album in Appendix N Group 6, a single and major splitting crack line occurred along the longitudinal length of the loaded end rebar with occasional transverse and flexural cracks which were minor. As the

loading continued, the cracks formed along the entire length until the end of the bond region (free end). All the specimens in Group 6 failed in bond splitting except for M4-R25-L300-C40-A, where the failure was both splitting and shear. However, the companion specimen (M4-R25-L300-C40-B) splitting failure load was similar and was included in the analysis. The shear failure could be due to the dislocation of the stirrups within the specimen during the concrete pour since all other specimens and set-up was the same.

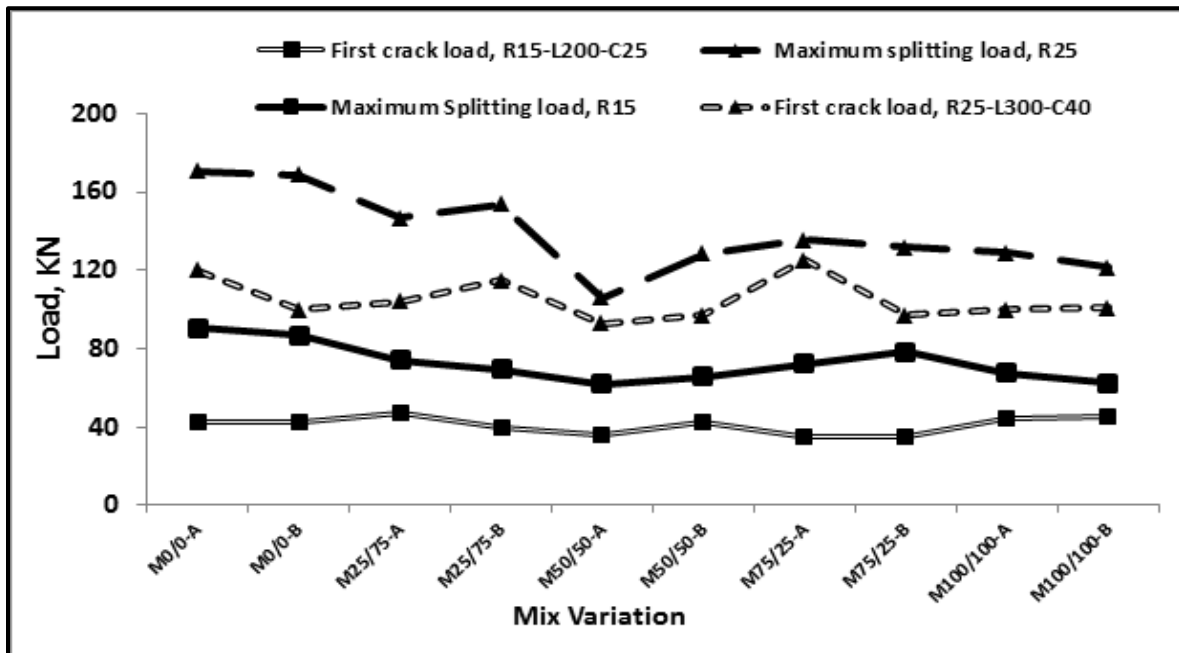


Figure 4.13 Trendline of the first crack and splitting loads for Group 1& 6 (Effect of bar size)

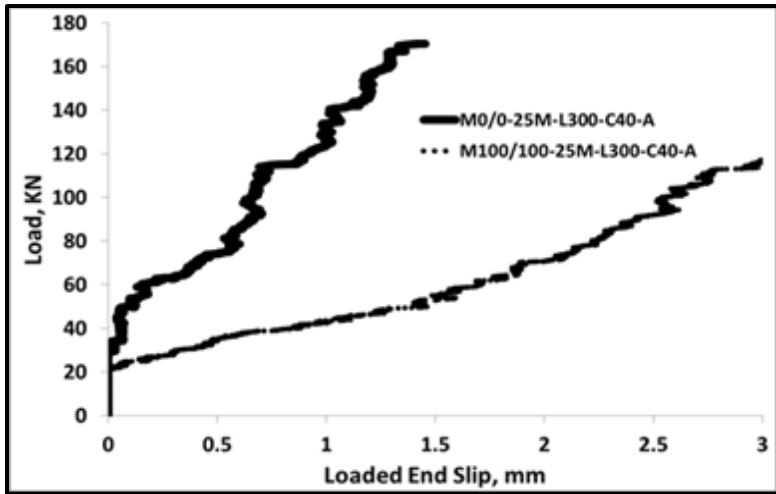
It can further be observed in Figure 4.13 that there is a slight reduction in the general trend of first crack load within each specimen type when comparing the conventional and recycled concrete mixes. The increase in bar size also increased correspondingly the first crack load from a range of (35 to 45)kN for the 15M rebars to (97 to 120)kN for the 25M rebars, where the proportion of the maximum splitting load was (35 to 47)% and (59 to 92)% respectively. The crack behavior is expected as the recycled concrete mixes have an embedded secondary ITZ

layer which aids in the crack widening and propagation, compared to the conventional concrete. The larger bar forces causing splitting cracks from the 25M rebars compared to the 15M can be attributed to the larger mass of concrete around the 25M, thus requiring greater forces to break the bonds between the concrete and rebars.

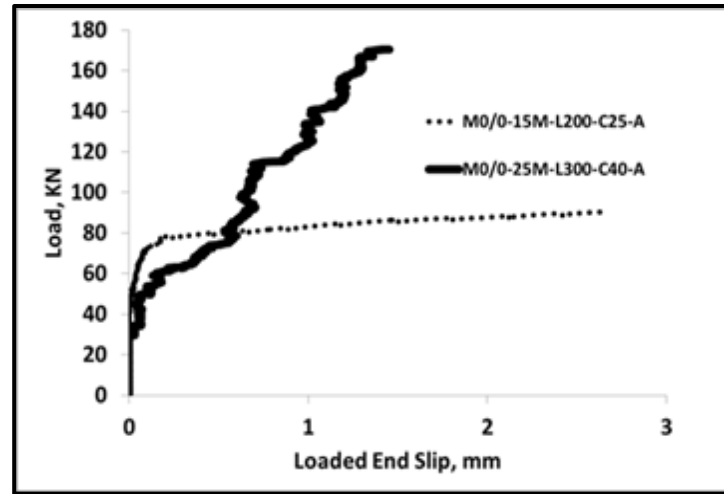
#### ***4.5.3 Effect of bar size on bond force vs slip curve***

The bond-slip curves in Figure 4.14-A show that the M0/0 mix was much stiffer (steep load vs slip gradient) than the M100/100 mix. In addition, maximum load and slip were 170kN & 1.5mm and 121kN & 2.5mm respectively for M0/0 and M100/100 mixes. The behavior confirms the influence of the splitting crack formation on the slips, and thus reduced slips from the M0/0 mix will result in a lesser deformation of a structural member than the increased slip from the M100/100 mix.

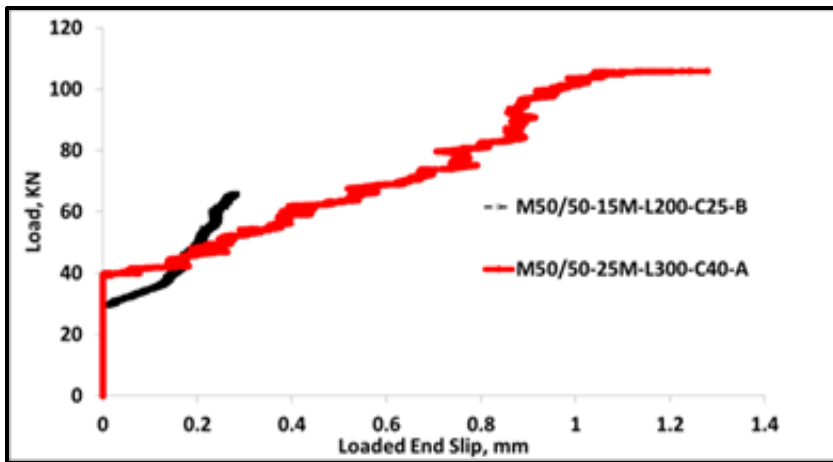
Consequently, for the change in bar size from 15M to 25M when using the conventional M0/0 mix (Figure 4.14-B), the 15M slipped much greater than 25M bar indicating a larger deformation and less brittle behavior for the 15M compared to the 25M. Once again the slip for the 25M rebars was about 1.5mm. Similar behavior of 15M and 25M using M50/50 is observed in Figure 4.14-C however, the LVDT recorded up to 0.3mm for the 15M, whereas



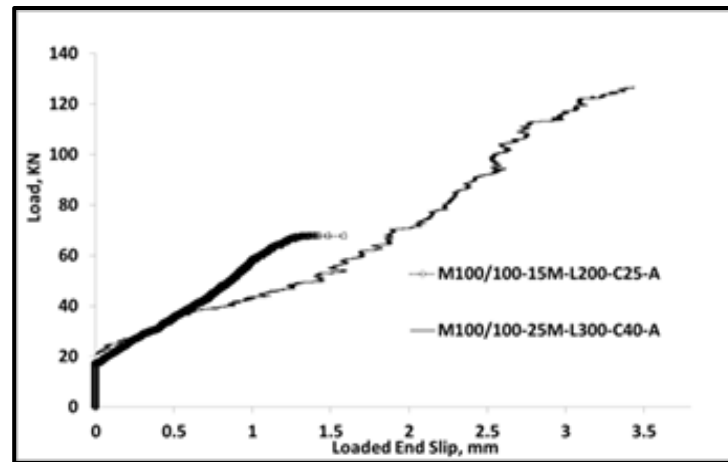
A-Comparison within mix-RCA slips early



B-Effect of bar size for M0/0 mix



C-Effect of bar size for M50/50 mix



D-Effect of bar size for M100/100 mix

Figure 4.14 Load-slip and mix variations on the effect on changing bar size (15M to 25M)

1.3mm slip was recorded for the 25M rebar. As observed for the M50/50 mix, a similar low slip was recorded for the M100/100 mix when comparing the 15M and 25M rebars bond behavior (shown in Figure 4.14-D). The trend in the behavior can be attributed to the reduced shearing area (bonded area) from the 15M bars compared to the 25M rebars which are nearly 234% more.

#### 4.6 Effect of bar position on bond (Groups 1 and 7)

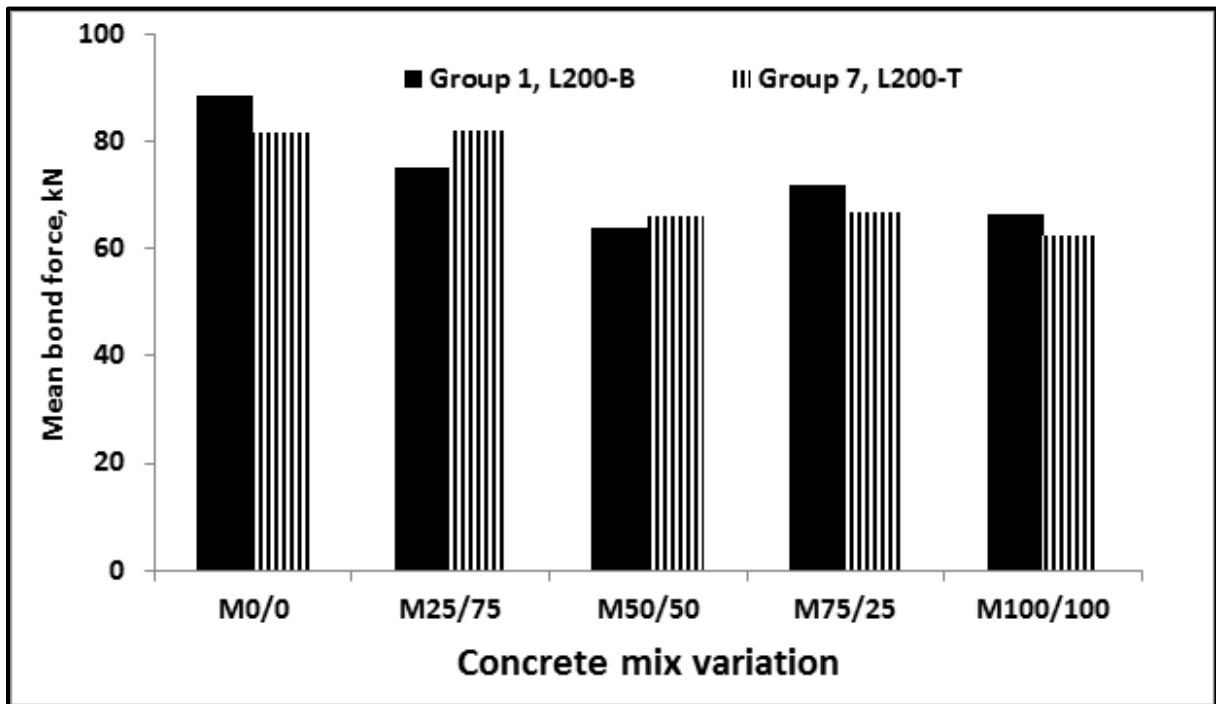


Figure 4.15 Bond force effect and variation on bar position (200 to 300)mm

Though the bond force variation was marginal (less than +/- 10)% across the comparative specimens, several other studies have reported a slight increase or reduction when using conventional concrete mixes with bar positions at the top (ACI Committee 408, 2003). In contrast, Looney, Arezoumandi, Volz, & Myers, (2012) concluded that when using self-consolidating concrete specimens (beam or pullout), there was a slightly greater bond for top located rebars. Because of the contrary reports, the ACI 318M-11 and the CSA A23.3

proposition of increasing the bond length by 30% may remain the same until more experiments are made available.

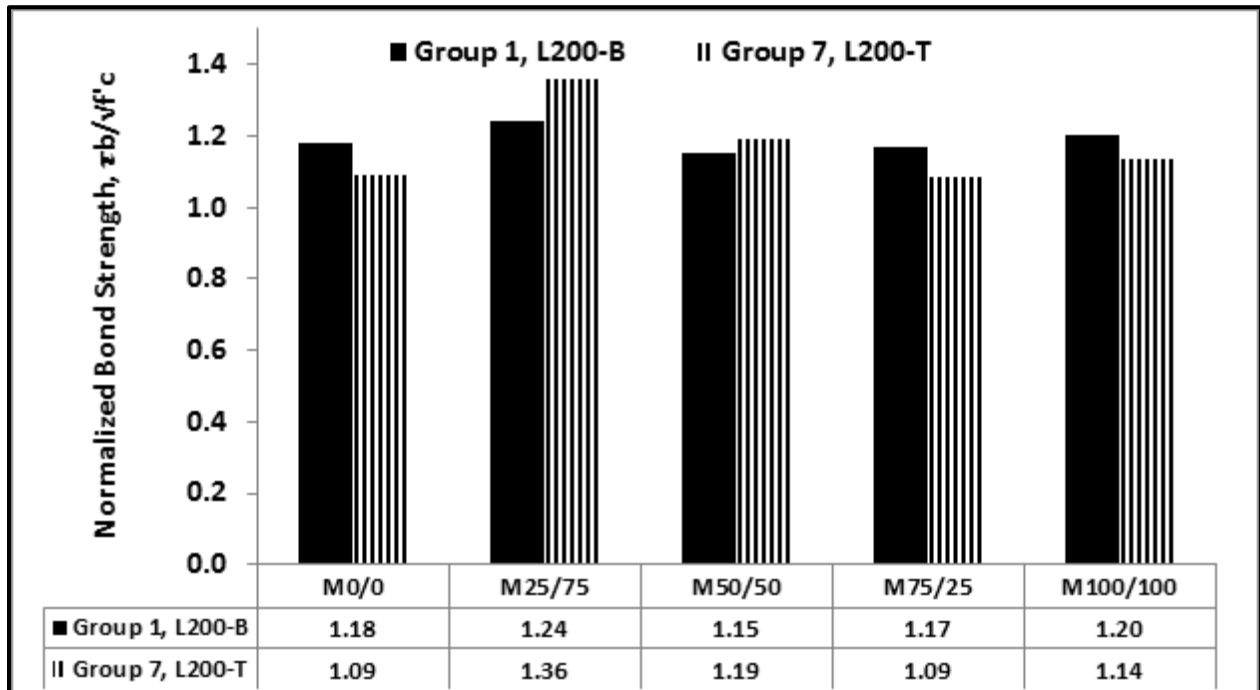


Figure 4.16 Normalized bond strength effect and variation on bar position (200 to 300)mm

#### 4.6.1 Effect of bar position on normalized bond strengths

The normalized bond strengths variations shown in Table 4.8 reveals that within the mix specimens, Group 7 showed a marginal increase of (0 to 9)% for M50/50, M75/25 and M100/100, whereas there was a 24% increase for the M25/75 which may be considered as an outlier. However, to conclude on the effect of bar position (across similar specimens), the M0/0 showed a reduction of -8% compared to (-6 to +9)% for the range of recycled concrete mixes used. If the M25/75 mix normalized bond strength is discounted, the remaining observations (+3 to -7)% are marginal and confirms some of the experimental observations in ACI Committee 408, (2003) and Looney et al., (2012), hence quality recycled structural concrete may not

significantly affect the bond due to the top bar position. However, this observation does not eliminate the occurrence of bleeding and voids around the top positioned rebars in concrete.

Table 4.8 Group 1 and 7 normalized bond strength

	<b>Normalized bond strength effect on bar position</b>				
	<b>Concrete mix variation</b>				
	M0/0	M25/75	M50/50	M75/25	M100/100
<b>Group 1, G1</b>	1.18	1.24	1.15	1.17	1.20
<i>Variation within mix specimens, G1</i>		5%	-2%	-1%	2%
<b>Group 7, G7</b>	1.09	1.36	1.19	1.09	1.14
<i>Variation within mix specimens, G7</i>		24%	9%	0%	4%
<i>Variation across specimens (Effect of variable)</i>	-8%	9%	3%	-7%	-6%

As the test results are in sharp contrast to the standards and codes ACI Committee 318, (2011) and CSA A23.1, (2014), the ACI Committee 408, (2003) report argues that the 30% enhanced factor for the development length is “arbitrary”. It further provides evidence of studies to the effect that concrete which has been internally vibrated, and rebars placed at depths of 380mm above the forms (with low slumps and good compaction) are not affected by reduced bond strength. In addition, Hamad, (1995) also observed a similar behaviour of comparable bond strengths in beams of 305mm depth in high strength concrete (70MPa) containing silica fume and superplasticizers.

#### **4.6.2 Effect of bar position on bond force and slip**

Based on the load-slip curves in Figure 4.18 (A to D) it can be observed that the top position rebars generally started to slip at lower loads than for the bottom bar positions. Thus, the top positioned rebars slipped faster with increasing load compared to the bottom-placed bars though

failure loads were comparable or similar. This confirms the theoretical concept of more void formation, bleeding, and settlement around the rebars when positioned at the top compared to the bottom cast rebars. These have an impact on the crack formation and are discussed in section 4.6.3, on the crack behavior, which is fundamental when considering bond behavior.

#### ***4.6.3 Effect of first crack load on bar position***

The crack formation album shown in Appendix O reveals similar splitting crack patterns for the conventional and recycled concrete mixes. Figure 4.17 shows the trend line for the bottom and top positions of the rebars. The trend and formation of cracks and splitting behaviour of the top positioned rebars are similar to the specimens in Group 3, where brittle failure was observed when the cover was increased. However, less brittle mode of failure was observed for the bottom-placed specimens in Group 1 as discussed earlier. For example, specimen M25/75-Top (L200-C25) had a first crack load of 76kN, and splitting failure occurred at 77kN (98%) whereas the comparable specimen with bottom-placed M25/75 -Bottom (L200-C25) had a first crack load of 35kN and splitting failure at 72kN (49%). Similar observations were made for all the top positioned rebar specimens including the conventional concrete where M0/0-Top (L200-C25) specimen recorded 81kN and 91kN (90%) accordingly. Thus it can be concluded that failure behaviour of top positioned rebars when using quality recycled concrete is not largely at variance with conventional concrete placed in the same position. However, when the failure mode is compared to the bottom-placed rebars the failure mode for the top placed rebars are more brittle whereas the companion bottom-placed rebars are less brittle. This behaviour can best be explained that though the failure loads were largely similar, there was damage accumulation as a result of the crack formation along the embedment length at the top rebar compared to the

bottom rebars, which was not evident until almost at the peak load when the first crack and the ultimate loads occurred almost concurrently.

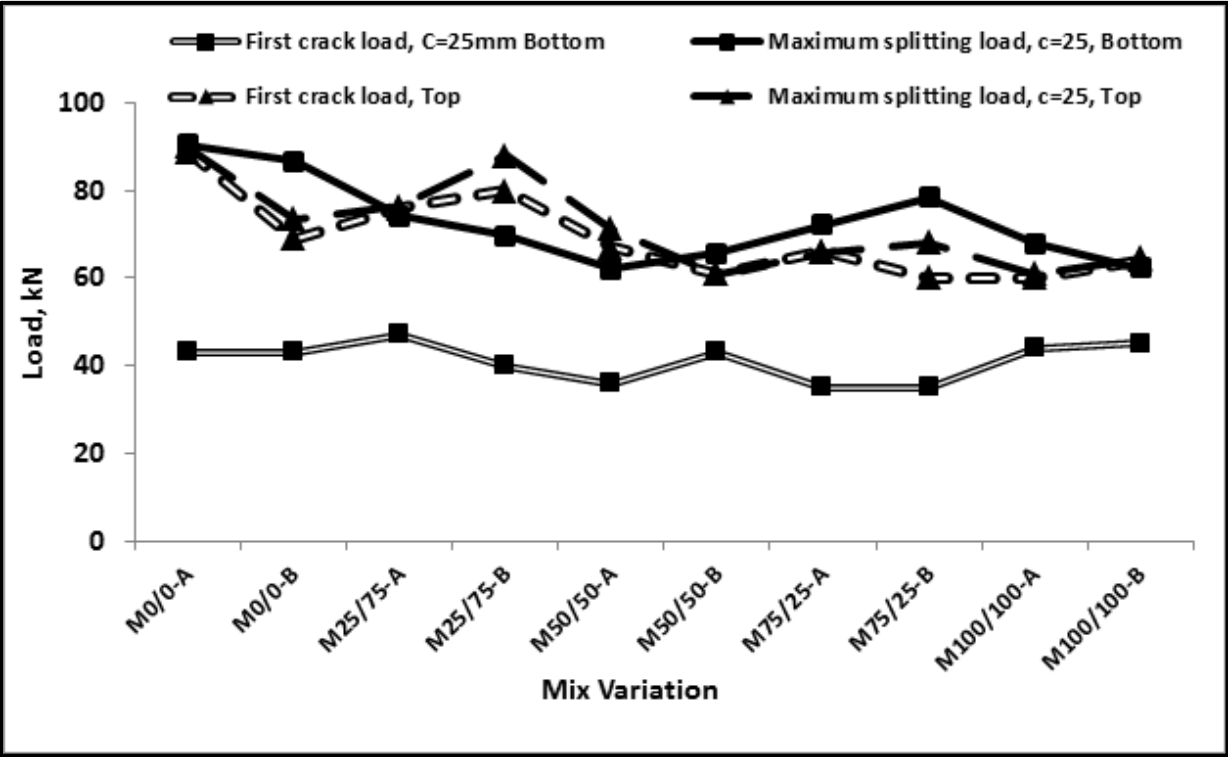


Figure 4.17 Trendline of the first crack and splitting loads for Group 1 & 7 (Effect of bar position)

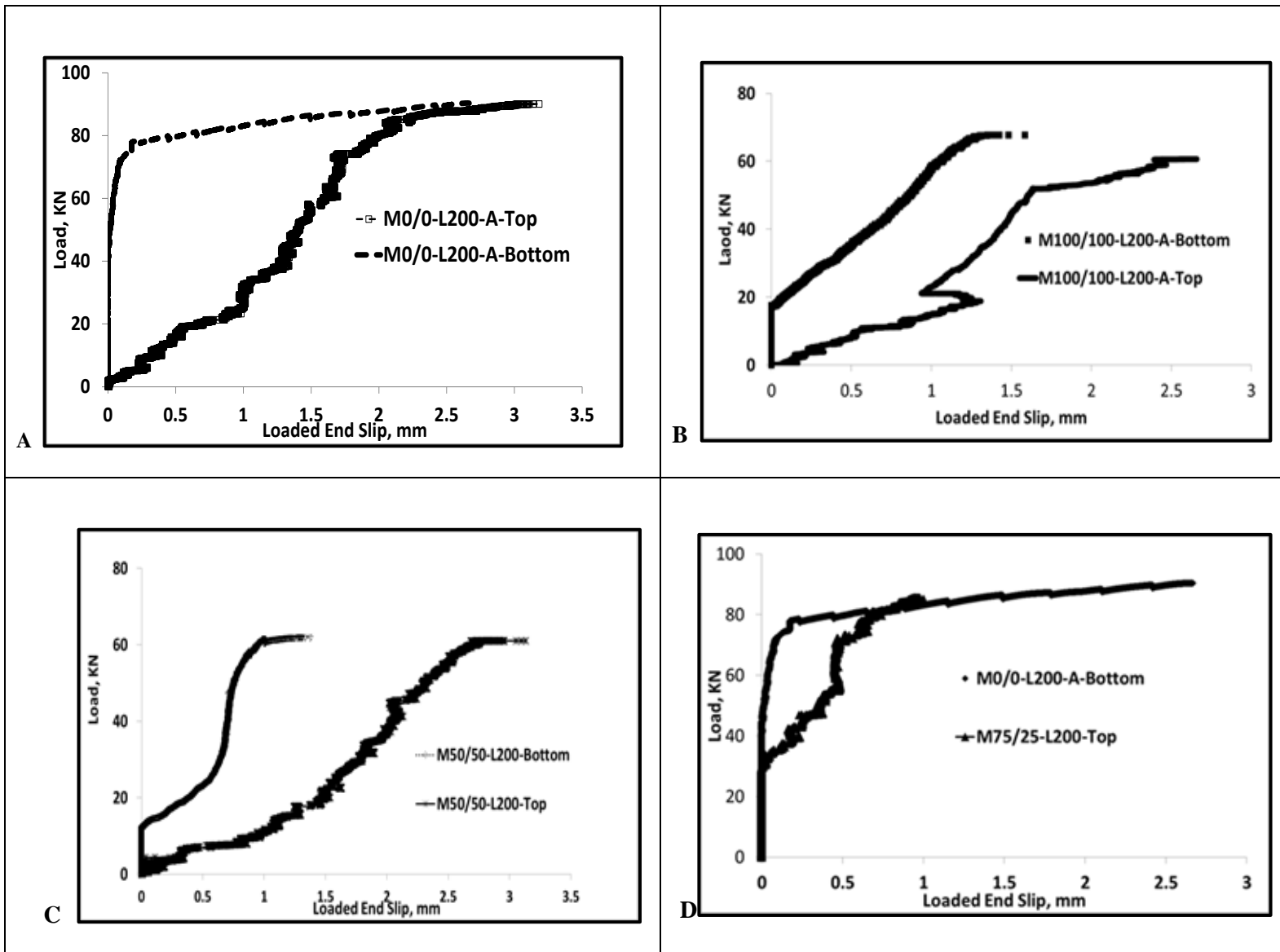


Figure 4.18 Typical load-slip curves (A to D) showing bar position of various specimens and mixes

#### **4.7 Effect of transverse reinforcement on bond force (Groups 1, 2 and 4)**

The 20 beams tested in Groups 2 and 4 (ten each) were used in determining the bond capacity, and bond-slip behavior when using quality recycled structural concrete with stirrups present within the bonded region. The mean bond forces for Group 2 and 4 were compared with the conventional concrete in Group 1 to observe the effect of the mean bond forces across the five mixes. The bond forces were further used to calculate the mean bond force which was then normalized with the concrete compressive strengths to allow a similar and rational comparison of the bond between the specimens tested and its effect.

Figure 4.19 shows the bond force variation across the spectrum of concrete mixes, and all the bond forces in Groups 2 and 4 exceeded 85kN (420MPa) confirming that the rebars yielded. As expected and shown in Figure 4.19, the use of the transverse reinforcement improved the bond capacity for all the concrete mixes compared to Group 1 where no transverse reinforcement was used. For the conventional concrete specimens in Group 2, the increase was 21% whereas for the recycled concrete mixes, M25/75 to M100/100, the increase was about 27% to 38% respectively. Similarly, for Group 4 specimens, a 27% increase was recorded for the conventional concrete compared to (25 to 34)% for the recycled concrete mixes. However, one test specimen (M0/0) had a fractured rebar, and the result was ignored. The reduced proportion for the conventional concrete may be due to its high strength concrete and brittle nature of the conventional concrete and hence reducing the wedging action between the concrete and rebars. Thus crack propagation at the concrete rebar interface split cracked the concrete faster than for the reduced compressive strengths of concrete in the recycled concrete mixes. Though the concrete mixes are a contributory factor, the results were normalized with the square root function of the concrete compressive strength where a greater proportion was still observed, as shown in Table 4.9 where

the normalized bond strength and the variations within the specimen groups. Whereas (+5 to -13)% was reported within Group 4 specimens, Group 2 specimens reported a wider difference of (+9 to +29)%.

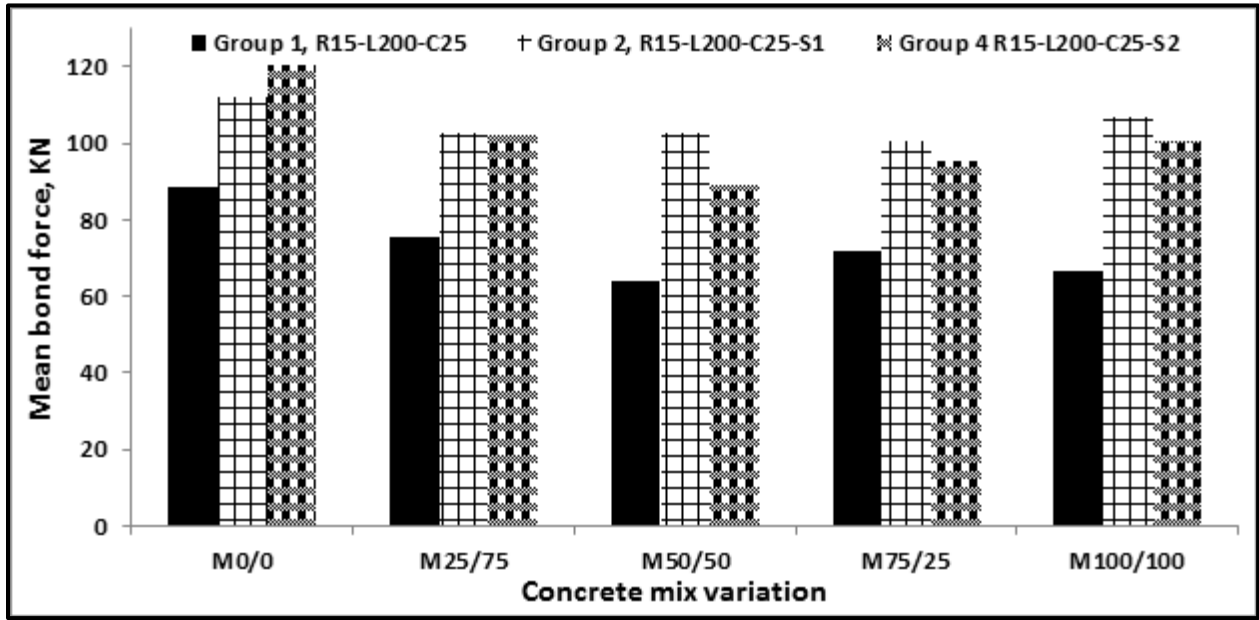


Figure 4.19 Bond force effect on transverse reinforcement and spacing (100mm to 200mm)

Table 4.9 Groups 1, 2 and 4 normalized bond strength effect of using stirrups

	<b>Normalized bond strength (NBS)</b>				
	<b>Concrete mix variation</b>				
	M0/0	M25/75	M50/50	M75/25	M100/100
<b>Group 1(NBS)</b>	1.18	1.24	1.15	1.17	1.20
Variation within mix specimens		5%	-2%	-1%	2%
<b>Group 2(NBS)</b>	1.50	1.70	1.85	1.64	1.94
Variation within mix specimens, (spacing=100mm)		13%	24%	9%	29%
<b>Group 4(NBS)</b>	1.60	1.69	1.61	1.55	1.82
Variation within mix specimens, (spacing=200mm)		5%	0%	-4%	-13%
<b>Group 2</b>					
Variation across (Effect of spacing, 100mm)	27%	37%	61%	40%	61%
<b>Group 4</b>					
Variation across (Effect of spacing, 200mm)	36%	36%	40%	33%	51%

Though there was increased bond capacity recorded in this test experiment, when the transverse reinforcement was used, the wider variations may be due to the fewer samples (2) tested in each type of concrete mixes used. However, more experiments may be carried out to validate or explain the differences. In a similar vein, it can be reasoned that the high strength concrete and brittle nature of the conventional concrete reduced the wedging action between the concrete and rebars, as explained in section 2.1.3. Also, the ACI Committee 408, (2003), confirms that placing additional stirrups beyond what is needed to cause splitting instead of the pullout failure, may become “progressively less effective”. Thus spacing of stirrups is critical in evaluating the bond capacity in any future work.

#### ***4.7.1 Effect of transverse reinforcement (stirrups) on bond contribution***

The total bond force is thus the sum of concrete contribution ( $T_c$ ) of the bond force without the transverse reinforcement and the steel contribution ( $T_s$ ) which is the additional bond force provided by the transverse steel. The transverse steel contribution is dependent on the rebar properties (cross-sectional area, yield strength, etc) crossing the crack planes from the bonded rebar and the concrete strength. It is also worth noting that transverse reinforcement does not generally yield and has been proven in several experiments since it only delays the crack propagation than being under tension due to the bond from concrete (ACI Committee 408, 2003).

As can be observed in Table 4.9, except for the conventional concrete mix, all the recycled concrete mixes recorded additional bond strength when the spacing was reduced from 200mm to 100mm. This confirms the general theoretical background of increased bond when using stirrups but not proportionally with the reduced amount of spacing from 200mm to 100mm.

Table 4.10 Group 1, 2 and 4 bond strength contribution from stirrups

	<b>Bond Strength, MPa and contribution from stirrups</b>				
	<b>Concrete mix variation</b>				
	M0/0	M25/75	M50/50	M75/25	M100/100
<b>Group 1</b>	8.81	7.49	6.36	7.16	6.62
<b>Group 2-L200-S100</b>	11.16	10.23	10.22	10.04	10.65
Stirrups contribution, (spacing=100mm)	2.35	2.74	3.86	2.88	4.03
<b>Group 4-L200-S200</b>	11.98*	10.18	8.88	9.51	10.02
Stirrups contribution, (spacing=200mm)	3.17*	2.69	2.52	2.35	3.4

\*One specimen fractured and was ignored in the results

As pointed out in the literature, no studies investigated the bond capacity of recycled structural concrete when stirrups were placed within the bonded region, but the RILEM twin-beam bond study by Pandurangan et al., (2016) which is close to this experiment also omitted the effect of stirrup spacing. However, when using conventional high strength concrete mixes of 65MPa with 25M rebars in splice beams, Hamad & Machaka, (1999) reported bond strengths in between 7.87 to 10.11 MPa when the stirrup spacing was from 102 to 305mm, which is comparable to this experimental results (8.88 to 10.65 MPa) for recycled structural concrete of 35MPa. In addition, the increased bond as a result of the stirrups presence and contribution was (0.73 to 2.97) MPa whereas this experiment demonstrated a minimum of 2.88MPa and 2.35MPa for the M75/25 recycled structural concrete mix. It is worth noting that the stirrups used in this experiment and that of Hamad & Machaka, (1999) were both 10M rebars. The foregoing is an indication that the bond capacity of recycled structural concrete as in this experiment may perform similarly in bond as conventional concrete.

#### **4.7.2 Effect of transverse reinforcement on cracking load and cracking behavior**

The initial and first cracks in all the beams occurred at the tip of the loaded end as in previous specimens when the rebars were tensioned. As can be observed in the crack album,

Appendix J and Appendix L (Group 2 and Group 4), the cracks were generally finer (less than 0.2mm) for the conventional mixes with some occasional transverse cracks compared to the specimens in Group 1. It can also be observed that due to the presence of the transverse reinforcement at the loaded end, the specimen faces were generally brittle (with mass concrete pulling out of place at the loaded end, see the summary of specimens in Appendix J) compared to the test face where the cover splitting cracks propagated longitudinally. A close-up fine crack and transverse reinforcement are shown in Figure 4.20. All the specimens in Group 2 and Group 4 failed in splitting except one specimen where the rebar fractured while testing. However, this occurrence was not expected but the yielding of the rebars of all the companion specimens is an indication that fracturing of the rebars was inevitable and could have occurred in any of the specimens in the groups.

The general trend of the first crack load shown in Figure 4.21 for the stirrup spacing at 100mm and 200mm were similar in range since all the specimens had 10M stirrups at the face of the beam loaded end. It can also be observed that the maximum splitting load for the specimens without transverse reinforcement was within the first cracking loads of the specimens with transverse reinforcement. This behavior supports the theoretical concept of a delayed crack formation and propagation when stirrups are introduced in beams and hence increasing the beam stiffness as would be discussed further on the load-slip behavior of the specimens.

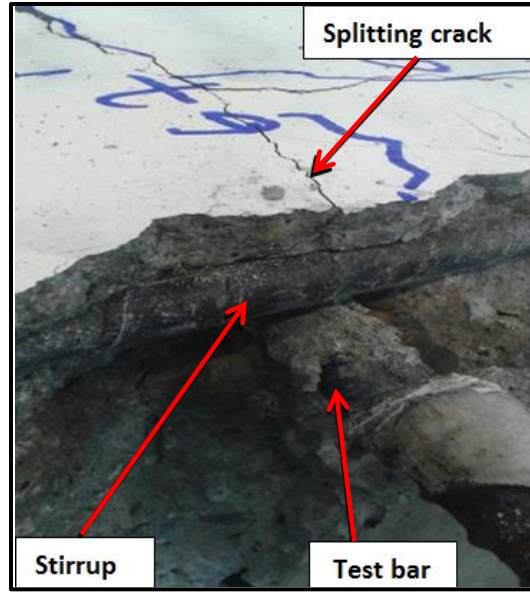


Figure 4.20 Splitting failure of concrete cover with stirrups

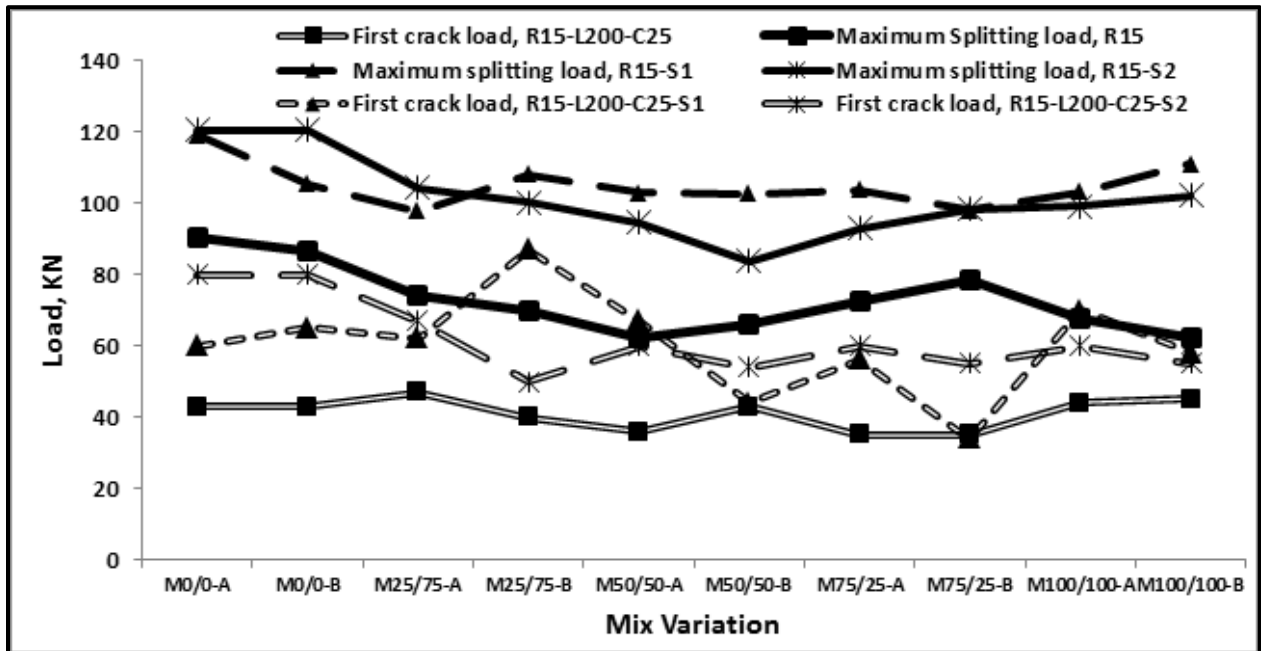


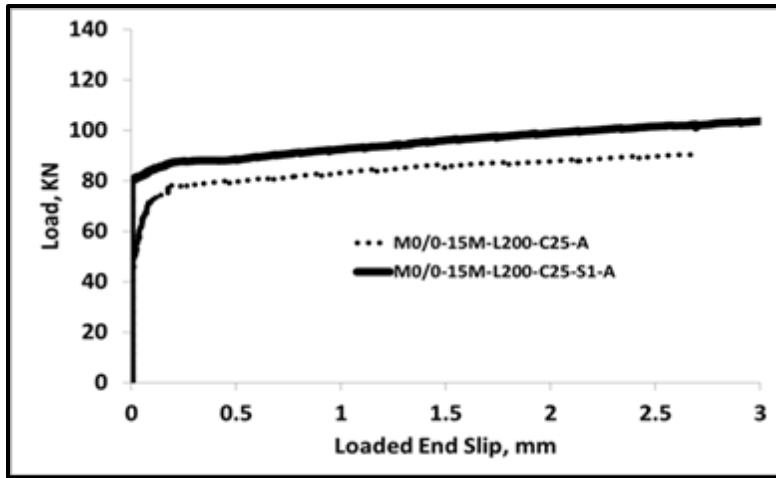
Figure 4.21 Trendline of the first crack and splitting loads for Group 1, 2 & 4 (Effect of stirrups/spacing)

### ***4.7.3 Effect of stirrups spacing on bond force (load) and slip curve***

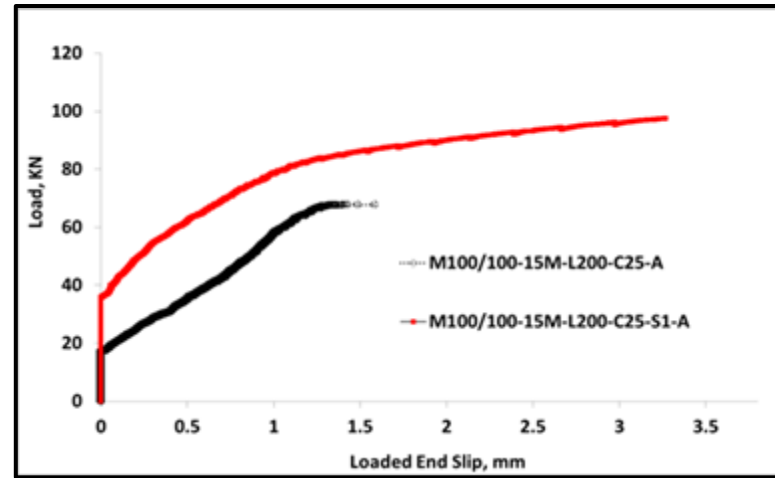
The load slip curves in Figure 4.22 shows the slip behaviour of the pair of mix specimens based on the use of stirrups. As can be seen Figure 4.22-A the M0/0-S1 specimen increased in both load and slip when compared with M0/0 with no stirrup confinement. This confirms the ductility of the beams with stirrups and is expected since, in conventional beams, the stirrups presence not only makes a beam ductile but also reduces the occurrence of shear failure. Similar behavior was also observed when M100/100 was compared and shown in Figure 4.22-B. However, the slip started occurring after a load of 20kN when there were no stirrups but for the specimen with stirrups, the slip occurred around 40kN load. Similar load-slip behavior was also observed in Figure 4.22-B. Thus the presence of the stirrups increased the slip of the rebar and similar can also be observed in Figure 4.22-A. However, a similar slip was observed when mix M50/50 (Figure 4.22-C) was evaluated. Though this behavior is expected in practical experiments, the final slips and load at failure confirm that the specimen with stirrups was more ductile in behavior when compared to a similar M50/50 specimen without stirrups.

A comparable behavior of ductility was again observed when the M0/0 was compared to M25/75-S1 where the stirrup containing specimen not only resulted in higher splitting loads but increased slip as well. The unconfined specimen of M100/100 when compared with the confined (stirrups) specimen with mixes M50/50 and M100/100 as in Figure 4.22-F showed that the M100/100 specimen performed as a stiffer beam where the slip started occurring around 40kN whereas for the confined and unconfined specimens of M50/50 and M100/100 the slips started at loads below 20kN.

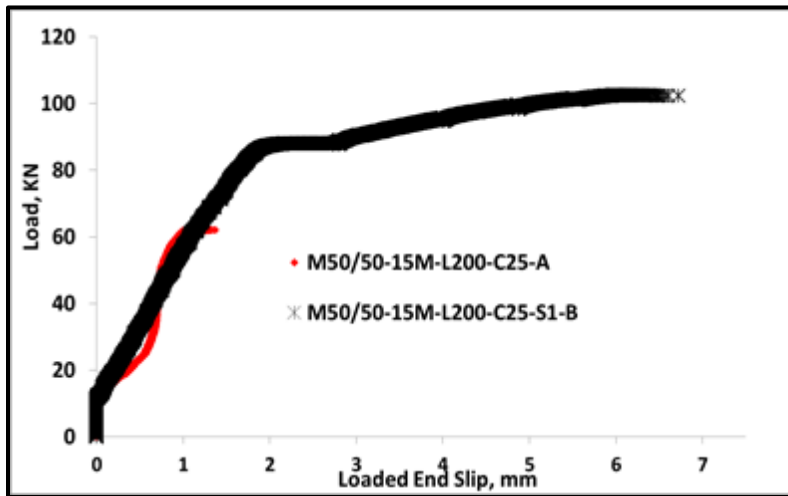
The observations of load and slips can be concluded that the use of quality recycled coarse and fine aggregates did not largely impact the bond-slip behavior and thus the use of stirrups enhanced the beam bond force while the spacing of the stirrups also marginally influenced the bond performance.



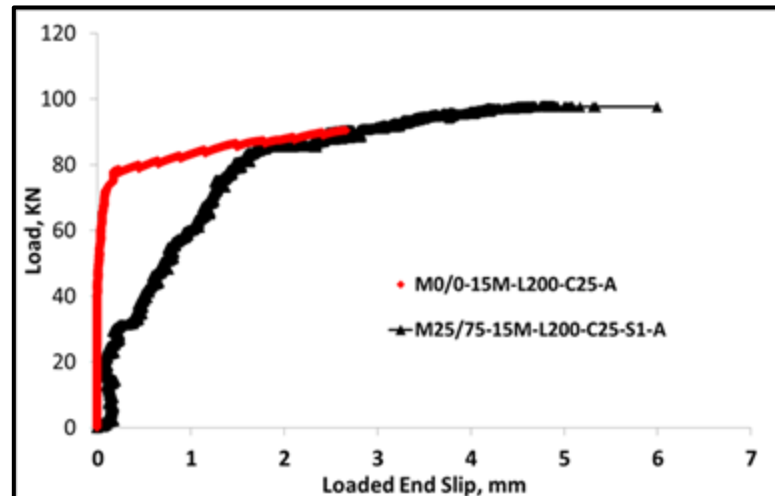
A



B



C



D

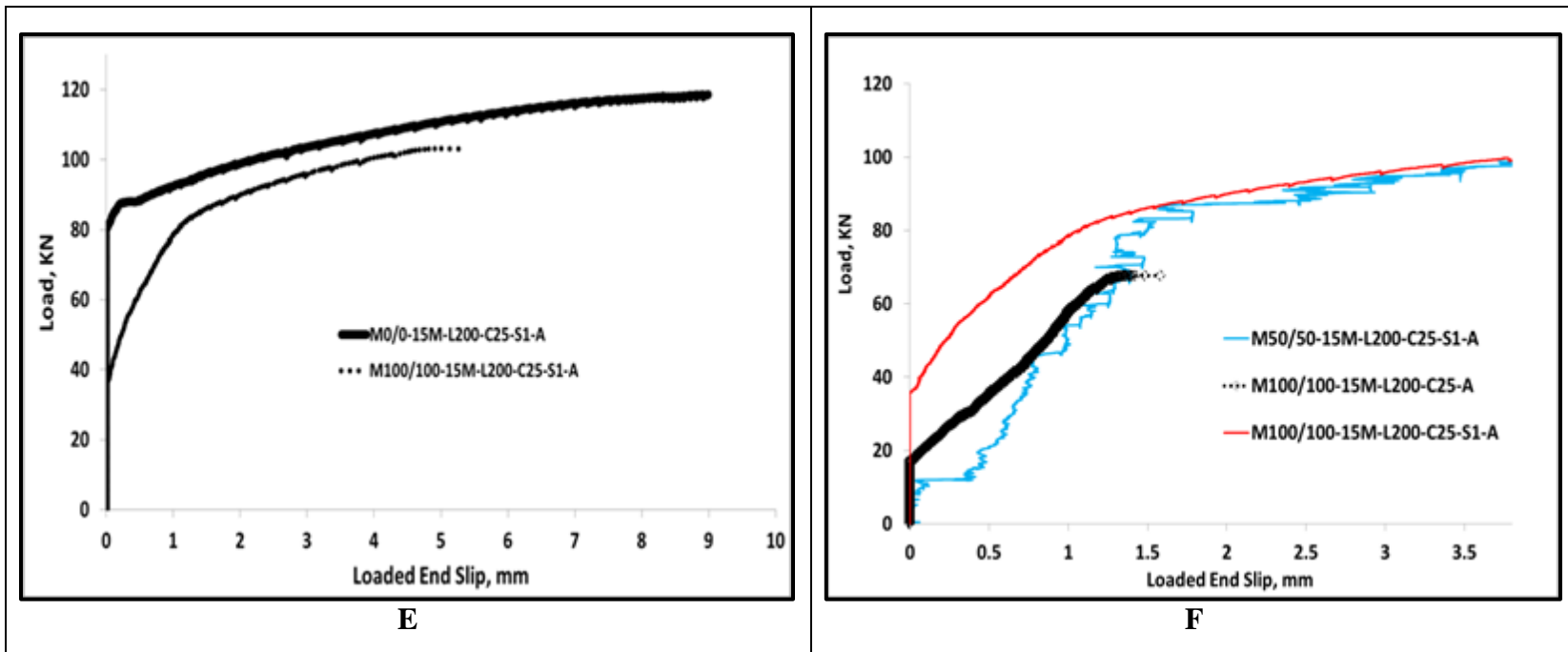


Figure 4.22 Bond slip effect on transverse reinforcement and spacing on concrete mixes

## **CHAPTER 5: EMPIRICAL EQUATIONS AND STATISTICAL MODELLING**

### **5.1 Background**

The use of descriptive and design (empirical) equations is predominant in the literature and can be found in Appendix G and several other documents such as the ACI Committee 408, (2003). Many of the expressions were developed based on the statistical analysis from experimental data, for which a significant one is the Orangun, Jirsa and Breen (1975, 1977). Prior to this development, the ACI 318-71 code was one of the first in North America to introduce the concept of development length (rebar yielding) when a rebar is anchored in concrete, which was meant to fulfill both the flexural and bond requirement in structural elements. However, the concept of bond stress has taken precedence over the flexural concept in structural elements.

Though the concept of development lengths is paramount and is fundamentally required to highly stress rebars to yield, it also causes splitting of thin sections of the surrounding concrete (ACI 318M-11). To this end, an average bond resistance over a full development length of the reinforcement has become more meaningful, since all bond tests use an average bond resistance over an embedment length of rebars, and unaccounted for variations exist around the bond stresses and flexural cracks (ACI 318M-11).

Thus, the use of rebars to achieve the purpose of yielding through development length dovetails into the economy of construction works as well as aiding the structural integrity and detailing of reinforcement at rebar terminations in splices and joints. Though several types of concrete properties shown in Table 2.1 and cited in ACI Committee 408, (2003) have proven to

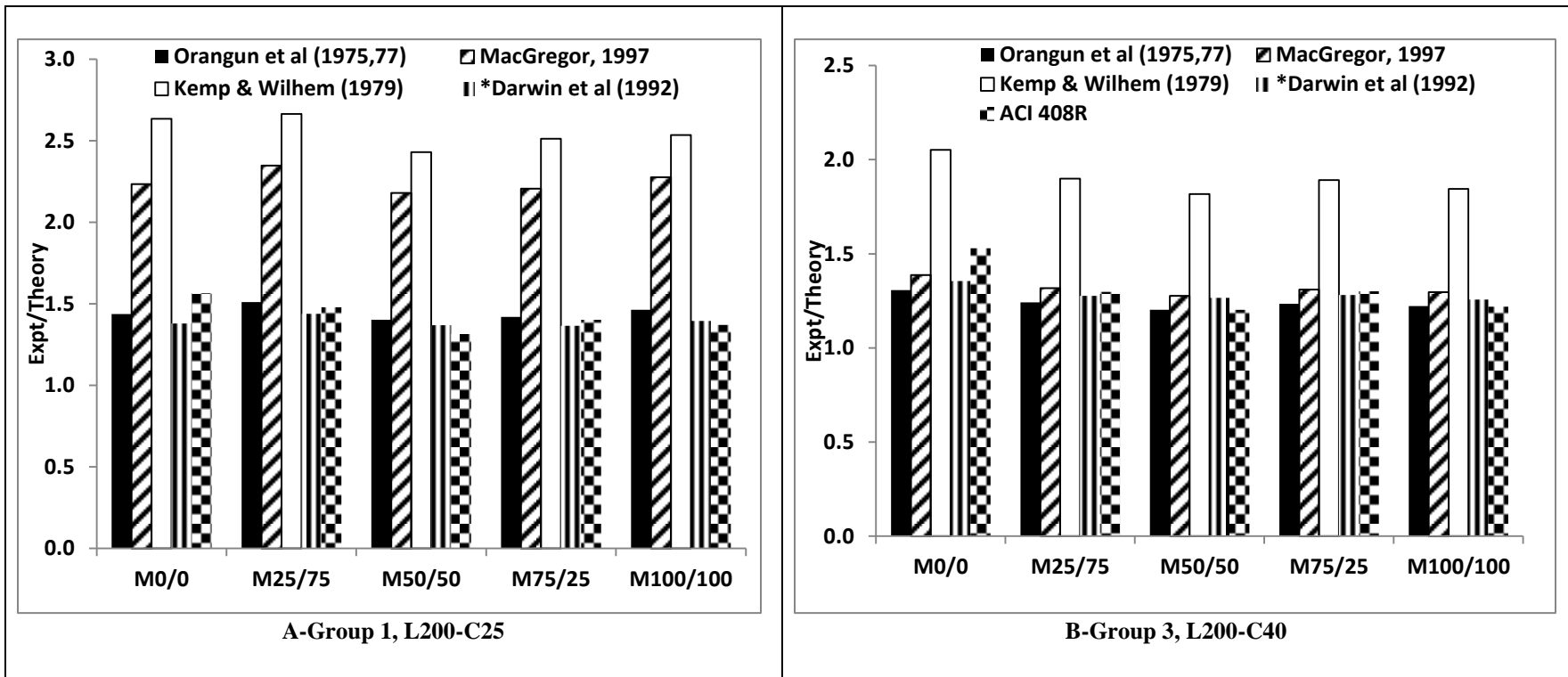
affect the bond capacity, the need to validate this when using recycled structural cannot be overemphasized since:

- a- There is a reduced density of recycled aggregates and recycled concrete due to the attached mortar as observed in this experiment and the literature ( Kim et al., 2015).
- b- Lightweight aggregates have density modification factors to account for development length as found in ACI 408 1963, ACI 408 1979 and ACI 408 2003
- c- The processing of recycled aggregates can significantly affect any remaining amount of the attached mortar.

This chapter considers five descriptive and design equations and undertakes an in-depth statistical analysis of the considered variables (cover, bar size, bond length, and concrete strength) to predict the bond strength based on the experimental data.

## **5.2 Descriptive Equations**

The five descriptive equations (shown in Appendix G) used in determining the compliance of the experimental recycled structural concrete are illustrated in Figure 5.1 and has been demonstrated to largely comply with the empirically computed bond strengths. Except for Group 6 (Figure 5.1-D where marginal bond ratio (less than 150%) was computed for all the mixes except when using the MacGregor equation MacGregor, (1997) all the other bond ratio was more than 150%.



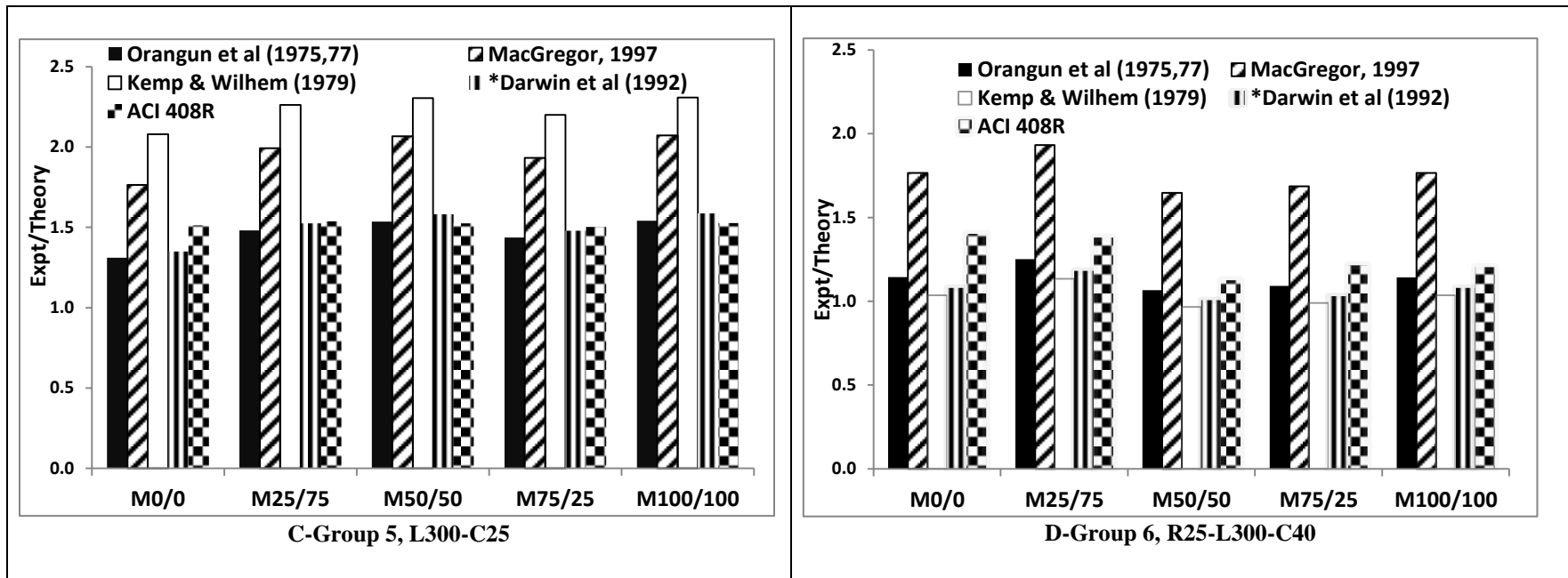


Figure 5.1 Bond ratios of descriptive equations compared with recycled concrete mixes

### **5.2.1 Summary discussions on descriptive equations**

From the graphs in Figure 5.1, it can generally be concluded that using quality recycled structural concrete may not need any correction factors based on the experimental data in this research. This observation supports the work of (Robert et al., 2017; Sadati et al., 2017) which showed that recycled structural concrete, in general, did not need correction factors in order to develop the rebars. In contrast, the works of Kim et al, (2012) proposed a correction based on the MacGregor's (1997) model of determining the bond strength in recycled concrete. However, it is important to note that the test method adopted was a pullout method and recycled aggregates used were also from the laboratory.

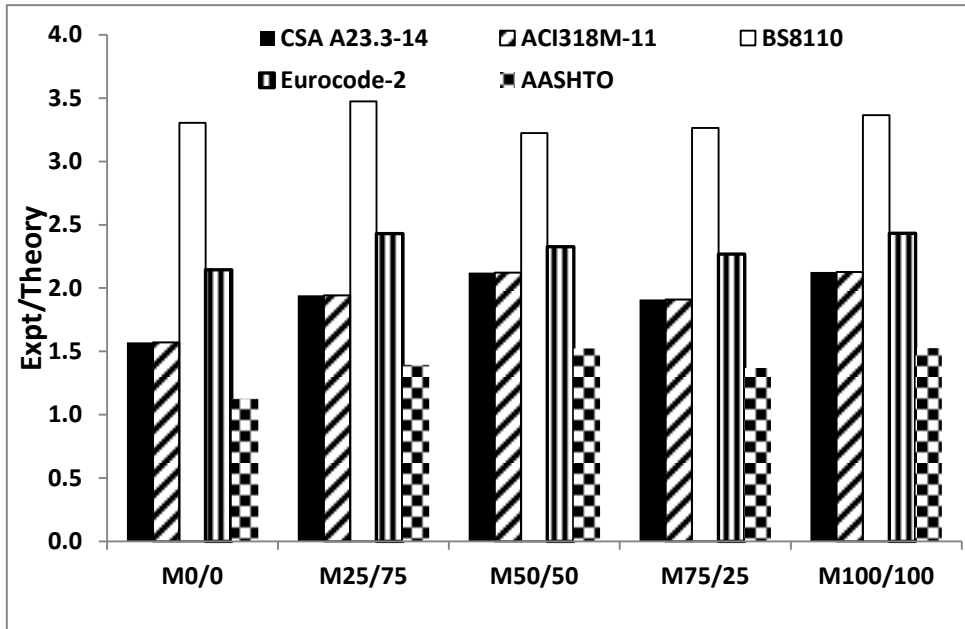
On the other hand, the ACI 408-03 reports similar bond strengths for lightweight aggregates and describes the state of art leading to the use of a modified factor as “paucity”. After that, extensive research by Graybeal in Highway, (2014) concluded that for lightweight aggregates (density of less than  $1920\text{kg/m}^3$ ), the descriptive equation in ACI Committee 408-03 requires some modifications to correct and achieve development length but not the design expression contained in ACI 318M-11.

Overall, divergent opinions and conclusions exist for the need of modification factors if the descriptive equations are to be considered but this experiment supports the fact that no modification factors are required.

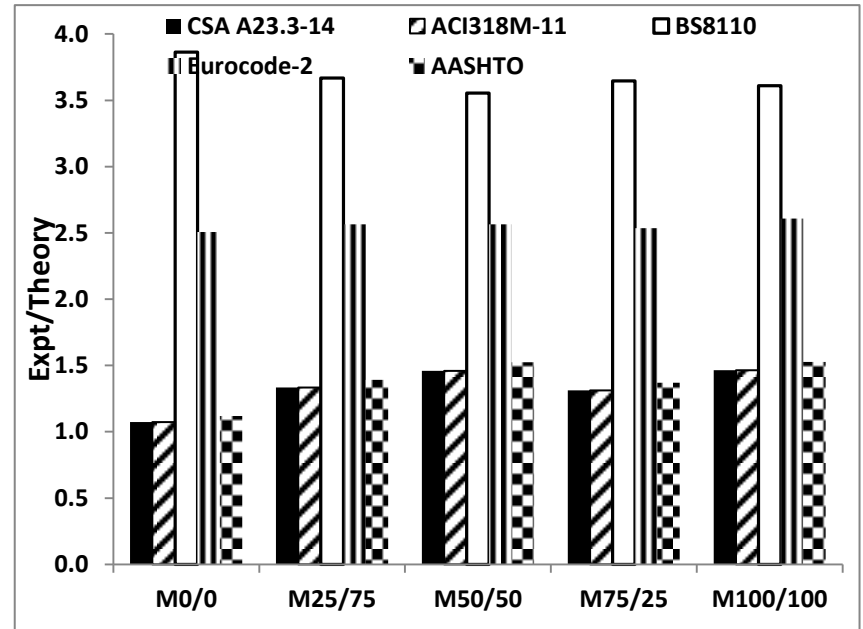
## **5.3 Design Equations**

The basic design provisions for bond and anchorage lengths for rebars, splices, bends, and hooks are generally outlined in Codes of Practice for conventional concrete structures. In both the ACI 318M-11 and CSA A.23.3-14 the content can be found in Chapter 12 of both to guide in

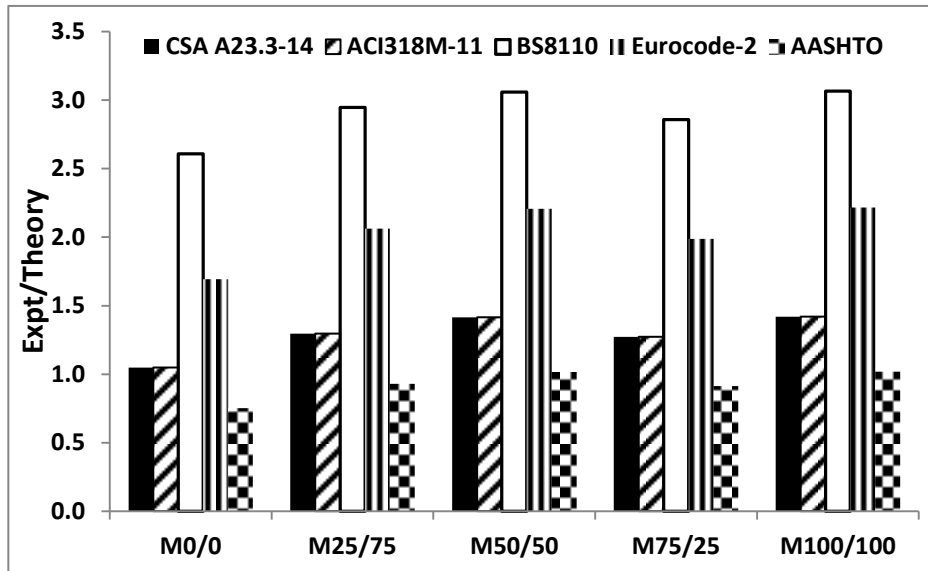
the safe design of structures. In this section, the experimental results were computed as average bond strength and compared with the code of practice provisions taking cognizance of the detailing requirements as per the experimental test specimens.



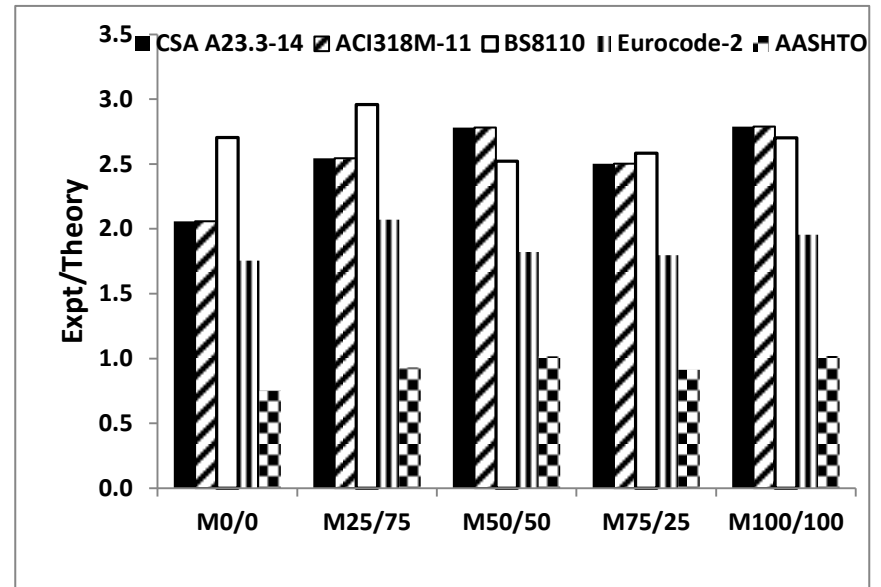
A-Group 1-R15-L200-C25mm



B-Group 3-(R15-L200-C40mm)



**C-Group 5-R15-L300-C25mm**



**D-Group 6-R25-L300-C40mm**

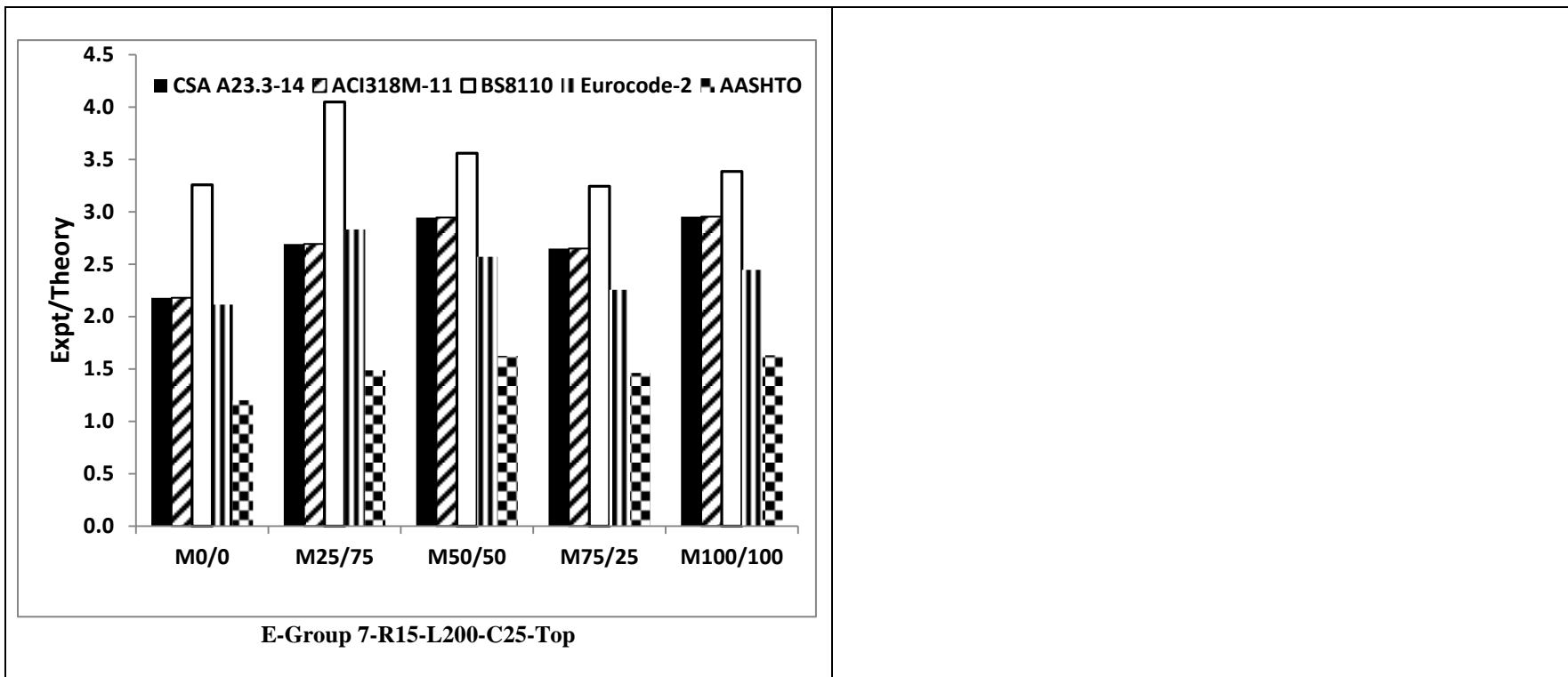


Figure 5.2 Bond ratios of design equations compared with recycled concrete mixes

### **5.3.1 Design equation using ACI 318M-11 and CSA A23.3-14**

Though the ACI 318 and the CSA A23 development length equations appear different they are mathematically the same and the governing coefficient which shows the results are also the same.

In Figure 5.2 (A&B) it can be observed that the increase in concrete cover for the conventional concrete resulted in a reduced bond efficiency from about (157 to 107)% of the experimental/theoretical which was expected because of the cover factor,  $d_{cs}$  which is a denominator and hence reduces the development length required. However, the bond force increased as discussed in Chapter 4 was within a similar range of reduction. For the specimens within Group 1, the RCA mixes showed higher bond efficiency (190 to 210)% compared to the conventional concrete of 157%. A reduced range of bond efficiency was obtained for Groups 3 and 5 (127 to 146)% RCA specimens, whereas a further increase was observed in Groups 6 and 7 (250 to 300)%. The observation confirms the conservativeness of the ACI 318 and the CSA A23.3 in calculating the development length but it is marginal when the cover and bond length is increased which confirms that the development length equation can closely predict the experimental results as seen in Groups 3 and 5 specimens. It also further confirms the economic advantage of considering all the factors as outlined in Table 2.1 to provide an optimum anchorage and development length.

### **5.3.2 Design equation using BS8100**

The BS8100 provision on the bond is a simplified approach and does not consider many variables contrary to the ACI 318 and CSA A23. It can be observed from Figure 5.2 that all the experimental and predicted ratios were generally high (above 250%) for any of the changed

variables from the experiment. However, in respect of the bond performance within the specimen groups, there were no significant variations from the conventional concrete bond calculations but the variations were mainly from the experimental average bond strength values obtained, which was expected.

Nevertheless, certain detailing requirements are critical to be considered when using such a code. An example is a top cast, where the BS code makes a provision of 1.4 in detailing requirement for laps at the top cast position for cases where the minimum cover is less than twice the length of the lapped rebars. Thus for the top cast rebars in Group 7 the average bond strength of when considering the 1.4 factor resulted in a bond efficiency of 230% for the conventional concrete whereas the recycled concrete mixes resulted in (230 to 290)% bond efficiency.

Thus the recycled concrete mixes used in the experiment have been conservatively demonstrated to satisfy the use of BS8100 in bond efficiency when considering the variables in this study.

### ***5.3.3 Design equation using Eurocode-2 and AASHTO***

Figure 5.2 (A-E) showed that the bond performance based on the BS 8100 was trailed by the Eurocode followed by the AASHTO code provision for all the groups and variables investigated in this experiment. Except for Groups 5 and 6 where the conventional concrete mixes bond efficiency was 75% in each case for the AASHTO, the recycled concrete mixes were generally above 90% to almost 160% for the AASHTO and can be concluded as conservative within the limits of this experimental work. However, the Eurocode-2 bond efficiency was a minimum of 169% for the conventional concrete whereas the recycled concrete mixes were minimum 180% up to about 280%. Thus the recycled concrete mixes used in the experiment have been

conservatively demonstrated to satisfy the use of Eurocode and AASHTO for bond efficiency when considering the variables in this study.

It must be noted that the Eurocode provision on bond performance for poor bond condition (Clause 8.4.2) is only attributable to rebars positioned above 300mm and in slip forms, and is not comparable to the generic provision in ACI 318M-11 and CSA A23.3 poor bond provision.

On the other hand, the AASHTO code for development length provision **Appendix G** is a direct equation of the earlier ACI 318-63 version and requires an update since new experimental data to support the development length of rebars are currently available.

#### ***5.3.4 Summary discussion of design equation compliance***

Because of the difficulty in finding two similar studies with the same variables investigated in research, this section will delve into discussing the summary of findings in Appendix C with a focus on using 100%RCA and/or partial replacement of RFA with NFA.

The 100% recycled quality aggregates used by Morohashi, Sakurada, & Yanagibashi, (2007) met the specification requirements of JIS A-5021-H and was used for the bond testing. The conclusion was that the bond splitting strength of RCA was similar to the NCA concrete, and the NFA, and hence the substitution rate of RFA as used in this experiment was not critical but rather the high-quality RCA is paramount. It may be inferred from the research that the aggregates and concrete were produced from the industry, and hence confirming the objectives of this research in using quality recycled aggregates for concrete to achieve a good bond between the concrete and rebar.

The above was also buttressed by Fathifazl et al., (2012) who concluded that by modifying the experimental mix design and using 100% RCA, the CSA A23.3-04 development length equation can be used satisfactorily without modification. Similarly, Hamad et al., (2018) confirmed that the ACI 318-11 does not need modifications when using 100% RCA. On the contrary, Arezoumandi, Steele, & Volz, (2018) concluded that only 50% RCA can be used to achieve a similar bond strength when using the ACI 318 development length relationship and emphasized the need to be cautious on the substitution rate (50% maximum) of RCA for structural concrete to achieve a good bond.

As a departure from using dense natural aggregates, lightweight aggregates have also been demonstrated in some experiments as structural concrete and performs similarly in bond, when compared to natural aggregates and complies with ACI 318-11 (Highway, 2014). However, the same report concludes that the AASHTO Bridge Design Code requires some modifications to meet the design specification criteria. This is in tandem with the observation in this thesis in Chapter 5.

#### **5.4 Proposed code provisions**

Because of the divergent opinions and based on the experimental evidence contained in this thesis, there may be no need to modify the current bond provisions in the design equations considered here until some contrary and compelling evidence to warrant a change. More importantly is when the recycled aggregates, coarse, and fine have been processed and tested to achieve a similar quality as required by ASTM C33 (ASTM, 2018). However, the AASHTO development length provision may need updating since a majority of recycled concrete is

expected from demolishing of road and bridge infrastructure and would serve as a huge source of recycled aggregates and concrete.

### 5.5 Statistical analysis and modelling

The statistical summary outputs in Table 5.1 and Table 5.2 show two different regression outputs from Groups 1, 3, 5, and 6 where 40 specimens of bottom cast unconfined rebars were considered.

Table 5.1 was obtained based on the average bond strength whereas Table 5.2 was based on the raw forces resulting in adjusted R-squared\* of 0.68 and 0.21 respectively using Excel statistical regression package. The lower adjusted R-squared=0.21 for the raw forces (non-normalized) compared to the normalized average bond strength confirms the non-linearity of the bond along the bar surface. However, based on the common linearity assumption, Table 5.1 has been used to predict the average bond strength as an outcome for the 40 specimens without transverse reinforcement and presented as equation (2).

$$\tau_b = \left[ -2.34 + 1.6 \frac{c}{d_b} - \frac{0.03l_d}{d_b} + 1.10\sqrt{f'_c} \right] \dots\dots\dots (2)$$

Table 5.1 Regression and ANOVA results of average (normalized) bond strength

Summary	
Multiple R	0.840
R Square	0.706
*Adjusted R Square	0.681
Standard Error	0.700
Observations	40

	<i>df</i>	<i>SS</i>	<i>MS</i>	<i>F</i>	<i>Significance F</i>
Regression	3	42.285	14.095	28.762	1.14E-09
Residual	36	17.642	0.490		
Total	39	59.927			

	<i>Coefficients</i>	<i>Standard Error</i>	<i>t Stat</i>	<i>P-value</i>	<i>Lower 95%</i>	<i>Upper 95%</i>
Intercept	-2.340	1.316	-1.779	0.084	-5.009	0.328
SQRT-f*c	1.096	0.155	7.051	2.82E-08	0.781	1.410
c/d	1.603	0.291	5.505	3.19E-06	1.013	2.194
l/d	-0.026	0.042	-0.623	0.537	-0.111	0.059

Table 5.2 Regression and ANOVA results of raw (non-normalized bond strength)

Summary	
Multiple R	0.522
R Square	0.272
*Adjusted R Square	0.212
Standard Error	25.614
Observations	40

	<i>df</i>	<i>SS</i>	<i>MS</i>	<i>F</i>	<i>Significance F</i>
Regression	3	8844.096	2948.032	4.494	0.0089
Residual	36	23618.32	656.064		
Total	39	32462.41			

	<i>Coefficients</i>	<i>Standard Error</i>	<i>t Stat</i>	<i>P-value</i>	<i>Lower 95%</i>	<i>Upper 95%</i>
Intercept	82.806	48.141	1.720	0.094	-14.829	180.441
SQRT-f*c	15.091	5.686	2.654	0.012	3.559	26.623
c/d	-25.917	10.657	-2.432	0.020	-47.530	-4.304
l/d	-2.236	1.533	-1.458	0.153	-5.345	0.8737

(\*NB-the adjusted R-squared is used where more than one variable is being considered)

The model from the data used was further compared with other descriptive model equations (eg Orangun, MacGregor's expression to determine the RMSE (Root Mean Square Error). Table

5.3 shows a summary and confirms that the proposed model has a lower RMSE and can be adopted in this limited scope of work in this research. In addition, the omission of  $l_d/d_b$  in the MacGregor's equation results in a higher RMSE, and thus some modifications are recommended such as the other compared models.

Table 5.3 Root mean square error (RMSE) of the experimental and descriptive models

<b>Model</b>	<b>RMSE</b>
Experimental Model ( <i>Equation-2</i> )	17.69
Orangun et al (1975,77)	127.00
MacGregor, (1997)	372.87
Kemp & Wilhelm, (1979)	29.54
Combined Model (data in Appendix C)	435.32

Again the model was validated by collating data from 48 experiments contained in Appendix C (Summary table of beam bond test of various researchers using 100%) where only 100% RCA was used and shown in equation 3. The statistical regression and ANOVA output is shown in Table 5.4 and indicates a very low adjusted R-squared (1.1%), high p-values for  $c/d_b$  &  $l_d/d_b$  (shown in Table 5.4) and high RMSE of 435 (as shown in Table 5.3) and thus supporting the proposed model in this research.

$$\tau_b = \left[ 0.787 + 0.131 \frac{c}{d_b} - \frac{0.031d}{d_b} \right] \sqrt{f'_c} \quad \text{-----Equation (3)}$$

Table 5.4 Regression and ANOVA results of combined 100% RCA from literature

ANOVA Summary	
Multiple R	0.230
R Square	0.053
*Adjusted R Square	0.011
Standard Error	0.223
Observations	48

	<i>df</i>	<i>SS</i>	<i>MS</i>	<i>F</i>	<i>Significance F</i>
Regression	2	0.124	0.062	1.251	0.296
Residual	45	2.236	0.050		
Total	47	2.360			

	<i>Coefficients</i>	<i>Standard Error</i>	<i>t Stat</i>	<i>P-value</i>	<i>Lower 95%</i>	<i>Upper 95%</i>
Intercept	0.787	0.118	6.665	3.2E-08	0.549	1.025
c/d	0.131	0.084	1.562	0.125	-0.038	0.301
l/d	-0.003	0.005	-0.690	0.494	-0.013	0.006

## 5.6 Bond behaviour and ACI 408 database comparison

### 5.6.1 Background on bond behavior

The bond strength between concrete and rebar is generally assumed to be average over the anchored length of rebar. However several experimental tests have demonstrated that the bond strength varies along the embedded rebar which depends on the type of experimental method employed to quantify the bond strength. In addition, the location and initial occurrence of a crack influence greatly the maximum bond strength along the rebar. Thus the bond problem between concrete and steel is a complex phenomenon and has been difficult to determine exactly not only through experiments but also mathematical theories. Though the mathematical theories have not yielded a simple solution based on a second-order differential function, the implied boundary conditions have also contributed to its complexity (Lutz & Gergely, 1967; Mains, 1951; Perry & Thompson, 1966; Watstein, 1947).

In addition, numerical analysis has been used in understanding the bond behavior by Lutz, (1970) where the underlying assumptions of the bond between concrete and rebar were by both failure/separation between concrete and steel at a crack, in addition to crushing of the concrete. Similar bond behavior of failure and separation is reported in ACI 408-03 and was observed in this experiment and shown in Figure 5.3, where the concrete at the loaded end separated from the rebar at the loaded end without crushing of the concrete. This effect tends to reduce the effective bond length.

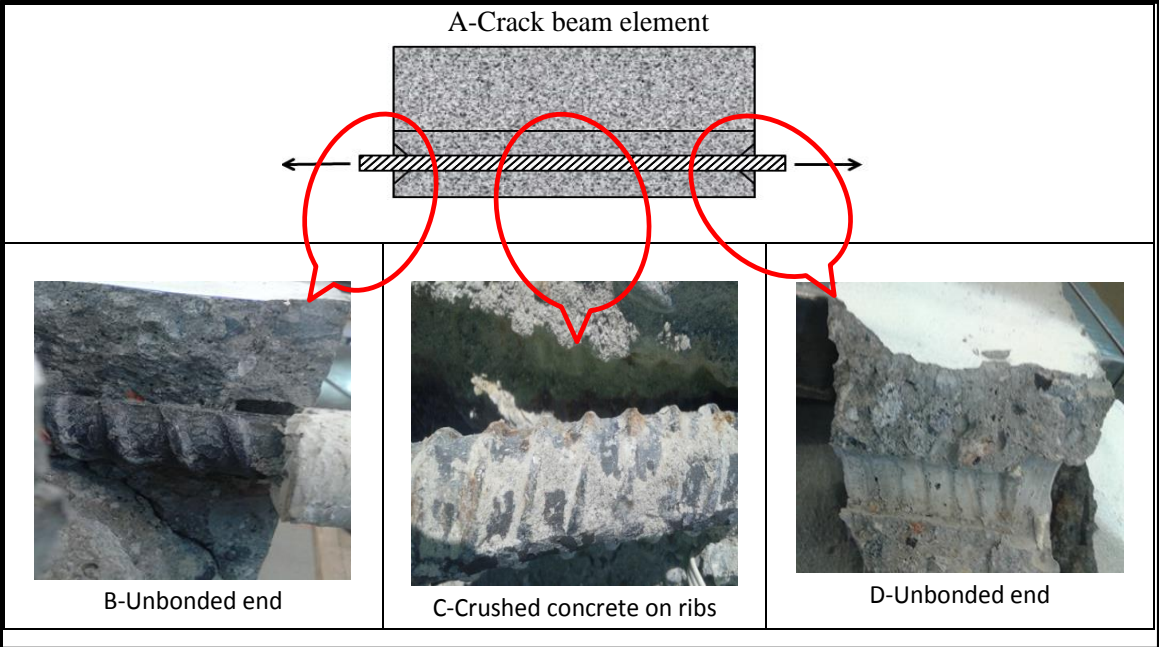
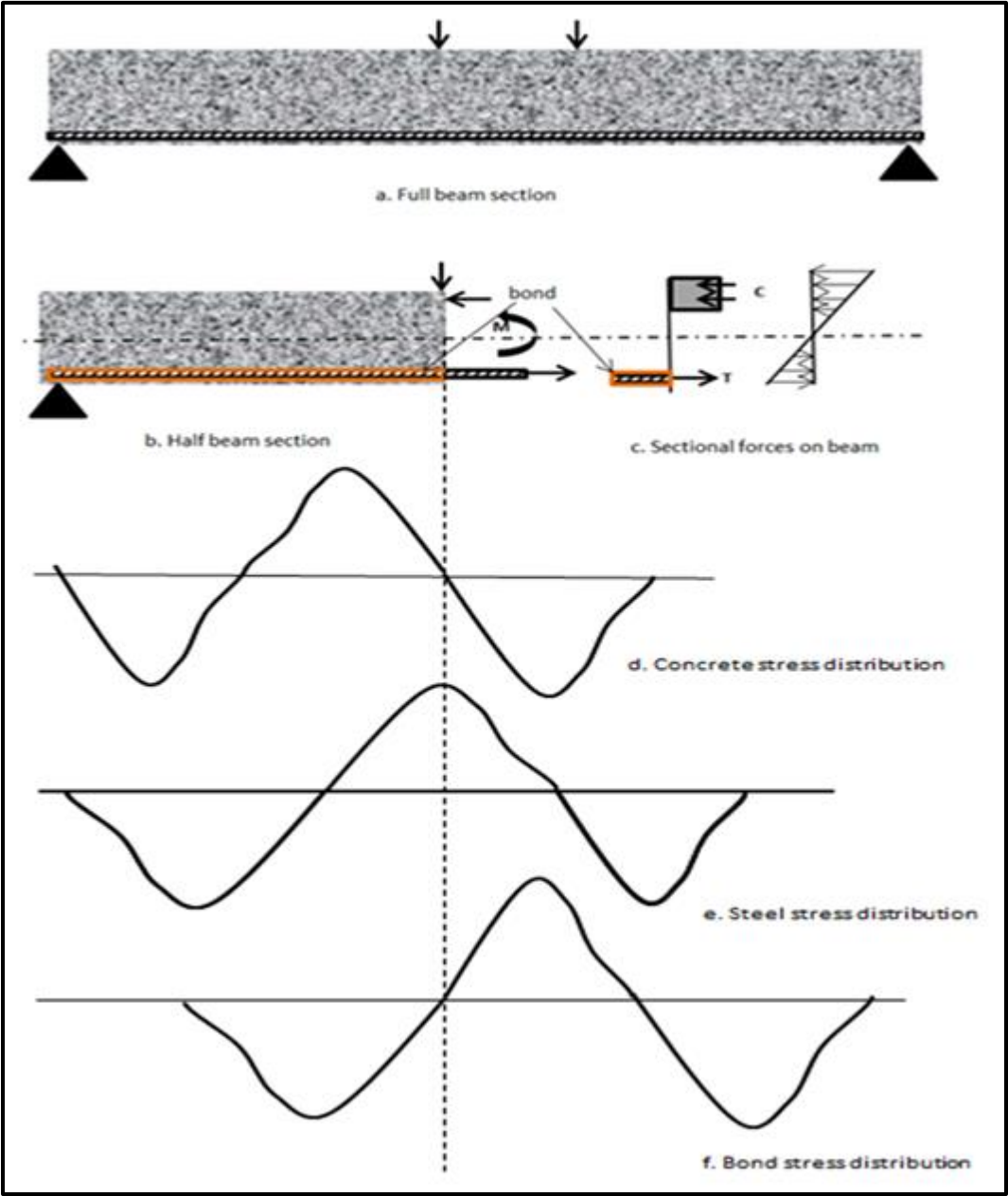


Figure 5.3 Experimental crack/separation and crushing failure of specimens

Figure 5.3 supports the assertion that though the rebar embedded length is 200mm, effectively less than 200mm is truly bonded to the surrounding concrete during load transfer from steel to concrete as the crack formation and concrete separation occurs at the loaded and unloaded ends. From Figure 5.4, the stress distribution for steel concrete and bond varies along the embedded

length and the distributions are non-uniform compared to the general assumption of average bond strength over the anchorage length.



a, beam free body diagram; b & c, concrete, and steel section analysis, d, concrete stress distribution e. Steel tensile stress distribution, f. Bond stress distribution

Figure 5.4 Reinforced beam section and stress distribution

### **5.6.2 ACI 408 database comparison**

The extensive research on bond since 1990 has demonstrated wide differences in results on bond test which may not only be due to the type of concrete as a material but other factors (such as fracture energy, slump, etc) which affects bond but not generally considered in design (ACI-408R, 2003).

Juxtaposing new test results of an experiment with a reliable experimental database in the case of new material such as recycled structural concrete would be important since the database compilation by the ACI committee 408 and the CEB task group VI on bond currently requires an update. The experimental test data compiled using test beams with both rebars and concrete in tension has been used for over four decades and new research data has become available. However, some researchers Gaurav & Singh, (2017); Sadati et al., (2017) have earlier compared test results when using recycled structural concrete, and it is important to undertake a similar comparison. The comparison is important since empirical bond models and design equations have proven generally conservative when using recycled structural concrete as demonstrated in Chapter 5. The ACI 408 database plot and the experimental plot in this research is shown in Figure 5.5, Figure 5.6 and Figure 5.7, and have been found to be tandem with all previous work on conventional concrete in the ACI 408 Committee database on bond experiments. However, more experiments are needed especially in Group 7 where the rebars are positioned at the top (more than 300mm) to validate the provisions in ACI 408-03, ACI 318-11 and CSA A23.3-14.

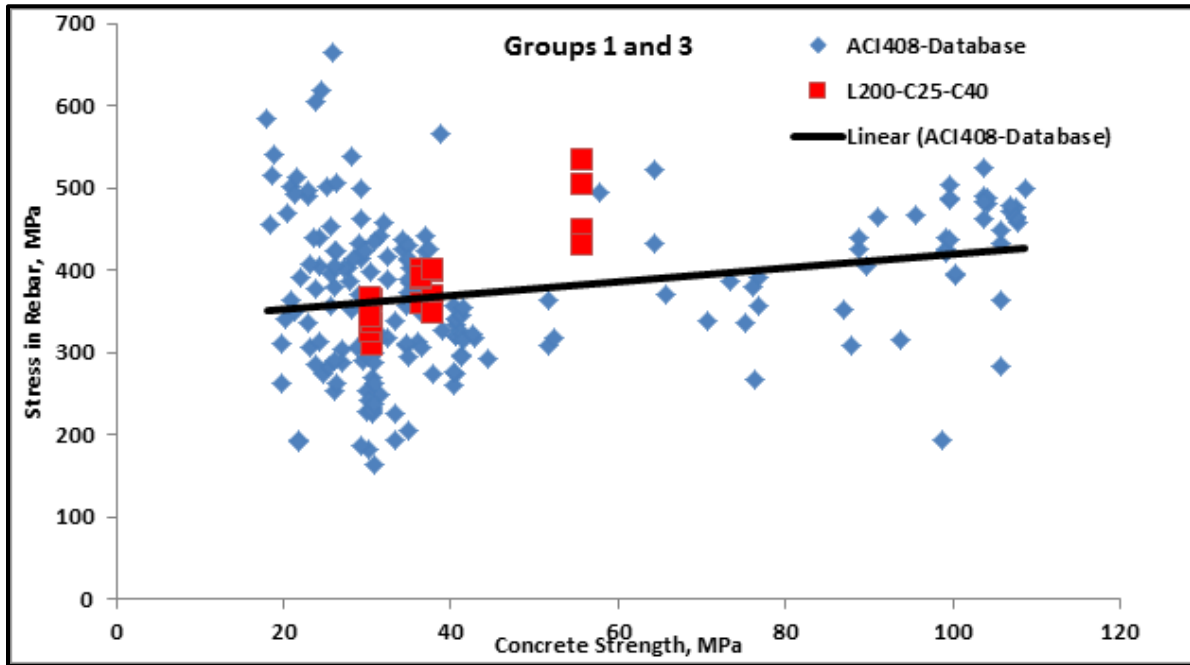


Figure 5.5 ACI 408 Database comparisons for 200 mm bond length for 15M (c=25 mm & 40 mm)

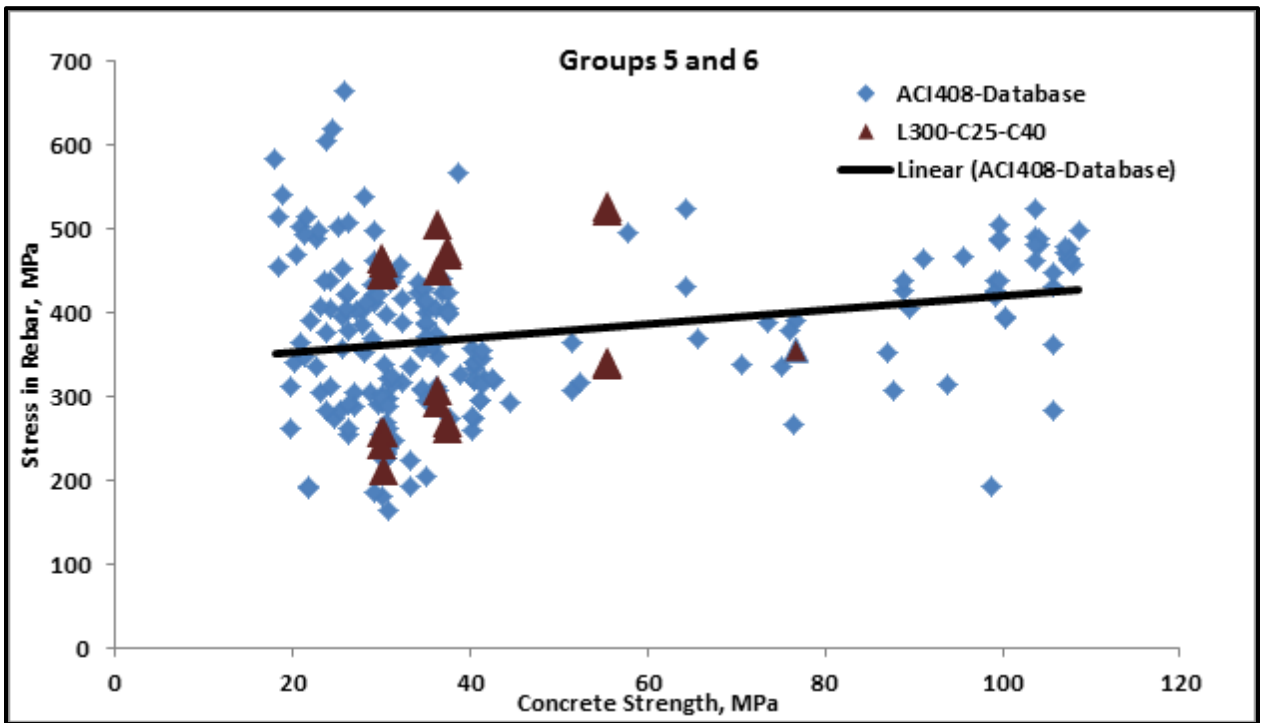


Figure 5.6 ACI 408 Database comparisons for 300 mm bond length (15M and 25M)

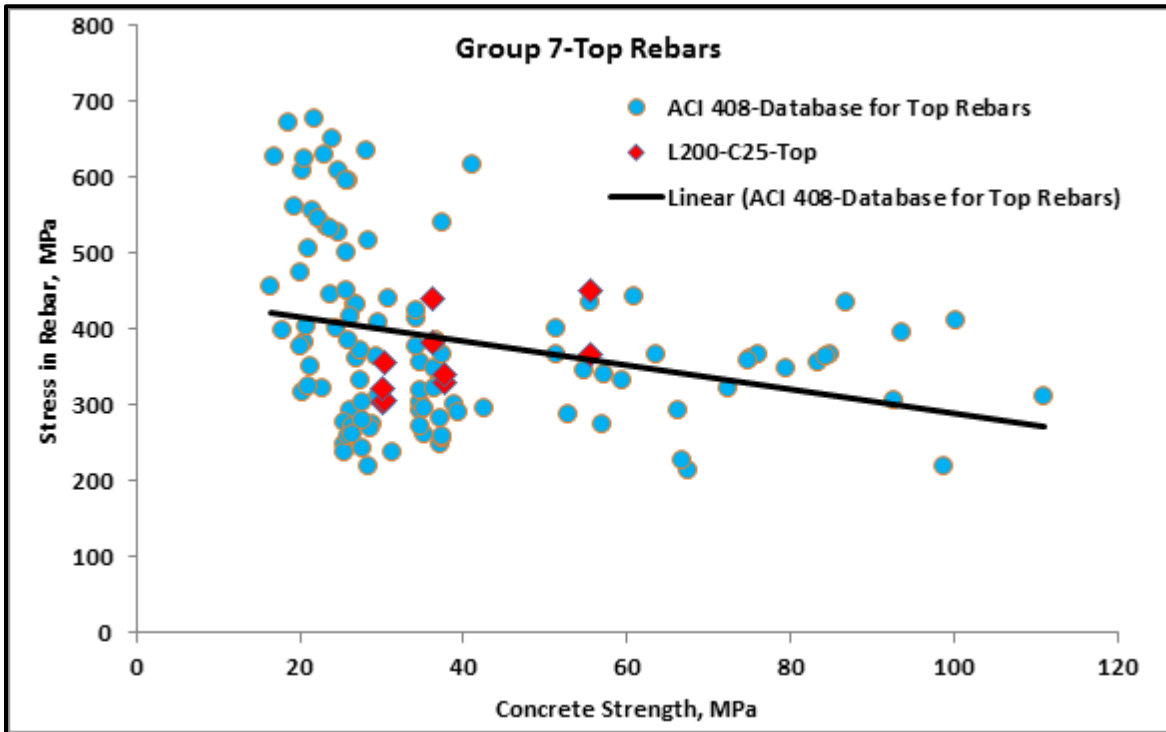


Figure 5.7 ACI 408 Database comparison for top rebar positions

## CHAPTER 6: CONCLUSIONS, LIMITATIONS, RECOMMENDATIONS FOR FUTURE RESEARCH AND NOVELTY

### 6.1 Conclusions on studied effect on bond variables

The experimental analysis of the 70 beam-end specimens that were tested to determine the bond between recycled structural concrete and rebars under monotonic loading can be concluded and presented under the following headings of the critical variables.

#### 6.1.1 *Effect of rebar cover on bond Group 1 and 3)*

- Bond vs slip performance can generally be concluded as similar for both the recycled and conventional structural concrete.
- The first crack load of conventional and quality recycled concrete is similar.
- The differences in the normalized bond strength between conventional and recycled concrete mixes were marginal. When the cover was 25mm the normalized bond strength was 1.18 and 1.20 for the conventional concrete and 100% recycled concrete specimens while it was 1.20 and 1.29 when the cover was 40mm for the same respective specimens.
- A good correlation coefficient was observed using  $\sqrt[4]{f_c'}$  which supports some principal investigations.

#### 6.1.2 *Effect of embedment length on bond (Group1 and Group5)*

- When the embedment length increased from 200mm to 300mm, the average bond force variation generally reduced across all the specimens. On the contrary, the slips increased when the bond length was increased.

- The bar stresses  $f_s$  developed within each pair of the specimens in Group 5 met the minimum development length of 300mm as required by CSA A23.3 and ACI 318M-11 and yielded the entire test bars for both conventional and recycled concrete.
- The normalized bond strength of 1.1 and 0.93 was obtained for the full recycled concrete and conventional concrete mixes respectively. The minimal differences confirm that the quality recycled concrete may perform similarly in bond to the conventional concrete.
- The crack widths were generally wider for the recycled concrete mixes than for the conventional concrete mixes and confirm that the inherent voids in the recycled aggregates used as structural concrete may affect the serviceability of structural elements. However, the effect on bond and crack formation when using quality recycled aggregates were minimal based on the normalized bond strength comparisons and in literature.

### ***6.1.3 Effect of bar size on bond (Group6)***

- The change in bar size generally reduced the bond strength comparatively across all specimens of conventional and recycled concrete. The bond capacity when considering the design standards also showed no effect on the bond when using quality recycled concrete.
- The change in bar size resulted in an increased slip when considering the Mix M0/0 and M100/100 and influenced the splitting crack behavior and hence may impact on the deformation.

- The differences in the normalized bond strength between conventional and recycled concrete mixes were marginal when the bar size increased from 15M to 25M. For the conventional concrete mix, M0/0, the reduced normalized bond strength was -18% whereas it was -20% for the M100/100, and thus confirming the similarity in bond capacity.
- The minimum development length of 300mm is not applicable in a larger sized bar such as 25M and similarly confirmed in (ACI Committee 408, 2003).
- Recycled concrete mixes generally slipped early compared to the conventional concrete mixes and the cracks for the 25M rebars were generally larger than the 15M rebars.

#### ***6.1.4 Effect of bar position on bond (Group 7)***

- There was marginal bond force variation (-6% to +8%) when bottom-placed rebars were compared with top placed rebars. Thus the failure loads of top positioned rebars were similar to the conventional concrete placed in the same position.
- The failure modes of top-placed rebars were more brittle, whereas the companion bottom-placed rebars are less brittle. However, the slips for top-placed rebars started at reduced loads and in some instances just after the beginning of testing.
- The normalized bond strength between the conventional and recycled concrete mixes was similar when the rebar position changed from bottom to top with 380mm depth of concrete. For the conventional concrete mix, M0/0, the normalized bond strength

was -8% whereas it was -6% for the M100/100, and hence confirming the similarity in bond capacity at the increased depth of concrete beneath the rebar.

- The comparison of the test results with design equations met the criteria for the top placed bars and was conservative, for all the conventional and recycled concrete mixes.

#### **6.1.5 *Effect of transverse reinforcement and spacing on bond (Groups 2 and 4)***

- The bond capacity of quality recycled structural concrete in the presence of stirrups was determined and its contribution was within 2.35 to 2.88 MPa whereas these values were between 0.73 to 2.97 MPa for conventional concrete experiments which demonstrated similar behavior.
- Loads were generally greater for the stirrups confined specimens (Groups 2 and 4) than for the specimens without transverse reinforcement (Group 1). The normalized bond strength for the conventional concrete increased by 27% and 36% when the spacing was 100mm and 200mm respectively whereas it increased by 61% and 51% for the 100% RCA and RFA.
- Cracks formed on the confined specimens with stirrups (were generally finer compared to unconfined specimens in Group 1 where there were no stirrups.
- The stirrups confined specimens (in Group 2 and 4) were less brittle compared to the concrete only confined specimens in Group 1
- Slips at the loaded end were generally greater for the stirrups confined specimens than the concrete only confined specimens and was accompanied by both rebar yielding and near ultimate.

## **6.2 Conclusions on effect of bond strength on bond equations and modelling**

The experimental results after analysis provide additional evidence that when structural concrete is produced from quality recycled aggregates it can be compared with several descriptive, design bond model equations as well as the ACI 408 database. A summary of the pieces of evidence and its effects are presented in the subsequent sections.

### ***6.2.1 Effect of descriptive equations***

It can generally be concluded that using quality recycled structural concrete may not need any correction factors based on the experimental data in this research. This has been validated using the most common five descriptive equations where all the equations were conservative compared to the experimental results.

### ***6.2.2 Effect of design equations***

- The analysis in this thesis supports the fact that the ACI 318, CSA A23.3, BS 8110, Eurocode-2 and AASHTO does not generally require modifications except for the instance of specimens in Groups 5 and 6 for the conventional concrete where AASHTO Bridge Design Code may require some modifications to meet the design specification criteria.
- The AASHTO design code formula though simple is an older version of the ACI 318 in 1963 and may require an update or remain the same until a full understanding of bond and rebar development is fully researched.

### **6.2.3 Proposed descriptive model and ACI Database**

- A new descriptive model based on ANOVA and regression analysis from the experimental data has been proposed. The model is similar to MacGregor, Orangun, Jirsa and Breen, Kemp & Wilhelm, Darwin et al and the ACI 408R-03 where the main variables are the cover, bar size, bond length and the compressive strength of concrete.
- The proposed model was validated and proved to have a low RMSE than all the other known models in the context of this experimental results
- The experimental results when compared with the ACI 408 database fitted well within the scope of previous experimental works for both bottom-placed and top placed rebar.

### **6.3 Limitations of this study**

Though this study may have unknown inherent errors and limitations, the following are some highlights:

- Few samples per variable were used, but future studies may focus on an increased and equal number of conventional and 100% recycled aggregates for the concrete production
- There was a wide difference in the conventional concrete strength (55 MPa) and the recycled concrete mix (30-37 MPa). However, quality control of the recycled concrete mixes resulted in minimal variation as this is expected in real life.
- Coring of the specimens was used for compressive strength testing, however, a comparable assessment of both cored and cylinder tests may be useful. Although the

cored specimens could be conservative due to inherent cracks after coring, it may be a preferred option especially if flat end caps of the specimens are ensured.

- Though petrographic and aggregate strength of recycled aggregates exists, similar studies in addition to the bond test could have been done to support the quality of the recycled aggregates.
- Cracks were measured after testing with a ruler, but digitally measuring the crack growth at specified locations during the test will remove any human errors similar to how the pullout force was obtained from the MTS

#### **6.4 Recommendations for future research**

Though the study of the bond is evolving (due to its complexity and variability), using quality recycled concrete not only unveils a new structural concrete material but introduces a new paradigm of quantifying bond. In this thesis many variables have been investigated to unearth the bond behavior, the results have largely proven positive and it is critical to consider the following in the future.

- Concrete cores and cylinder specimens should be obtained in future works to determine if the normalized bond strengths may have any significant impact in the result analysis.
- The effect of bond behaviour under cyclic loading when using quality recycled concrete compared with conventional concrete.
- The effects on the bond behaviour using epoxy coated, corroded, and galvanized rebars need to be investigated since conventional concrete per CSA A23.3 and ACI 318-14 standards require modification factors for rebar development length.

- There is a need to study the deformation effect in beams and its impact on code equations when considering similar quality mixes “M0/0 and M100/100” and when the bar size is also changed since the slipping behaviour changed.
- Additional experiments are needed especially in Group 7 (where the rebars are positioned at the top with more than 300mm of concrete beneath) to validate the code provisions in the ACI 408-03, ACI 318-11, CSA A23.3-14. The minimum development length of 300 mm is worth investigating than the 200mm in this case. A precaution is required to cap the bonded area with formwork (as in the case of bottom-placed rebars) and avoid any hand surface finishing (eg trowelling) the concrete as it may affect the amount of cover or the densified concrete in the bonded test region.
- Concerning the bar position, vertically oriented bars where the cast direction is either vertical or horizontal needs to be tested to represent practical case studies such as in retaining and shear walls.

## **6.5 Novelty of this study**

To this end, the novelty of this study/thesis has addressed some of the identified gaps in the literature and hence contributed significantly to enhancing the knowledge within the scientific community such as:

1. Using recycled aggregates prepared from a commercial source and of good quality.
2. Using both recycled coarse and fine aggregates in large proportions to unearth any effect on bond capacity if present.

3. Studying the effect of critical variables to detail structures and their effects on the bond performance, such as cover to rebar, bond length, bar size, transverse reinforcement, and rebar position.
4. Adopting a beam test method which will create the required tension stress state in both steel and concrete.

## REFERENCES

- ACI Committee 318. (2011). *Building Code Requirements for Structural Concrete and Commentary (ACI 318M-14)*. American Concrete Institute. American Concrete Institute, Farmington Hill, MI. [https://doi.org/10.1016/0262-5075\(85\)90032-6](https://doi.org/10.1016/0262-5075(85)90032-6)
- ACI Committee 408. (2003). Bond and Development of Straight Reinforcing Bars in Tension Reported by ACI Committee 408. *ACI Special Publication*, 1–49.
- ACI Committee 555R-01. (2002). *Removal and reuse of hardened concrete*. *ACI Report* (Vol. 99).
- ACI Committee 701. (2016). *ACI E701*. *ACI Materials Journal*. Farmington Hills, MI.
- Agg-Net. (2018, November 27). Fraunhofer Institute creates new process for recycling construction waste.
- Ahmed, K., Siddiqi, Z. A., Ashraf, M., & Ghaffar, A. (2008). Effect of Rebar Cover and Development Length on Bond and Slip in High Strength Concrete. *Pak. J. Engg. & Appl. Sci.*, 2(Development Length), 9. <https://doi.org/10.1016/j.eswa.2011.08.103>
- Ajdukiewicz, A., & Kliszczewicz, A. (2002). Influence of recycled aggregates on mechanical properties of HS/HPC. *Cement and Concrete Composites*, 24(2), 269–279. [https://doi.org/10.1016/S0958-9465\(01\)00012-9](https://doi.org/10.1016/S0958-9465(01)00012-9)
- Arezoumandi, M., Steele, A. R., & Volz, J. S. (2018). Evaluation of the Bond Strengths Between Concrete and Reinforcement as a Function of Recycled Concrete Aggregate Replacement Level. *Structures*, 16, 1–9.

- ASTM-A944. (2015). Standard Test Method for Comparing Bond Strength of Steel Reinforcing Bars to Concrete, (Reapproved 2015), 2015–2018. <https://doi.org/10.1520/A0944-10R15.2>
- ASTM. (2018). Standard Specification for Concrete Aggregates. *ASTM C33M*. <https://doi.org/10.1520/C0033>
- Behera, M., Bhattacharyya, S. K., Minocha, a K., Deoliya, R., & Maiti, S. (2014). Recycled aggregate from C&D waste & its use in concrete – A breakthrough towards sustainability in construction sector: A review. *Construction and Building Materials*, 68(0), 501–516. <https://doi.org/http://dx.doi.org/10.1016/j.conbuildmat.2014.07.003>
- Bhattacharyya, M. C. R. S. K. (2011). Influence of field recycled coarse aggregate on properties of concrete Bureau of Indian Standards, 205–220. <https://doi.org/10.1617/s11527-010-9620-x>
- Brecolotti, M., & Materazzi, A. L. (2013). Structural reliability of bonding between steel rebars and recycled aggregate concrete. *Construction and Building Materials*, 47, 927–934. <https://doi.org/10.1016/j.conbuildmat.2013.05.017>
- BS8100 British Standard. (1997). *Structural use of concrete-code of practice for design and construction*.
- Brown, T., & Taylor, A. H. (2001). Performance of concrete made with commercially produced coarse recycled concrete aggregate, 31.
- Butler, L. J., West, J. S., & Tighe, S. L. (2015). Bond of Reinforcement in Concrete Incorporating Recycled Concrete Aggregates. *Journal of Structural Engineering*, 141(3), 1–12. [https://doi.org/10.1061/\(ASCE\)ST.1943-541X.0000928](https://doi.org/10.1061/(ASCE)ST.1943-541X.0000928).

- Butler, L., West, J. S., & Tighe, S. L. (2011). The effect of recycled concrete aggregate properties on the bond strength between RCA concrete and steel reinforcement. *Cement and Concrete Research*, 41(10), 1037–1049. <https://doi.org/10.1016/j.cemconres.2011.06.004>
- Canbay, E., & Frosch, R. J. (2006). Bond Strength of Lap-Spliced Bars. *ACI Structural Journal*, (102).
- Choi, H. B., & Kang, K. I. (2008). Bond Behaviour of Deformed bars embedded in Recycled Aggregates Concrete. *Magazine of Concrete Research*, 399–410. <https://doi.org/10.1680/macrc.2008.60.6.399>
- Clark, A. (1949). Bond of Concrete to Reinforcing Bars. *ACI Journal Proceedings*, 46(11), 161–184. Retrieved from <http://www.concrete.org/PUBS/JOURNALS/OLJDetails.asp?Home=JP&ID=12050>
- Corinaldesi, V. (2010). Mechanical and elastic behaviour of concretes made of recycled-concrete coarse aggregates. *Construction and Building Materials*, 24(9), 1616–1620. <https://doi.org/10.1016/j.conbuildmat.2010.02.031>
- CSA A23.1. (2014). *Design of Concrete Structures CSA A23.3*. Canadian Standards Association.
- Darwin, D., & Graham, E. K. (1993). Effect of deformation height and spacing on bond strength of reinforcing bars. *ACI Materials Journal*, 90(6), 646–657. <https://doi.org/10.14359/4459>
- Dosho, Y. (2007). Development of a sustainable concrete waste recycling system: Application of recycled aggregate concrete produced by aggregate replacing method. *Journal of Advanced Concrete Technology*, 5(1), 27–42. <https://doi.org/10.3151/jact.5.27>

- Duan, Z. H., Kou, S. C., & Poon, C. S. (2013). Prediction of compressive strength of recycled aggregate concrete using artificial neural networks. *Construction and Building Materials*, 40, 1200–1206. <https://doi.org/10.1016/j.conbuildmat.2012.04.063>
- Eiras-López, Javier Seara-Paz, Sindy González-Fonteboa, Belén Martínez-Abella, F. (2017). Bond behavior of recycled concrete : analysis and prediction of bond stress – slip curve. *Journal of Material*, 29(10), 1–12. [https://doi.org/10.1061/\(ASCE\)MT.1943-5533.0002000](https://doi.org/10.1061/(ASCE)MT.1943-5533.0002000).
- Eurocode 2. (2003). *Design of concrete structures-Part1-1: General rules and rules for buildings*.
- Evangelista, L, & Brito, J. De. (2007). Mechanical behaviour of concrete made with fine recycled concrete aggregates. *Cement and Concrete Composites*, 29(5), 397–401.
- Evangelista, Luis. (2013). Concrete with fine recycled aggregates : A review. *European Journal of Environmental and Civil Engineering*, 18(April 2015). <https://doi.org/10.1080/19648189.2013.851038>
- Fathifazl, G., Abbas, a., Razaqpur, a. G., Isgor, O. B., Fournier, B., & Foo, S. (2009). New Mixture Proportioning Method for Concrete Made with Coarse Recycled Concrete Aggregate. *Journal of Materials in Civil Engineering*, 21(10), 601–611. [https://doi.org/10.1061/\(ASCE\)0899-1561\(2009\)21:10\(601\)](https://doi.org/10.1061/(ASCE)0899-1561(2009)21:10(601))
- Fathifazl, Gholamreza, Razaqpur, a. G., Isgor, O. B., Abbas, A., Fournier, B., & Foo, S. (2012). Bond performance of deformed steel bars in concrete produced with coarse recycled concrete aggregate. *Canadian Journal of Civil Engineering*, 39(2), 128–139. <https://doi.org/10.1139/111-120>

- Gaurav, G., & Singh, B. (2017). Bond strength prediction of tension lap splice for deformed steel bars in recycled aggregate concrete. *Materials and Structures*, 50(5), 1–20. <https://doi.org/10.1617/s11527-017-1101-z>
- Gonçalves, P., & Brito, J. d. (2010). Recycled aggregate concrete (RAC) – comparative analysis of existing specifications. *Magazine of Concrete Research*, 62(5), 339–346. <https://doi.org/10.1680/mac.2008.62.5.339>
- Gonzalez-Fontebao, B., & Martinez-Abella, F. (2007). Shear strength of recycled concrete beams. *Construction and Building Materials*, 21(4), 887–893. <https://doi.org/10.1016/j.conbuildmat.2005.12.018>
- Guerra, M., Ceia, F., De Brito, J., & Júlio, E. (2014). Anchorage of steel rebars to recycled aggregates concrete. *Construction and Building Materials*, 72, 113–123. <https://doi.org/10.1016/j.conbuildmat.2014.08.081>
- Guo, H., Shi, C., Guan, X., Zhu, J., Ding, Y., Ling, T. C., ... Wang, Y. (2018). Durability of recycled aggregate concrete – A review. *Cement and Concrete Composites*, 89, 251–259. <https://doi.org/10.1016/j.cemconcomp.2018.03.008>
- Hamad, B S, & Machaka, M. F. (1999). Effect of transverse reinforcement on bond strength of reinforcing bars in silica fume concrete. *Materials and Structures/Materiaux et Constructions*, 32(July), 468–476.
- Hamad, Bilal S. (1995). Bond strength improvement of reinforcing bars with specially designed rib geometries. *ACI Structural Journal*, 92(1), 3–13. <https://doi.org/10.14359/1464>
- Hamad, Bilal S, Dawi, A. H., Daou, A., & Chehab, G. R. (2018). Studies of the effect of

- recycled aggregates on flexural , shear , and bond splitting beam structural behavior. *Case Studies in Construction Materials*, 1–17. <https://doi.org/10.1016/j.cscm.2018.e00186>
- Highway, F. A. (2014). Lightweight Concrete : Development of Mild Steel in Tension. *Technical Research Report, FHWA-HRT14(202)*, 1–12.
- Huang, Q. F., & Wang, D. F. (2011). Experimental Study on Bond-Slip between Steel Bar and Recycled Aggregate Concrete. *Advanced Materials Research*, 250–253, 1651–1656. <https://doi.org/10.4028/www.scientific.net/AMR.250-253.1651>
- Huda, S. B., & Alam, M. S. (2014). Mechanical behavior of three generations of 100 % repeated recycled coarse aggregate concrete. *Construction and Building Materials*, 65, 574–582. <https://doi.org/10.1016/j.conbuildmat.2014.05.010>
- Jeanty, P. R., Mitchell, D., & Mirza, M. S. (1988). Investigation of “Top Bar” Effects in Beams. *ACI Structural Journal*, 85(3), 251–257.
- John Robert Prince, M., & Singh, B. (2013). Bond behaviour of deformed steel bars embedded in recycled aggregate concrete. *Construction and Building Materials*, 49, 852–862. <https://doi.org/10.1016/j.conbuildmat.2013.08.031>
- John Robert Prince, M., & Singh, B. (2014). Bond behaviour between recycled aggregate concrete and deformed steel bars. *Journal of Structural Engineering (India)*, 41(2), 132–143. <https://doi.org/10.1002/suco.201300042>
- Kaarthik, M., & Subramanian, N. (2014). Fine Aggregate and Steel Fibres. In *International Conference on Biological, Civil and Environmental Engineering (BCEE-2014)* (pp. 48–52). Dubai, UAE.

- Kang, H., & Kee, S. (2017). Improving the Quality of Mixed Recycled Coarse Aggregates from Construction and Demolition Waste Using Heavy Media Separation with Fe<sub>3</sub>O<sub>4</sub> Suspension, 2017.
- Katz, A. (2003). Properties of concrete made with recycled aggregate from partially hydrated old concrete, 33, 703–711. [https://doi.org/10.1016/S0008-8846\(02\)01033-5](https://doi.org/10.1016/S0008-8846(02)01033-5)
- Kayali, O., & Yeomans, S. R. (2000). Bond of ribbed galvanized reinforcing steel in concrete. *Cement and Concrete Composites*, 22, 459–469.
- Kim, S. W., Park, W. S., Jang, Y. Il, Jang, S. J., & Yun, H. Do. (2017). Bonding behavior of deformed steel rebars in sustainable concrete containing both fine and coarse recycled aggregates. *Materials*, 10(9). <https://doi.org/10.3390/ma10091082>
- Kim, S. W., & Yun, H. Do. (2014). Evaluation of the bond behavior of steel reinforcing bars in recycled fine aggregate concrete. *Cement and Concrete Composites*, 46, 8–18. <https://doi.org/10.1016/j.cemconcomp.2013.10.013>
- Kim, S. W., Yun, H. Do, Park, W. S., & Jang, Y. Il. (2015). Bond strength prediction for deformed steel rebar embedded in recycled coarse aggregate concrete. *Materials and Design*, 83, 257–269. <https://doi.org/10.1016/j.matdes.2015.06.008>
- Kim, Y., Sim, J., & Park, C. (2012). Mechanical properties of recycled aggregate concrete with deformed steel re-bar. *Journal of Marine Science and Technology*, 20(3), 274–280. Retrieved from <http://jmst.ntou.edu.tw/marine/20-3/274-280.pdf>
- Lima, C., Caggiano, A., Faella, C., Martinelli, E., Pepe, M., & Realfonzo, R. (2013). Physical properties and mechanical behaviour of concrete made with recycled aggregates and fly ash.

*Construction and Building Materials*, 47, 547–559.  
<https://doi.org/10.1016/j.conbuildmat.2013.04.051>

Lin, H., & Zhao, Y. (2016). Effects of confinements on the bond strength between concrete and corroded steel bars, *118*, 127–138.

Looney, T. J., Arezoumandi, M., Volz, J. S., & Myers, J. J. (2012). An Experimental Study on Bond Strength of Reinforcing Steel in Self-Consolidating Concrete. *International Journal of Concrete Structures and Materials*, 6(3), 187–197. <https://doi.org/10.1007/s40069-012-0017-9>

Lotfi, S., Eggimann, M., Wagner, E., Mróz, R., & Deja, J. (2015). Performance of recycled aggregate concrete based on a new concrete recycling technology. *Construction and Building Materials*, 95, 243–256. <https://doi.org/10.1016/j.conbuildmat.2015.07.021>

Lotfy, A., & Al-fayez, M. (2015). Performance evaluation of structural concrete using controlled quality coarse and fine recycled concrete aggregate, *61*, 36–43.

Lutz, B. L. A., & Gergely, P. (1967). Mechanics of Bond and Slip of Deformed Bars in Concrete. *American Concrete Institute*, (64), 711–721.

Lutz, L. A. (1970). Analysis of Stresses in Concrete Near a Reinforcing Bar Due to Bond and Transverse Cracking. *ACI Journal*, 67(67), 778–787.

Mains, R. (1951). Measurement of the distribution of tensile and bond stresses along reinforcing bars. *American Concrete Institute*, 48(11), 225–252. <https://doi.org/10.14359/11882>

Malešev, M., Radonjanin, V., & Marinković, S. (2010). Recycled concrete as aggregate for

structural concrete production. *Sustainability*, 2(5), 1204–1225.  
<https://doi.org/10.3390/su2051204>

Manzi, S., Mazzotti, C., & Bignozzi, M. C. (2013). Short and long-term behavior of structural concrete with recycled concrete aggregate. *Cement and Concrete Composites*, 37(March), 312–318. <https://doi.org/10.1016/j.cemconcomp.2013.01.003>

Marco, P. (2015). *A conceptual model to design recycled aggregate concrete for structural applications*. University of Salerno, Italy.

Martí-Vargas, J. R., & García-Taengua, E. (2015). Discussion of “bond of reinforcement in concrete incorporating recycled concrete aggregates” by Liam J. Butler, Jeffrey S. West, and Susan L. Tighe. *Journal of Structural Engineering (United States)*, 141(2), 1–2. [https://doi.org/10.1061/\(ASCE\)ST.1943-541X.0001232](https://doi.org/10.1061/(ASCE)ST.1943-541X.0001232)

Matias, D., Brito, J. De, Rosa, A., & Pedro, D. (2014). Durability of Concrete with Recycled Coarse Aggregates : Influence of Superplasticizers, *06014011*(5), 1–5. [https://doi.org/10.1061/\(ASCE\)MT.1943-5533.0000961](https://doi.org/10.1061/(ASCE)MT.1943-5533.0000961).

McNeil, K., & Kang, T. H. K. (2013). Recycled Concrete Aggregates: A Review. *International Journal of Concrete Structures and Materials*, 7(1), 61–69. <https://doi.org/10.1007/s40069-013-0032-5>

Mohamad, N., Khalifa, H., Abdul Samad, A. A., Mendis, P., & Goh, W. I. (2016). Structural performance of recycled aggregate in CSP slab subjected to flexure load. *Construction and Building Materials*, 115, 669–680. <https://doi.org/10.1016/j.conbuildmat.2016.04.086>

Morohashi, N., Sakurada, T., & Yanagibashi, K. (2007). Bond splitting strength of high-quality

- recycled coarse aggregate concrete beams. *Journal of Asian Architecture and Building Engineering*, 6(2), 331–337. <https://doi.org/10.3130/jaabe.6.331>
- Neville, A. M. M., & Brooks, J. J. J. (2010). *Concrete Technology. Building and Environment* (Vol. 11). [https://doi.org/10.1016/0360-1323\(76\)90009-3](https://doi.org/10.1016/0360-1323(76)90009-3)
- Noguchi, T. (2010). Toward sustainable resource recycling in concrete society. *2nd International Conference on Sustainable Construction Materials and Technologies*, 321–334.
- Oikonomou, N. D. (2005). Recycled concrete aggregates. *Cement and Concrete Composites*, 27(2), 315–318. <https://doi.org/10.1016/j.cemconcomp.2004.02.020>
- Orangun, C. O., Jirsa, J. O., & Breen, J. E. (1975). *A Reevaluation of Test Data on Development Length and Splices. Technical Research Report* (Vol. 74). <https://doi.org/10.14359/10993>
- Pandurangan, K., Dayanithy, A., & Prakash, S. O. (2016). Influence of treatment methods on the bond strength of recycled aggregate concrete. *Construction and Building Materials*, 120, 212–221. <https://doi.org/10.1016/j.conbuildmat.2016.05.093>
- Pedro, D, Brito, J. De, & Evangelista, L. (2017). Structural concrete with simultaneous incorporation of fine and coarse recycled concrete aggregates : Mechanical , durability and long-term properties. *Construction and Building Materials*, 154, 294–309. <https://doi.org/10.1016/j.conbuildmat.2017.07.215>
- Pedro, D, Guedes, M., De Brito, J., & Evangelista, L. (2019). Microstructural Features of Recycled aggregate concrete: from non-structural to high-performance concrete. *Microscopy and Microanalysis*, 601–616. <https://doi.org/10.1017/S1431927619000096>

- Perry, E.S. and Thompson, J. (1966). Bond Stress Distribution on Reinforcing Steel in Beams and Pullout Specimens. *ACI Journal Proceedings*, 63(8). <https://doi.org/10.14359/7656>
- Robert, M. J., Gaurav, G., & Singh, B. (2017). Splice strength of deformed steel bars embedded in recycled aggregate concrete. *Structures*, 10, 130–138. <https://doi.org/10.1016/j.istruc.2017.03.001>
- Sadati, S., Arezoumandi, M., Khayat, K. H., & Volz, J. S. (2017). Bond performance of sustainable reinforced concrete beams. *ACI Materials Journal*, 114(4), 537–547. <https://doi.org/10.14359/51689776>
- Sago-Crentsil, K. K., Brown, T., & Taylor, A. H. (2001). Performance of concrete made with commercially produced coarse recycled concrete aggregate. *Cement and Concrete Research*, 31, 707–712.
- Sato, R., Maruyama, I., Sogabe, T., & Sogo, M. (2007). Flexural Behavior of Reinforced Recycled Concrete Beams. *Journal of Advanced Concrete Technology*, 5(1), 43–61. <https://doi.org/10.3151/jact.5.43>
- Seara-Paz, S., González-Fontebo, B., Eiras-López, J., & Herrador, M. F. (2013). Bond behavior between steel reinforcement and recycled concrete. *Materials and Structures*, 47(1–2), 323–334. <https://doi.org/10.1617/s11527-013-0063-z>
- Senaratne, S., Lambrousis, G., Mirza, O., Tam, V. W. Y., & Kang, W. H. (2017). Recycled Concrete in Structural Applications for Sustainable Construction Practices in Australia. *Procedia Engineering*, 180(0), 751–758. <https://doi.org/10.1016/j.proeng.2017.04.235>
- Silva, R. V., Brito, J. De, & Dhir, R. K. (2017). Availability and processing of recycled

aggregates within the construction and demolition supply chain : A review, *143*, 598–614.

Tam, V. W. Y. (2008). Economic comparison of concrete recycling: A case study approach. *Resources, Conservation and Recycling*, *52*(5), 821–828.  
<https://doi.org/10.1016/j.resconrec.2007.12.001>

Tam, V. W. Y., Tam, C. M., & Wang, Y. (2007). Optimization on proportion for recycled aggregate in concrete using two-stage mixing approach, *21*, 1928–1939.  
<https://doi.org/10.1016/j.conbuildmat.2006.05.040>

The Canadian Infrastructure Report Card. (2016). *Canadian Infrastructure Report Card: Informing the Future*. Retrieved from [canadianinfrastructure.ca](http://canadianinfrastructure.ca)

Tokyo Sokki Kenkyujo. (2017). Strain gauge adhesives.

Tu, T. Y., Chen, Y. Y., & Hwang, C. L. (2006). Properties of HPC with recycled aggregates. *Cement and Concrete Research*, *36*(5), 943–950.  
<https://doi.org/10.1016/j.cemconres.2005.11.022>

Wang, H. L. (2019). Steel-concrete bond behaviour of self-compacting concrete with recycled aggregates. *Magazine of Concrete Research*, *68*(13), 678–691.

Watstein, D. (1947). Distribution of Bond Stress in Concrete Pull-Out Specimens. *ACI Journal*, *18*(9), 1041–1052.

Watsteint, B. D. (1941). Bond Stress in Concrete Pull-Out Specimens. *American Concrete Institute*, *38*(1).

Wernisch, G. R. (1937). Bond studies of different types of reinforcing bars. *Journal of the*

*American Concrete Institute*, 34(11), 145–164.

Xiao, J., & Falkner, H. (2007). Bond behaviour between recycled aggregate concrete and steel rebars. *Construction and Building Materials*, 21(2), 395–401.  
<https://doi.org/10.1016/j.conbuildmat.2005.08.008>

Xiao, J., Li, L., Tam, V. W. Y., & Li, H. (2014). The state of the art regarding the long-term properties of recycled concrete. *Structural Concrete*, 15(1), 3–12.  
<https://doi.org/10.1002/suco.201300024>

Xing, G., Zhou, C., Wu, T., & Liu, B. (2015). Experimental Study on Bond Behavior between Plain Reinforcing Bars and Concrete. *Advances in Materials Science and Engineering*, 2015. <https://doi.org/10.1155/2015/604280>

Yang, H., Deng, Z., & Ingham, J. M. (2016). Bond position function between corroded reinforcement and recycled aggregate concrete using beam tests, 127, 518–526.

Zhao, Y., Lin, H., Wu, K., & Jin, W. (2013). Bond behaviour of normal/recycled concrete and corroded steel bars. *Construction and Building Materials*, 48, 348–359.  
<https://doi.org/10.1016/j.conbuildmat.2013.06.091>

## Appendix A Summary of recycled coarse and fine aggregates applications

Institution (Country)	Concrete Application	Aggregates Size	Maximum Replacement Percentage (%)	Allowable Compressive Strength (28days) MPa	Researcher
Australia CCAA (2008)	Grade 2 Concrete	Coarse	100	25	(Marco, 2015)
	Grade 1 Concrete	Coarse	30	40	
Belgium CRIC (2004)	Structural	Coarse	100	Not Specified	(McNeil & Kang, 2013)
	Non-Structural	Fine	Limits Imposed		
BSI-8500-2 (2006)	Not Specified	Coarse	20	20-40	(Marco, 2015)
Canada CSA A23.1 (2014)	Not Specified	Coarse	Not Specified	10	CSA A23.1&2 (2014)
Denmark DS481 (1998)	Structural	Coarse	100	Not Specified	(McNeil & Kang, 2013)
		Fine	20		
German DAFStB (1998)	Structural	Coarse	35	25	(Marco, 2015)
			25	35	(Marco, 2015)
		Fines	Not Allowed		(McNeil & Kang, 2013)
Hong Kong BD (2009)	Non-Structural	Coarse	100	20	(Marco, 2015)
	Structural	Coarse	20	25-30	
Italian Ministry of Infrastructure (NTC 2008)	Non-Structural	Coarse	100	10	(Marco, 2015)
			30	37	(Marco, 2015)
			60	25	(Marco, 2015)
Netherlands NEN5950 (1995)	Structural	Coarse	20	Not Specified	(McNeil & Kang, 2013)
		Fine	20		
UK BS EN12620 (2002)	Structural	Coarse	20	Not Specified	(McNeil & Kang, 2013)
	Non-Structural	Fine	Not Allowed		
RILEM (1994)	Not Specified	Coarse	100	50	(Marco, 2015)
		Fines	Not Allowed		

## Appendix B Summary table of pullout bond test method and conclusions

### Aggregates and Concrete Proportion and Production Source

Researcher(s)	Bond Length, (mm)	Bar Size(s) (mm)	Concrete Strength, (MPa)	Aggregate Production Source (C/F)	RC A	RFA or NFA	Concrete Source	RCA Proportion (%)	Conclusions on Bond Strength
1. (Ajdukiewicz & Kliszczewicz, 2002)	50	14	40-85	Laboratory-C	Yes	NFA	Laboratory	0, 20, 50, 100	Bond Strength reduced with increasing RCA content
2. (Xiao & Falkner, 2007)	50	10	35-44	Laboratory-C	Yes	NFA	Laboratory	0, 50, 100	Similar Bond strength for both RCA and NCA
3. (Choi & Kang, 2008)	150	16	23-38	Laboratory-C	Yes	NFA	Laboratory	0, 30, 50, 100	Similar Bond strength for both RCA and NCA
4. (Malešev et al., 2010)	150	12	43-46	Laboratory-C	Yes	NFA	Laboratory	0, 50, 100	Similar Bond strength for both RCA and NCA and high quality RCA is recommended
5. (Corinaldesi, 2010)	80	16	35	Industry-C	Yes	NFA	Laboratory	0, 50	Similar Bond strength for both RCA and NCA
6. (Huang & Wang, 2011)	80, 180	16	32-37	Laboratory-C	Yes	NFA	Laboratory	0, 30, 50, 75, 100	RCA bond strength reduces if tensile strength reduces
7. (Y. Kim et al., 2012b)	150	19	39-45	Laboratory-C	Yes	RFA/NFA	Laboratory	0, 30(C/F), 60(C/F), 100	Similar Bond Strength up to 60% RCA and 18% reduction in bond with 100% RCA
8. (Seara-Paz et al., 2013)	50	10	42-64	Laboratory-C	Yes	NFA	Laboratory	0, 20, 50, 100	Similar Bond strength for both RCA and NCA
9. (S. W. Kim & Yun, 2014)	64	16	27-32	Industry-C/F	No	RFA&NFA	Industry*	0, 30(C/F), 60(C/F), 100	The bond strength reduction was 12%. The focus was on using RFA than RCA and for up to 60% RFA and the bond strength was similar, but at 100%RFA. <b>NB: No RCA was used</b>
10. (Guerra et al., 2014)	60-240	12, 16	43-48	Laboratory-C	Yes	NFA	Laboratory	0, 20, 50, 100	Similar bond strength up to 50% RCA and 12% reduction in bond with 100% RCA
11. (John Robert Prince & Singh, 2014)	40, 50	8, 10	24-37	Laboratory-C	Yes	NFA	Laboratory	0, 25, 50, 75, 100	Normalized bond strengths across RCA replacement percentages were higher for the RCA concrete compared to the natural coarse aggregate concrete
12. (S. W. Kim, Yun, Park, & Jang, 2015c)	64	16	27-44	Industry-C**	Yes	NFA	Industry	0,30,60,100	Bond Strength reduced with increasing RCA content

## Appendix C Summary table of beam bond test with varied experimental settings and conclusions

<u>Test Specimen Details</u>				<u>Concrete and Aggregates Production Details</u>						
Researcher(s)	Beam Specimen or Test Method	Bond Length, mm	Rebar Sizes mm	Concrete Strength, MPa	Aggregates. Production Source (C/F)	RCA	RFA/NFA	Concrete Source	RCA (%)	Bond strength conclusions
1. (Morohashi, Sakurada, & Yanagibashi, 2007a)	Splice Beam	570	19	34-44	Laboratory-C	Yes	NFA	Laboratory	0, 50, 100	Similar bond strength obtained but high quality RCA is to be used
2. (Gholamreza Fathifazl et al., 2012)	Beam End	250-291	16,25	34-49	Laboratory-C	Yes	NFA	Laboratory	0, 100	18-33% reduction in bond strength depending on mixing method
3. (L. J. Butler et al., 2015)	Beam End	125, 375, 450	25	30-60	Laboratory-C	Yes	NFA	Laboratory	0, 100	10-21% reduction in bond strength
4. (Pandurangan et al., 2016)	RILEM Beam	100	10	37-43	Laboratory-C	Yes	NFA	Laboratory	0, 70-95	Bond strength reduced by 4%-Acid Tr. 10%-Mechanical Tr and 20%-Thermal Treatment
5. (Robert et al., 2017)	Splice Beam	300	6, 8, 12, 20	24-69	Laboratory-C	Yes	NFA	Laboratory	0, 50, 100	Similar bond strength
6. (Sadati et al., 2017)	Splice Beam	360	19	25-30	Industry-C <sup>*</sup>	Yes	NFA	Laboratory & Industry	0, 50	Similar bond strength
7. (Arezoumandi et al., 2018)	Splice	360	19	25-33	Industry <sup>#</sup>	Yes	NFA	Industry	0, 50, 100	Bond is similar up to 50%
8. (Bilal S Hamad et al., 2018)	Splice	305	12	29-33	Laboratory	Yes	NFA	Industry	0, 40, 100	2-16% greater BS in RCA mixes than NCA

**Notes:** \*=Crushers used not stated, #=Crushers were only primary and secondary, Tr=Treatment

**Appendix C-Cont'd Summary table of beam bond test of various researchers using 100%  
RCA**

Researcher	Specimen ID	Bond Force-T	$f'_c$	$d_b$	cover, c	$BL=l_d$	c/d	$l_d/d_b$	BS/ $f'_c$	Exp BS
<b>Bilal and Hamad, 2018</b>	NB100-1	120.2	29.5	12	30	305	2.5	25.417	0.776	4.214
	NB100-2	122.2	29.5	12	30	305	2.5	25.417	0.789	4.285
<b>Fathifazil et al, 2012</b>	CM-30		48.5	30	55	262	1.833	8.733	0.863	6.01
	CM-15		49.5	16	52	279	3.250	17.438	1.151	8.1
	CV30		49	30	55	263	1.833	8.767	0.899	6.29
<b>Liam et al, 2015</b>	RAC1-30-125A	56.2	30.7	25	30	125	1.200	5.000	1.034	5.727
	RAC1-30-125B	56.7	30.7	25	30	125	1.200	5.000	1.043	5.778
	RAC1-40-125A	60.6	38.6	25	30	125	1.200	5.000	0.994	6.176
	RAC1-40-125B	68.8	38.6	25	30	125	1.200	5.000	1.129	7.011
	RAC1-50-125A	61.4	48.2	25	30	125	1.200	5.000	0.901	6.257
	RAC1-50-125B	57.8	48.2	25	30	125	1.200	5.000	0.848	5.890
	RAC1-60-125A	62.8	60.1	25	30	125	1.200	5.000	0.826	6.400
	RAC1-60-125B	68.3	60.1	25	30	125	1.200	5.000	0.898	6.961
	RAC2-30-125A	50.6	31.3	25	30	125	1.200	5.000	0.922	5.157
	RAC2-30-125B	59.1	31.3	25	30	125	1.200	5.000	1.077	6.023
	RAC2-50-125A	57.7	49.4	25	30	125	1.200	5.000	0.837	5.880
	RAC2-50-125B	59.2	49.4	25	30	125	1.200	5.000	0.858	6.033
	RAC3-40-125A	63.8	41.4	25	30	125	1.200	5.000	1.011	6.502
	RAC3-40-125B	55.2	41.5	25	30	125	1.200	5.000	0.873	5.625
	RAC3-60-125A	65.9	56.2	25	30	125	1.200	5.000	0.896	6.716
	RAC3-60-125B	63.9	57	25	30	125	1.200	5.000	0.863	6.512
	RAC1-30-375A	150.8	30.9	25	30	375	1.200	15.000	0.922	5.123
	RAC1-30-375B	151.1	30.9	25	30	375	1.200	15.000	0.923	5.133
	RAC1-50-375A	161.9	47.9	25	30	375	1.200	15.000	0.795	5.500
	RAC1-50-375B	152.5	47.9	25	30	375	1.200	15.000	0.749	5.180
	RAC2-30-375A	148.5	31.3	25	30	375	1.200	15.000	0.902	5.045
	RAC2-30-375B	150.4	31.3	25	30	375	1.200	15.000	0.913	5.109
	RAC2-50-375A	164.6	49.4	25	30	375	1.200	15.000	0.796	5.592
	RAC2-50-375B	153.5	49.4	25	30	375	1.200	15.000	0.742	5.214
	RAC1-40-450A	190.6	43.7	25	30	450	1.200	18.000	0.816	5.396
	RAC1-40-450B	189.5	42.6	25	30	450	1.200	18.000	0.822	5.364
	RAC1-60-450A	182.2	53.8	25	30	450	1.200	18.000	0.703	5.158
	RAC1-60-450B	191.2	49.9	25	30	450	1.200	18.000	0.766	5.413
	RAC3-40-450A	187	56.2	25	30	450	1.200	18.000	0.706	5.294
	RAC3-40-450B	185.4	57	25	30	450	1.200	18.000	0.695	5.248
RAC3-60-450A	181.3	56.2	25	30	450	1.200	18.000	0.685	5.132	
RAC3-60-450B	179.3	57	25	30	450	1.200	18.000	0.672	5.076	

Researcher	Specimen ID	Bond Force-T	$f'_c$	$d_b$	cover, c	BL= $l_d$	c/d	$l_d/d_b$	BS/ $f'_c$	Exp BS
Robert et al, 2017	AS12R100-1	77.28	24.71	12	15	300	1.250	25.000	1.052	5.23
	AS12R100-2	66.93	24.71	12	15	300	1.250	25.000	0.907	4.51
	AS20R100-1	180.3	24.71	20	25	400	1.250	20.000	1.066	5.3
	AS20R100-2	176.32	24.71	20	25	400	1.250	20.000	1.034	5.14
	CS12R100-1	94.23	50.3	12	15	300	1.250	25.000	0.750	5.32
	CS12R100-2	86.84	50.3	12	15	300	1.250	25.000	0.750	5.32
	CS20R100-1	200.36	50.3	20	25	400	1.250	20.000	0.830	5.89
	CS20R100-2	182.65	50.3	20	25	400	1.250	20.000	0.756	5.36
Arezoumandi, Steele, 2018	RAC-100-1	53	33.3	19	30	360	1.579	18.947	1.646	9.5
	RAC-100-2	53	33.3	19	30	360	1.579	18.947	1.646	9.5
	RAC-100-3	53	33.3	19	30	360	1.579	18.947	1.646	9.5

## Appendix D **Strain gage and adhesive installation**

The strain gauge application procedure is given as:

- 1) The location for the strain gauges was measured, marked, and then the surface was sanded down flat using a pneumatic drill and flap disk.
- 2) The surface was then sanded smoother using a 320 grit general use sand paper to provide a uniform surface to affix the gauges.
- 3) The flat section was cleaned used high pressure air and acetone to remove any particles or dust.
- 4) A thin coat of general use strain gauge cement (CC-33A) was applied to the surface of the bar and the strain gauge was applied while pressure was applied for a minute using a plastic sheet as per the cement manufacturers recommendations (Tokyo Sokki Kenkyujo, 2017).
- 5) A strain gauge terminal was applied directly next to the strain gauge using the same strain gauge cement and the process as in step 4.
- 6) The lead wires from the strain gauges were shaped towards the terminal and soldered down using rosin flux and soldering wire.
- 7) Long wires were soldered to the other side of the terminal to provide a connection to the data acquisition (DAQ) system.

- 8) The strain gauge and wires were sealed with an insulating compound to prevent electrical interference, and further sealed with bees wax to prevent and damage during the bonding process.
- 9) The strain gauges were tested from the far end of the wires using a handheld voltmeter to ensure the gauges still read  $120 \pm 0.5 \Omega$  meaning that no damage had occurred during the application process.

### Strain Gage Adhesive (CC-33A)

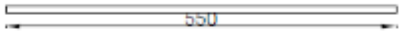
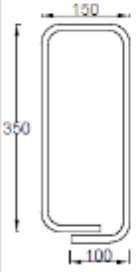
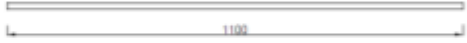
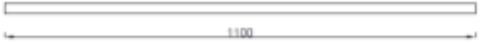
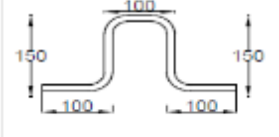
1  
-47  
STRAIN GAGES

## Adhesives and Bonding Tools

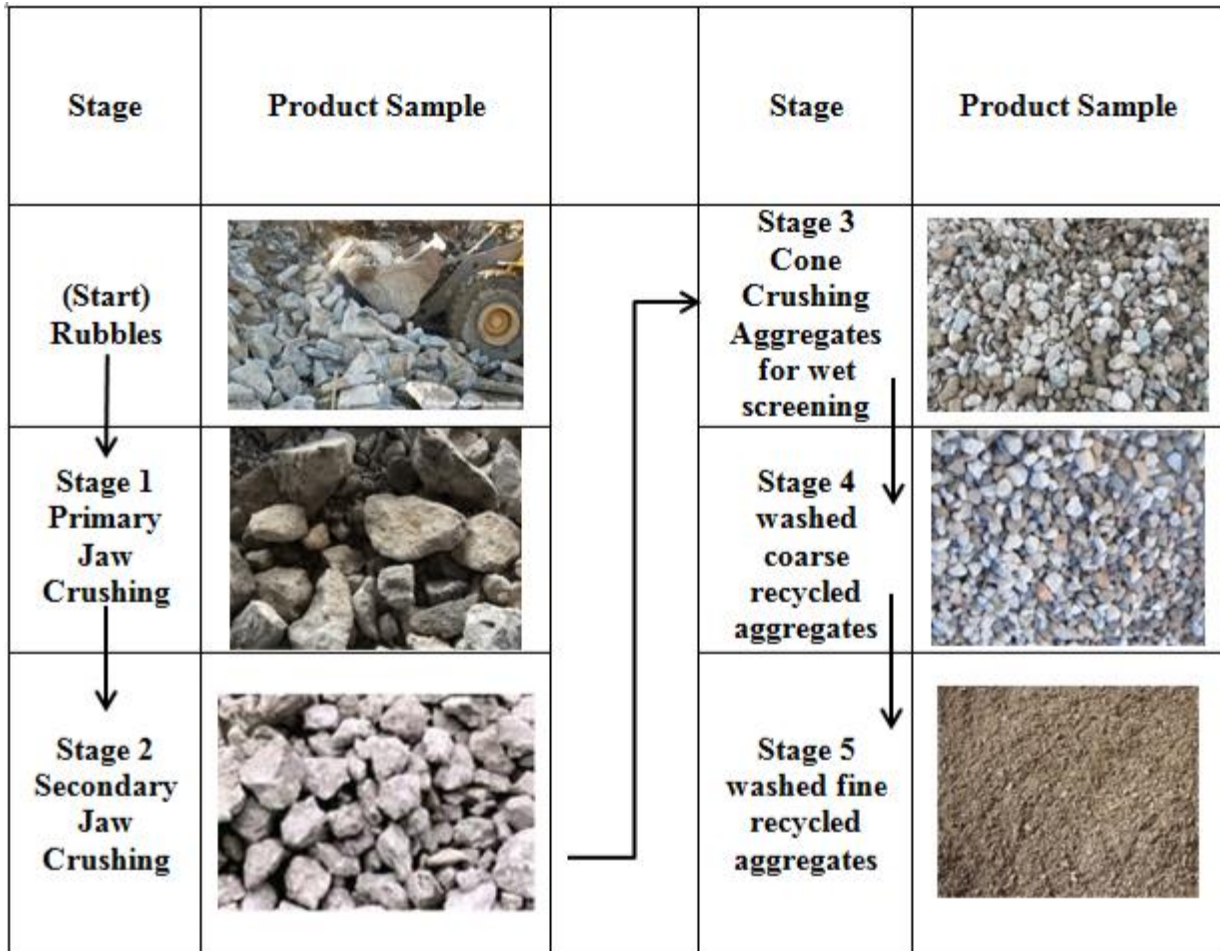
To obtain good measurement results, the strain gage must be bonded completely to the measuring object. Thus, it is important to select a suitable adhesive for the materials of measuring object and gage base and for measuring requirements.

Models	Types	Operating Temperature Range (°C)	Major Applicable Materials	Curing Requirements
 <b>CC-33A</b>	Instantaneous adhesive cured at normal temperature	-196 to 120	<ul style="list-style-type: none"> <li>•Metals (Steel, stainless steel, copper, aluminum alloys A1050, A2024, etc.)</li> <li>•Plastics (acrylate, vinyl chloride, nylon, etc.)</li> <li>•Composite materials (CFRP, GFRP, printed board, etc.)</li> <li>•Rubber</li> </ul>	Apply finger pressure (100 to 300 kPa) for 15 to 60 seconds. Then, leave the gage as it is for 1 hour. The finger pressure application time differs depending on temperature and humidity conditions. The lower the temperature and humidity, the longer the finger pressure application time required.
 <b>CC-35</b>	Instantaneous adhesive cured at normal temperature	-30 to 120	<ul style="list-style-type: none"> <li>•Concrete</li> <li>•Mortar</li> <li>•Lumber</li> </ul>	Apply finger pressure (100 to 300 kPa) for 30 to 60 seconds. Then, leave the gage as it is for 1 hour or more. The finger pressure application time differs depending on temperature and humidity conditions. The lower the temperature and humidity, the longer the finger pressure application time required.
 <b>CC-36</b>	Instantaneous adhesive cured at normal temperature	-30 to 100	<ul style="list-style-type: none"> <li>•Metals (Steel, stainless steel, copper, aluminum alloys A1050, A2024, A7075, magnesium alloy, etc.)</li> <li>•Plastics (acrylate, vinyl chloride, nylon, polypropylene, etc.)</li> <li>•Composite materials (CFRP, GFRP, PCB, etc.)</li> <li>•Concrete      •Mortar</li> <li>•Lumber        •Rubber</li> </ul>	Apply finger pressure (100 to 300 kPa) for 30 to 60 seconds. Then, leave the gage as it is for 1 hour or more. The finger pressure application time differs depending on temperature and humidity conditions. The lower the temperature and humidity, the longer the finger pressure application time required.

Appendix E **Bending schedule for test beam specimens**

Bar Mark	Bar size	Bar diameter (mm)	Shape Size	No.	Unit Weight (kg/m)	Total Weight (In kg)
R1	M10	11.3		150	0.785	95.38
R2	M10	11.3		300	0.785	294.38
R3	M15	16		64	1.57	144.69
R4	M25	25		11	3.93	71.67
U1	M10	11.3		75	0.79	35.33
					<b>Total Weight (In kg)</b>	<b>641.44</b>

Appendix F **Recycled concrete products and stages of crushing**



## Appendix G Descriptive and design equations

### APPENDIX 7A-Summary of descriptive equation

Orangun, Jirsa and Breen, (1975,1977)	$\tau_b = \left(0.1 + 0.25 \frac{C}{d_b} + \frac{4.15d_b}{l_d}\right) \sqrt{f'_c}$ $\tau_b = \left[0.1 + 0.25 \frac{C}{d_b} + \frac{4.15d_b}{l_d} + \frac{A_{tr}f_{yt}}{41.52sd_b}\right] \sqrt{f'_c}$ <p style="text-align: center;"><i>NB: Term with <math>A_{tr}</math> is accounting for transverse reinforcement</i></p>	(7.1)
MacGregor, (1997)	$\tau_b = 0.498 \left(\frac{C}{d_b} - 0.5\right) \sqrt{f'_c}$	(7.2)
Kemp & Wilhelm, (1979)	$\tau_b = \left(0.55 + 0.24 \frac{C}{d_b}\right) \sqrt{f'_c}$	(7.3)
Darwin et al, (1992)	$\frac{T_c}{\sqrt{f'_c}} = 0.554(C_{min} + 0.5d_b) \left(0.08 \frac{C_{max}}{C_{min}} + 0.92\right) \sqrt{f'_c} + 24.9A_b$	(7.4)
ACI 408R-03	$\frac{T_c}{\sqrt[4]{f'_c}} = \frac{A_b f_s}{\sqrt[4]{f'_c}} = (59.5l_d(C_{min} + 0.5d_b) + 2400A_b) \left(0.1 \frac{C_{max}}{C_{min}} + 0.9\right)$	(7.5)

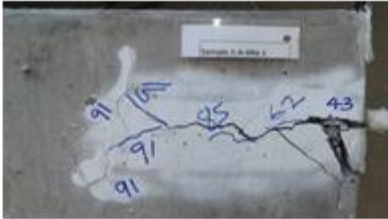
### APPENDIX 7B- Summary of design equations

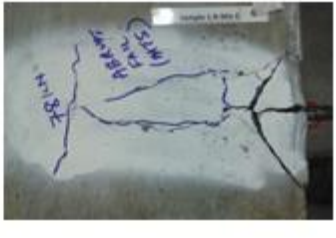
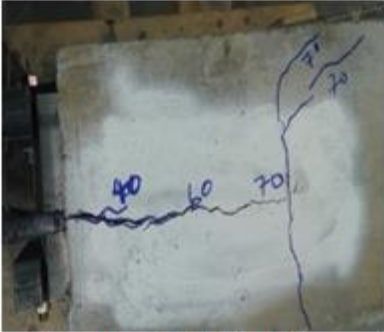
(ACI Committee 318, 2011)-Chapter 12	$l_d = \left(\frac{f_y}{1.1\lambda\sqrt{f'_c}}\right) \left(\frac{\psi_t\psi_e\psi_s}{\frac{c_b+K_{tr}}{d_b}}\right) d_b \quad \text{where, } K_{tr} = \frac{40A_{tr}}{sn}$	(7.6)
(CSA A23.1, 2014) Chapter 12	$l_d = \left(\frac{1.15k_1k_2k_3k_4}{\sqrt{f'_c}}\right) \left(\frac{f_y}{d_{cs}+K_{tr}}\right) A_b \quad \text{where, } K_{tr} = \frac{A_{tr}f_{yt}}{10.5sn}$	(7.7)
(British Standard, 1997) BS8100 clause 3.12.8.4	$\tau_b = 0.4\sqrt{f_{cu}} \quad \text{where } f_{cu} = 0.8f'_c$	(7.8)
(Eurocode 2, 2003) EC-2clause 8.4.2	$f_{bd} = 2.25\eta_1\eta_2f_{ctd}$ <p style="text-align: center;">where <math>f_{ctd} = (0.21\sqrt[3]{f_{cu}})/\gamma_c</math> and <math>\gamma_c = 1.5</math></p>	(7.9)
AASHTO/ACI 318-71	$l_d = \frac{0.02A_b f_y}{\sqrt{f'_c}}$	(7.10)

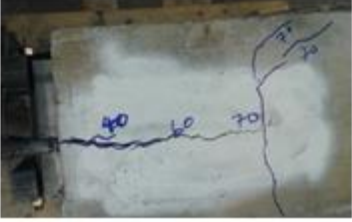
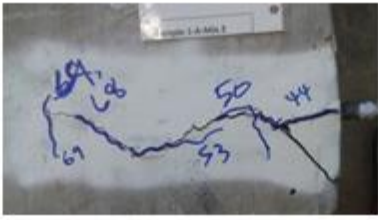
## Appendix H **Bond failure in specimens**

See **Appendix I to O** showing crack patterns in each specimen group and corresponding range of crack width in bracket ( )mm.

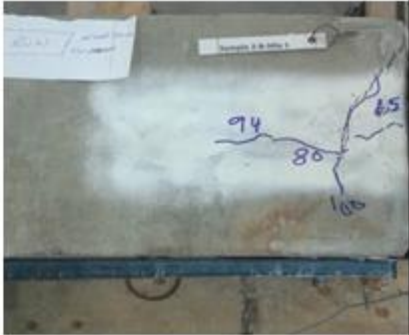
Appendix I Group 1 Test specimens R15-L200-C25

Mix Type	Specimen Types and Crack widths	
<b>M1-R15-L200-C25</b>	 <p data-bbox="565 751 927 785" style="text-align: center;"><b>Plan view of-A (3.5 to 0.1)mm</b></p>	 <p data-bbox="1015 751 1328 785" style="text-align: center;"><b>Plan view-B (5 to 0.1)mm</b></p>
	 <p data-bbox="667 1570 829 1604" style="text-align: center;"><b>Front view-A</b></p>	 <p data-bbox="1084 1570 1295 1604" style="text-align: center;"><b>Isometric view-B</b></p>

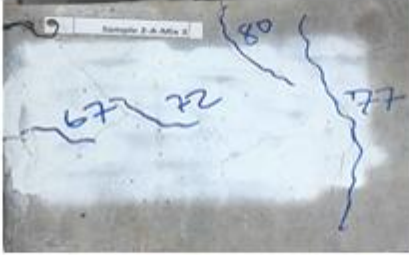
Mix Type	Specimen Types and Crack widths	
<b>M2-R15-L200-C25</b>	 <p data-bbox="544 596 878 632" style="text-align: center;"><b>Plan view-A (2.5 to 0.1)mm</b></p>	 <p data-bbox="1015 583 1330 619" style="text-align: center;"><b>Plan view-B (2 to 0.1)mm</b></p>
<b>M3-R15-L200-C25</b>	 <p data-bbox="500 1171 870 1207" style="text-align: center;"><b>Isometric view-A (3 to 0.1)mm</b></p>	 <p data-bbox="971 1171 1341 1207" style="text-align: center;"><b>Isometric view-B (4 to 0.1)mm</b></p>
<b>M4-R15-L200-C25</b>	<p data-bbox="639 1373 808 1409"><b>Not Available</b></p>	
	<p data-bbox="566 1598 881 1633" style="text-align: center;"><b>Plan view-A (2 to 0.2)mm</b></p>	 <p data-bbox="998 1591 1336 1627" style="text-align: center;"><b>Plan view-B (3.5 to 0.8)mm</b></p>

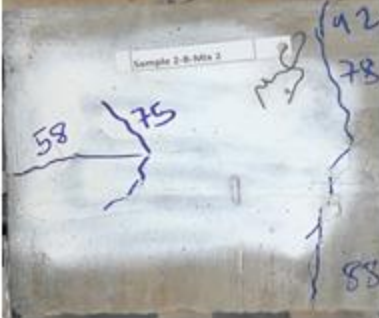
Mix Type	Specimen Types and Crack widths	
<b>M4-R15-L200-C25</b>	<p><b>Not Available</b></p> <p>(2 to 0.2)mm</p>	 <p style="text-align: center;"><b>Plan view-A (3.5 to 0.8)mm</b></p>
<b>M5-R15-L200-C25</b>	 <p style="text-align: center;"><b>Plan view-A (3 to 0.1)mm</b></p>	 <p style="text-align: center;"><b>Plan view-B (4 to 0.6)mm</b></p>
	 <p style="text-align: center;"><b>Front view-A</b></p>	 <p style="text-align: center;"><b>Front view-B</b></p>

Appendix J Group 2 Test specimens R15-L200-C25-S1

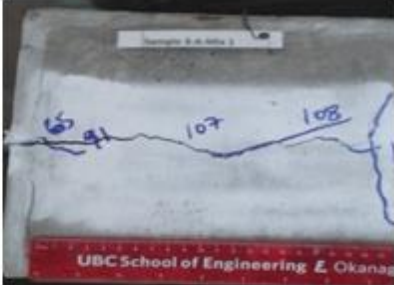
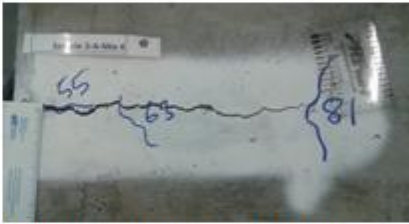
<b>Mix Type</b> Chart Area	<b>Specimen Types and Crack widths</b>	
M1-R15-L200-C25-S1	 <p data-bbox="540 743 878 842">                         Plan view-A (0.15mm-same through)                     </p>	 <p data-bbox="1015 1045 1328 1167">                         In test progress picture-B                          (0.18mm-same through)                     </p>
	 <p data-bbox="521 1493 896 1591">                         Side view-A (Flexural crack at 110KN)                     </p>	

Mix Type	Specimen Types and Crack widths	
M2-R15-L200-C25 -S1	 <p data-bbox="618 810 789 842"><b>Front view-A</b></p> <p data-bbox="618 898 797 930">(3.5 to 0.3)mm</p>	 <p data-bbox="1013 800 1325 831"><b>In test progress picture-B</b></p> <p data-bbox="1073 888 1265 919">(3.0 to 0.25)mm</p>
	 <p data-bbox="578 1524 834 1556"><b>Front view failure-A</b></p>	 <p data-bbox="1044 1520 1297 1551"><b>Front view failure-B</b></p>

Mix Type	Specimen Types and Crack widths	
<b>M3-R15-L200-C25-S1</b>	 <p data-bbox="597 625 818 659" style="text-align: center;"><b>In test progress A</b></p> <p data-bbox="618 716 797 749" style="text-align: center;"><b>(2.5 to 0.1)mm</b></p>	 <p data-bbox="1045 625 1295 659" style="text-align: center;"><b>Front view failure-B</b></p> <p data-bbox="1073 716 1268 749" style="text-align: center;"><b>(0.35 to 0.1)mm</b></p>
<b>M4-R15-L200-C25-B-S1</b>	 <p data-bbox="537 1171 878 1205" style="text-align: center;"><b>Plan view-A (2.5 to 0.1)mm</b></p>	 <p data-bbox="1062 1352 1273 1386" style="text-align: center;"><b>Isometric view-B</b></p> <p data-bbox="1078 1436 1256 1470" style="text-align: center;"><b>(2.5 to 0.1)mm</b></p>
	 <p data-bbox="602 1633 813 1667" style="text-align: center;"><b>Isometric view-A</b></p>	

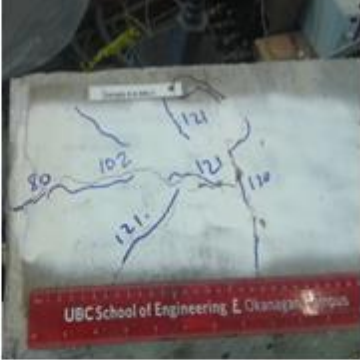
Mix Type	Specimen Types and Crack widths	
<b>M5-R15-L200-C25-B-S1</b>	 <p data-bbox="613 877 808 915">(0.4 to 0.15)mm</p>	 <p data-bbox="1097 781 1247 814">Plan view-B</p> <p data-bbox="1075 869 1269 907">(0.4 to 0.15)mm</p>
<b>SPECIMEN OVERVIEW OF GROUP 2</b>	 <p data-bbox="639 1499 1240 1537">General view of post tested specimens in Group 2</p>	

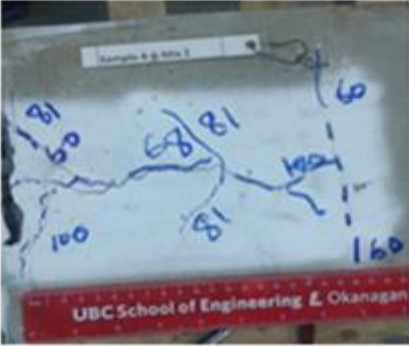
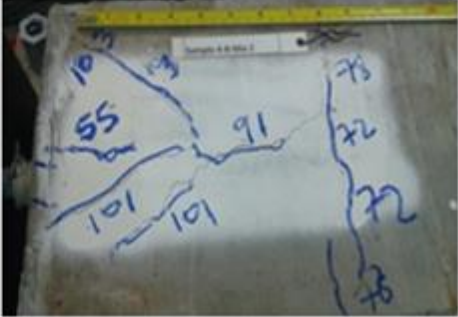
Appendix K Group 3 Test Specimens R15-L200-C40

Mix Type	Specimen types and crack widths	
M1-R15-L200-C40	 <p data-bbox="581 747 764 779">Plan view of A</p>	 <p data-bbox="1068 747 1252 779">Plan view of B</p>
M2-R15-L200-C40	 <p data-bbox="461 1062 841 1094">Plan view of A (3.5 to 0.35)mm</p>	 <p data-bbox="969 1089 1349 1121">Plan view of B (3.5 to 0.25)mm</p>
M3-R15-L200-C40-B	 <p data-bbox="492 1570 857 1602">Plan view of A (3.0 to 0.3)mm</p>	 <p data-bbox="969 1570 1349 1602">Plan view of B (3.5 to 0.35)mm</p>

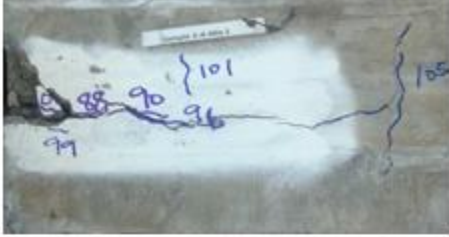
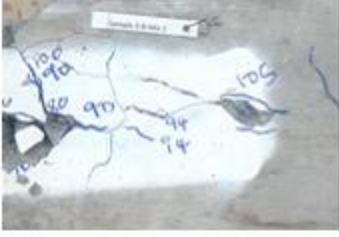
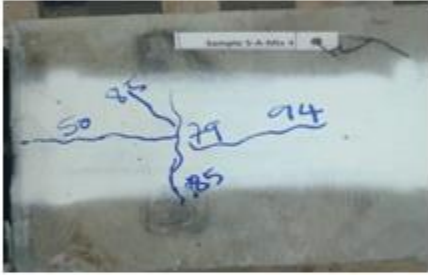
Mix Type	Specimen types and crack widths	
<b>M4-R15-L200-C40</b>	 <p data-bbox="553 972 792 1003"><b>Isometric view of A</b></p>	 <p data-bbox="1040 972 1279 1003"><b>Isometric view of B</b></p>
<b>M5-R15-L200-C40</b>	 <p data-bbox="574 1575 773 1606"><b>Front view of A</b></p>	 <p data-bbox="1062 1575 1260 1606"><b>Front view of B</b></p>

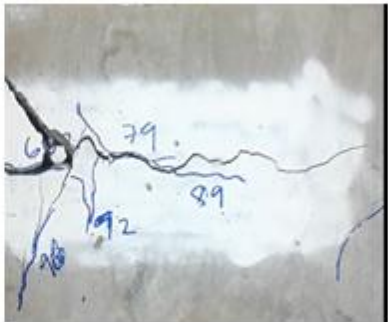
Appendix L Group 4 Test Specimens R15-L200-C25-S2

Mix Type	Specimen types and crack widths	
M1-R15-L200-C25-S2	 <p data-bbox="565 814 748 846">Plan view of A</p> <p data-bbox="565 905 748 936">(0.4 to 0.15)mm</p>	 <p data-bbox="922 842 1365 873">Isometric view of B-Fractured rebar</p>
M2-R15-L200-C25-S2	 <p data-bbox="529 1598 789 1629">In-progress testing A</p>	 <p data-bbox="1024 1598 1268 1629">Isometric view of A</p>

Mix Type	Specimen types and crack widths	
M3-R15-L200-C25-S2	 <p data-bbox="526 772 836 808">In-progress testing of A</p>	 <p data-bbox="911 762 1425 798">In-progress testing of B (0.8 to 0.15)mm</p>
M4-R15-L200-C25-S2	 <p data-bbox="466 1150 852 1186">Plan view of A (1.0 to 0.1)mm</p>	 <p data-bbox="982 1150 1369 1186">Plan view of B (0.5 to 0.3)mm</p>
M5-R15-L200-C25-B-S2	 <p data-bbox="475 1665 865 1701">Plan view of A (1.0 to 0.1)mm</p>	 <p data-bbox="1003 1640 1393 1675">Plan view of B (0.5 to 0.3)mm</p>

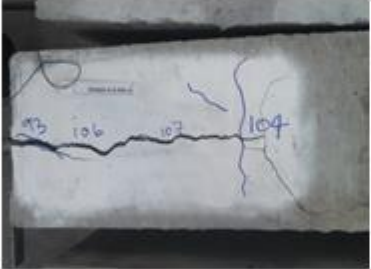
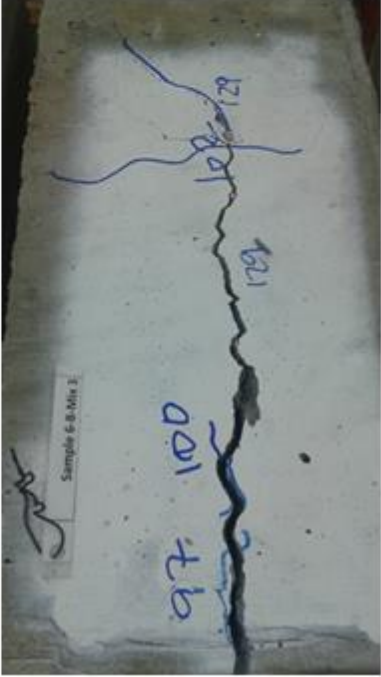
Appendix M Group 5 Test specimens R15-L300-C25

Mix Type	Specimen types and crack widths	
M1-R15-L300-C25	 <p data-bbox="597 659 781 688">Plan view of A</p>	 <p data-bbox="1084 659 1268 688">Plan view of B</p>
M2-R15-L300-C25-B	 <p data-bbox="472 1050 906 1079">In testing progress of A (3.5 to 0.1)mm</p>	 <p data-bbox="932 1066 1295 1096">Plan view of A (3.5 to 0.1)mm</p>
M3-R15-L300-C25-B	 <p data-bbox="477 1596 906 1625">Isometric view of A (1.5 to 0.1)mm</p>	 <p data-bbox="932 1596 1360 1625">In testing progress of B (2.5 to 0.1)mm</p>

Mix Type	Specimen types and crack widths	
M4-R15-L300-C25-B	 <p data-bbox="521 667 883 699">Plan view of A (3.5 to 0.1)mm</p>	 <p data-bbox="1008 667 1370 699">Plan view of B (3.5 to 0.1)mm</p>
M5-R15-L300-C25-B	 <p data-bbox="566 1104 1268 1136">Isometric view of A-(3.5 to 0.1)mm and B-(4.0 to 0.1)mm</p>	
Specimen overview of Group 5	 <p data-bbox="618 1619 1218 1650">General view of post tested specimens in Group 5</p>	

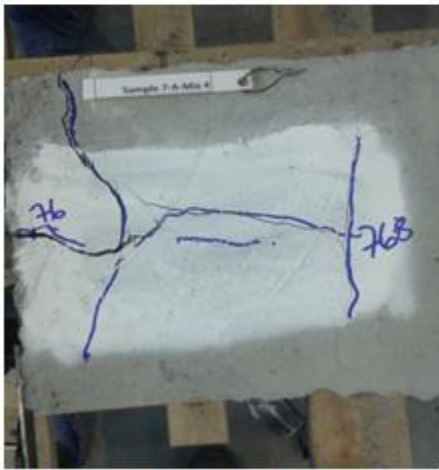
Appendix N **Group 6 Test specimens R25-L300-C40**

Mix Type	Specimen types and crack widths	
<p style="text-align: center;"><b>M1-R25-L300-C40</b></p>	 <p style="text-align: center;"><b>Isometric view-A (10 to 0.15)mm</b></p>	 <p style="text-align: center;"><b>Isometric view-B (5 to 0.15)mm</b></p>
	 <p style="text-align: center;"><b>Flexural crack on A</b></p>	

Mix Type	Specimen types and crack widths	
M2-R25-L300-C40	 <p data-bbox="399 877 797 911">Isometric view-A (3.5 to 0.2)mm</p>	 <p data-bbox="943 877 1279 911">Plan view-B (5.0 to 0.2)mm</p>
M3-R25-L300-C40	 <p data-bbox="444 1262 820 1295">Plan view of A (8.0 to 0.15)mm</p>  <p data-bbox="444 1625 829 1659">Flexural cracks on the side of A</p>	 <p data-bbox="899 1667 1273 1701">Plan view of B (8.0 to 0.15)mm</p>

Mix Type	Specimen types and crack widths	
<b>M4-R25-L300-C40</b>	 <p data-bbox="402 709 818 743" style="text-align: center;"><b>In-progress test A (4.5 to 0.15)mm</b></p>	 <p data-bbox="857 709 1224 743" style="text-align: center;"><b>Shear failure A (5.0 to 0.1)mm</b></p>
<b>M5-R25-L300-C40</b>	 <p data-bbox="542 1136 735 1169" style="text-align: center;"><b>(7.0 to 0.15)mm</b></p>	 <p data-bbox="1019 1136 1200 1169" style="text-align: center;"><b>(6.0 to 0.1)mm</b></p>
<b>Specimen overview of Group 6</b>	 <p data-bbox="581 1623 1187 1656" style="text-align: center;"><b>General view of post tested specimens in Group 6</b></p>	

Appendix O **Group 7 Test specimens R15-L200-C25-Top**

Mix Type	Specimen types and crack widths	
<b>M1-R15-L200-C25-Top</b>	 <p data-bbox="423 957 850 989">Isometric view of A (2.0 to 0.3)mm</p>	 <p data-bbox="911 968 1328 999">Isometric view of B (0.8 to 0.3)mm</p>
<b>M2-R15-L200-C25-Top</b>	 <p data-bbox="418 1514 797 1545">Plan view of A (3.5 to 0.15)mm</p>	<p data-bbox="1036 1226 1203 1257">Not Available</p>  <p data-bbox="1036 1493 1203 1524">(3.0 to 0.1)mm</p>

Mix Type	Specimen types and crack widths	
M3-R15-L200- C25-Top	Not Available (3.0 to 0.15)mm	 (3.0 to 0.15)mm
M4-R15-L200- C25-Top	 Isometric view of A(3.0 to 0.15)mm	 Isometric view of B (5.0 to 0.1)mm
M5-R15-L200- C25-Top	 Plan view of A (3.0 to 0.3)mm and B (4.0 to 0.3)mm	
	 Isometric view of A and B	